

Advancing savanna structural characterization at multiple scales for enhanced ecological insights

Dissertation

zur Erlangung des akademischen Grades doctor rerum naturalium
(Dr. rer.nat)

vorgelegt dem Rat der Chemisch-Geowissenschaftlichen Fakultät der
Friedrich-Schiller-Universität Jena
von M.Tech Jenia Singh geboren am
11.02.1992 in Haridwar, India

Gutachter:

1. Prof. Dr. Christiane Schmullius, FSU, Jena, Germany
2. Assoc. Prof. Dr. Shaun R Levick, Charles Darwin University, and CSIRO, Darwin, Australia

Tag der Verteidigung: 24.02.2020

Zugl.: Dissertation, Friedrich-Schiller-Universität Jena, [2020]

Acknowledgements

Firstly, I would like to thank my supervisor at Max Planck Institute of Biogeochemistry, Shaun R. Levick for introducing me to the fascinating world of *Savanna ecosystems*. I appreciate his involvement throughout my thesis work and pushing me towards the excellence. I am grateful for the freedom he gave me in taking up many exciting research internships beyond MPI-BGC. I am also thankful to my other committee member Prof. Susan Trumbore for her interest in my work and pertinent advices during PAC meetings, which have been precious for the development of this thesis.

I wish to express my sincere gratitude to my supervisor at the University - Prof. Christiane Schullius for her cooperation, suggestions during PAC meeting and most importantly making me believe in myself. I would like to thank Dr. Marcus Guderle for his invaluable assistance during terrestrial laser scanning survey in South Africa, data processing and contribution to the successful development of my PhD career, for that I am immensely grateful. I also appreciate his help in proof reading of manuscripts and translation of the abstract of this thesis to German language. I must greatly thank Dr. Christian Berger for his help and suggestions during Radar data processing.

Special thanks to Dr. Sassan Saatchi and Dr. Pasi Raunonen for welcoming me into their labs during my research stay abroad at Jet Propulsion Laboratory, Pasadena, California, and Tampere University of Technology, Tampere, Finland, which were intellectually intriguing experiences.

In addition, I am thankful to Steffi Rothhardt for her advices during PAC meeting and for organizing the scientific events, and to Kerstin Lohse for her support in organizing business trips. A warm thanks to my friends and colleagues at MPI-BGC for friendly chats, summer barbecues and hiking. I will always remember our yearly kayaking in Saale river with Ingo Schöning, Hueiyang Gan, Kasun Gayantha and Sung-Bin Park, thanks for your company. Thanks to Yan, Annu, Shivali and Pavan for the weekend dinners.

I gratefully acknowledge the International Max Planck Research School for Biogeochemical Cycles for funding my PhD work and several research stays. Thanks to John Kula, for all the administrative help. I acknowledge the help and support from Izak Smit, Navashni Govender, and Tercia Strydom at Sanparks, Kruger National Park, South Africa. I also thank all the game guards for their help in the field work during terrestrial laser scanning data acquisition.

I would like to thank my family - my parents, Rekha Singh and Devendra Singh and my brother, Piyush for their love and support, and cheering me up on every phone call. I would not have made it this far without you all.

Finally, I would like to thank the most important person in my life, my husband *Shivam*, my biggest cheerleader, who made sure that I followed a healthy work-life balance, even though he was miles apart. I look forward to sharing with you all wonderful experiences and next challenges.

Jena, December 18, 2019

Jenia Singh

Abstract

Savanna ecosystems make up a large proportion of land area and play a considerable role in the storage and cycling of carbon. *Vegetation structure* is the principle factor controlling carbon storage in these ecosystems, as it controls biomass carbon stocks and inputs to soil. However, vegetation structure in savannas is highly variable in space and time, depending on local factors such as disturbance (fire and herbivory) as well as regional factors like climate or nutrient availability. Previously, investigations to quantify vegetation structure have been limited by the manual field inventories at the plot scale or coarse spatial resolution satellite data. This paucity of precise vegetation structural data underlies our inability to determine trajectories of vegetation change under disturbance regimes and changing climate scenarios. Additionally, not all the processes influencing vegetation structural dynamics operate at the same spatial scale, and can not be understood with the same level of detail (grain).

This thesis addresses these shortcomings by exploring data on fine-scale vegetation structure in savanna landscapes through the use of structural inventories at multiple scales from high resolution 3D terrestrial LiDAR and Radar data. Furthermore, this work characterizes the synergy between disturbances, resources and vegetation structure. First, the response of savanna vegetation structure to long-term fire regimes were investigated across four distinct savanna types along a rainfall gradient in South Africa. This was achieved by acquiring 3D data with a Riegl VZ-2000 terrestrial laser scanner across long-term (63 years) experimental burning plots in Kruger National Park (KNP). The results from this study reveal that the relationship between vegetation and fire are context dependent, and are strongly influenced by rainfall. Second, knowledge of savanna vegetation dynamics is often constrained due to sparse landscape scale vegetation inventories that characterize the spatial heterogeneity. To enable the characterization of vegetation structure at landscape scale, we collected 106 long-range scans ($>2000\text{ m}$) from topographic vantage points and hill-slopes across the entire KNP. In order to validate the accuracy of long-range scanning in large area monitoring samplings, a canopy height and cover change matrix with respect to increasing distance from the scanner was produced. For this, we used reference plots of 1 *ha* from multiple scans in the footprint of long-range scans. The relationships were highly significant, and displayed a low RMSE of 1.0 *m* until 600 *m* from the scanner location. Furthermore, despite the decreasing point density, canopy cover metrics from long-range scans were comparable to those reported from the reference

plots. The high correlation of biophysical attributes derived from long-range scans allowed us to trace the trajectories of woody vegetation structure at landscape scale under diverse ecological settings. The last part of the dissertation discusses the scaling implications of long-range scanning for training and validating spaceborne Radar imagery for monitoring of larger areas. Overall this work demonstrates that vegetation responses to long-term burning regimes differ between savanna landscapes types, and management policies in protected areas need to take this into account while formulating conservation policies. Similarly, mapping methods differ in their efficiency at different sites which needs to be considered when designing mapping protocols in order to accurately reflect the present vegetation.

Keywords- Savanna ecosystem, vegetation structure, fire-regimes, Terrestrial Laser scanning, scaling, Radar remote sensing

Zusammenfassung

Savannen-Ökosysteme bilden einen großen Teil der Landfläche und spielen eine wichtige Rolle bei der Speicherung und dem Kreislauf von Kohlenstoff. Die Vegetationsstruktur ist der Hauptfaktor, der die Kohlenstoffspeicherung in diesen Ökosystemen steuert, da diese die Kohlenstoffvorräte und -eintragungen aus Biomasse in den Boden bestimmt. In Savannen ist die Vegetationsstruktur jedoch in Raum und Zeit sehr variabel, abhängig von lokalen Faktoren wie Störungen (Feuer und Pflanzenfresser) sowie regionalen Faktoren wie Klima oder Nährstoffverfügbarkeit. Bisher waren Studien zur Quantifizierung der Vegetationsstruktur durch manuelle Feldinventuren im Plot-Maßstab oder grob aufgelösten Satellitendaten eingeschränkt. Dieser Mangel an genauen Daten geht einher mit unserem Unvermögen, Veränderungen der Vegetationsstruktur durch Störungen sowie sich verändernden Klimaszenarien zu erfassen. Darüber hinaus finden nicht alle Prozesse, die die Dynamik der Vegetationsstruktur beeinflussen, mit der gleichen räumlichen Auflösung statt und können somit nicht in der gleichen Detailgenauigkeit verstanden werden.

Diese Arbeit untersucht das Potential von Inventuren der Vegetationsstruktur, welche auf den Skalen von hochaufgelösten 3D terrestrial LiDAR- und Radardaten durchgeführt werden. Darüber hinaus charakterisiert diese Arbeit das Zusammenwirken von Ökosystemstörungen, Ressourcen und Vegetationsstruktur. Zunächst wurden die Auswirkungen von langfristigen Feuerexperimenten auf die Vegetationsstruktur in vier verschiedenen Savanntypen in Südafrika entlang eines Niederschlagsgradienten untersucht. Hierfür wurden 3D-LiDAR Daten von 63 Jahre bestehenden Feuerexperimente im Krüger-Nationalpark (KNP) mittels eines terrestrischen Laserscanner VZ-2000 der Firma Riegl erhoben. Die Ergebnisse dieser Studie zeigen, dass die Beziehung zwischen Vegetation und Feuer kontextabhängig ist und stark vom Niederschlagsregime beeinflusst wird. Zweitens ist das Wissen über die Dynamik von Savannenvegetation durch die wenigen Vegetationsinventuren auf Landschaftsebene, welche die räumliche Heterogenität charakterisieren, limitiert. Um die Charakterisierung der Vegetationsstruktur auf Landschaftsmaßstab umzusetzen, wurden 106 „long-range scans“ (LiDAR-scans bis zu einer Entfernung von 2000 *m*) von topographischen Aussichtspunkten und Hügeln im gesamten KNP durchgeführt. Die Genauigkeit der „long-range scans“ beim Monitoring auf Landschaftsmaßstab wurde mittels der Änderung der Bestandeshöhe sowie des Bedeckungsgrades mit zunehmendem Abstand vom LiDAR Scanner validiert. Hierfür wurden Referenzflächen (jeweils 1 *ha*) im Footprint der „long-range scans“ durch sogenannte „Multiple Scans“ aufgenommen. Die abgeleiteten Variablen Bestandeshöhe und Bedeckungsgrad aus den „long-range scans“ und den Referenzflächen zeigen einen signifikanten Zusammenhang mit einem niedrigen RMSE für die Entfernung von 1,0 *m* bis 600 *m* vom Standort des Scanners. Trotz der abnehmenden Punktdichte in den „long-range scans“ waren die Werte der Bestandesbedeckung mit denen der Referenzplots vergleichbar. Auf Grund der hohen Korrelation zwischen den biophysikalischen Größen aus den „long-range scans“ mit den Referenzflächen ist es möglich, die verholzte Vegetationsstruktur auf Landschaftsmaßstab unter verschiedenen ökologischen Bedingungen

zu ermitteln. Ausgehend von diesen Ergebnissen werden im letzten Teil der Dissertation die Implikationen der Skalierung von „long-range scans“ auf das Training und die Validierung von weltraumgestützten Radarbildern zum Monitoring größerer Gebiete diskutiert. Diese Arbeit zeigt, dass die Reaktion der Vegetation auf Langzeit-Feuerregime unterschiedlich in den jeweiligen Savannenlandschaften ist, was bei der Ausarbeitung von Managementrichtlinien für Schutzgebiete beachtet werden muss. Ebenso unterscheiden sich die Kartierungsmethoden in ihrer Effizienz die verschiedenen Standorte zu erfassen, was bei der Entwicklung von Kartierungsprotokollen berücksichtigt werden muss, um die aktuelle Vegetation genau wiederzugeben.

Schlüsselwörter- Savannen-Ökosystem, Vegetationsstruktur, Feuerregime, Terrestrisches Laserscanning, Skalierung, Radarfernerkundung

Contents

	Page
Acknowledgements	iii
Abstract	v
Contents	ix
Chapter 1 State of the art and research questions	1
1.1 Background and motivation	2
1.2 Biotic and abiotic determinants of savanna structure	3
1.3 Woody encroachment and homogenization in savanna landscapes	8
1.4 Savanna vegetation structure estimation	9
1.5 Aims and research questions	13
1.6 Outline of the thesis	15
Chapter 2 Study site and instrumentation	19
2.1 Study Area	20
2.2 Woody vegetation data	21
Chapter 3 Effects of fire regimes on savanna vegetation structure - A local scale analysis	25
3.1 Introduction	27
3.2 Study site and experimental design	29
3.3 Results	34
3.4 Discussion	39
3.5 Conclusions	43
Chapter 4 Mapping savanna landscapes - A long-range terrestrial laser scanning approach	45
4.1 Introduction	47
4.2 Methods	49
4.3 Results	54
4.4 Discussion	61
4.5 Conclusions	65

Chapter 5 Improved characterization of woody vegetation at regional scales using earth observation data	67
5.1 Introduction	69
5.2 Long-range scans acquisition sites and processing	71
5.3 Results	76
5.4 Discussion	85
5.5 Conclusion	88
Chapter 6 Synthesis	89
6.1 Synthesis	90
6.2 Reflection	91
6.3 Closing thoughts	98
6.4 Looking to the future	99
References	105

List of Figures

- 1.1 Conceptual chart of biotic and abiotic factors influencing savanna vegetation structure at various scales. The outer box represents the boundary of savanna ecosystems, with climate, topography and substrate controlling ecosystem structure at larger scales, while interactive controls depicted inside the box act at smaller spatial scales. 4
- 1.2 (a) Derived relationship between woody cover and mean annual precipitation (MAP) at African savanna sites (Sankaran et al., 2005) (b) Woody cover estimates for Africa showing a bifurcated distribution with fewer sites in the 50-70% (Staver et al., 2011). 5
- 1.3 Illustration of terrestrial LiDAR data captured in South African savanna and coloured according to amplitude. Amplitude is higher for the woody component than the photosynthetic part of the vegetation. 12
- 1.4 Framework demonstrating the link between the objectives resulting from this dissertation. Upper boxes show the different topics and links studied in this dissertation. Colored boxes in the middle indicate objectives in this dissertation. Grey boxes in the bottom row indicate different data types and methodologies applied in the different objectives. 14
- 1.5 Conceptual representation for the chapters of this thesis in relation to the main objectives and research questions across various spatial scales. Figure style adapted from Schimel et al. (2019). 16

- 2.1 Location of the KNP with longitudinal geomorphological division and north-south rainfall gradient. 20
- 2.2 Riegl VZ-2000 terrestrial laser scanner at a terrestrial vantage point in KNP. 22

- 3.1 (a) Location of the four experimental burn plots within Kruger National Park, South Africa. Differences in vegetation structure along the precipitation gradient. (b) Upper photograph is from Mopani EBP receiving 496-mm mean annual precipitation (MAP) on basaltic soils. (c) Lower photograph is from Pretoriuskop EBP receiving 737-mm MAP on granitic soils. 30

3.2	The TLS scanning setup of the EBPs with solid black dots indicating the scan locations. Sampling of the EBPs was achieved by placing random circles of 40 m radii depicted with dotted circles.	31
3.3	Normalized height distribution of vegetation within a 100 x 30 m transect of the laser footprint, represented at 5 m height increments. The colour scale from green through red indicates increasing vegetation height. The panel shows data from biennially (B2-yr) and triennially (B3-yr) burnt plots, and fire exclusion (unburnt) from the Satara site, with maximum height of 12 m.	32
3.4	Average height (a), maximum height (b), and canopy cover (c) in plots subjected to different burn treatments. B2= biennial, B3= triennial and Unburnt= fire exclusion. Colour shading indicates the increasing MAP from Pretoriuskop to Mopane.	35
3.5	Structural responses of woody vegetation height to different fire frequencies as a function of landscape type.	37
3.6	Woody biomass in plots subjected to different burn treatments estimated from the terrestrial LiDAR point cloud data. Results are shown for the long-term experimental burn plots at Mopani and Satara, the dry savanna and Skukuza and Pretoriuskop, the wet savanna subjected to a burn frequency of B2= biennial, B3= triennial and Unburnt= fire exclusion.	38
4.1	(a) Location of the two sampling landscapes (shown with black circles) in Kruger National Park, South Africa. The rightmost panels show examples of 2D LiDAR data from the two sites, with the level-plots describing vegetation heterogeneity. Mathekenyani and Stevenson sites are shown in (b) and (c) respectively.	50
4.2	Conceptual representation of the long-range scanning set-up adopted in this study. The black outlined squares indicate the multi-scan reference plots positioned 100 m apart from each other, and overlaid in the long-range scan footprint up to 600 m, with an associated decreases in point density.	51
4.3	Reference-plot example, derived from multi-scan TLS and shown in oblique view with colour scale representing height above ground level. TLS instruments capture vegetation 3D structural detail in a holistic manner that cannot be recorded manually in the field.	53
4.4	Comparison of vertical height distribution derived from LR-TLS and reference-plots in vertical intervals of 0.5 m at increasing distances in the Mathekenyani landscape.	55
4.5	Comparison of vertical height distribution derived from LR-TLS and reference plots in vertical intervals of 0.5 m with increasing distances in the Stevenson-Hamilton landscape.	56
4.6	Canopy height (a) and canopy cover (b) differences between LR-TLS and reference-plots with increasing ranging distance.	59

4.7	(a) Deviation in canopy height, and (b) canopy ground projected area (GPA) with increasing ranging distance in the two study landscapes. The colour coding represents the linear interpolation model at different laser ranging distances.	60
4.8	An example of height normalized LiDAR returns of a single tree (a) and shrub (b) from reference-plots and LR-TLS at a ranging distance of 400 m.	63
5.1	(a) Location of study site with LiDAR sampled plots within Kruger National Park, South Africa overlaid on elevation data, (b) major geology in the study site, and (c) mean annual precipitation of the park at 5° grid size.	72
5.2	Landsat-8 and PALSAR-2 and Sentinel-1 SAR polarimetric imagery over the Kruger National Park in October 2015. The C and L band images are false colour composites.	74
5.3	a) Normalized long-range scan from the southern Kruger National Park. Lower panel represents the frequency distribution of LiDAR returns calculated for two sites situated in granite (b) and basalt substrate (c) with a MAP of 747 mm and 353 mm respectively.	77
5.4	Boxplots of estimates of mean canopy height, cover and AGB in two geologies and along a rainfall gradient.	78
5.5	Estimates of canopy cover at 1m and 1.5m height threshold derived for the scanned sites. Lines represent linear model fit with dashed line as 1:1 (a,b). Distribution of canopy cover at different height thresholds (c).	79
5.6	Distribution of R^2 between height thresholds used to determine woody cover and AGB in the scanned sites for ALOS-PALSAR 2 (a) and Sentinel-1 (b).	80
5.7	Relationship of L-band radar backscatter power (m^2m^2) at two polarizations of HH and HV with the woody cover (%) and AGB (Mg/ha).	81
5.8	Relationship of C-band radar backscatter power (m^2m^2) at two polarizations of VH and VV with the woody cover (%) and AGB (Mg/ha).	82
5.9	Errors in predicting AGB from the ALOS (a) and Sentinel-1 (b) backscatter plotted against long-range scan quantified woody properties.	83
5.10	AGB map of KNP and associated analyses. (a) Spatial pattern of AGB in KNP. Example A shows the riparian vegetation stands in the northern part of the park. Example B displays the catenas with high AGB. (b) frequency distribution of AGB for two substrate type, and (c) frequency distribution of AGB for each rainfall zone.	84
6.1	Bar plots for distribution of trees in 3 height classes with varying frequencies.	94
6.2	A graphical representation showing varying effects of fire regimes across basalt and granite substrate of KNP. Arrows indicate the strength of fire influence on vegetation, where red symbolises greater effect while black indicates a weak effect.	95

6.3	Estimation of aboveground biomass from the long-range and multi-scan setup for (a) Mathekenyani and (b) Stevenson.	96
6.4	Individual tree point clouds (a) Marula, (b) and (c) Mopane in Experimental burn plots of Kruger National Park, South Africa, coloured by height from low (blue) to high (yellow). The contrasting three-dimensional structures across EBPs are associated with the fire frequency and intensity. . .	100
6.5	a) TLS point cloud of a Marula (<i>Sclerocarya birrea</i>) coloured by height low (blue) to high (yellow). (b) QSM model derived from using (Raumonen et al., 2013) algorithm. The total volume, branch volume and DBH of the tree were 5210 cm ³ , 3841 cm ³ and 53 cm respectively.	101
6.6	Work task of the concept for LR-TLS benchmark study.	102
6.7	(a) TLS and (b) Unmanned aerial vehicle acquired point cloud across Northern Australian savanna sites. It is evident from UAV point clouds that stems of the vegetation are not properly characterized. The data quality from UAV is greatly influenced by the flight paths, overlap and laser sensor. (Data courtesy: Shaun Levick)	104

List of Tables

- 2.1 Specifications of Riegl VZ-2000 laser scanner (Data source Riegl VZ-2000 data sheet). 21
- 3.1 Results from an analysis of the effects of fire frequency and landscape upon three-dimensional vegetation characteristics at the EBPs in Kruger National Park, South Africa. Results are the Akaike’s Information Criterion for linear mixed effect models, with * referring to the most parsimonious model. 36
- 3.2 The importance of two variables (landscape and fire frequency) examined as predictors of average and maximum vegetation height, and woody cover, with * referring to the variables with reasonable level of support as predictors. 36
- 4.1 Characteristics of two study landscapes located in Kruger National Park, South Africa. Canopy cover and slope are calculated from the multi-scan TLS data. 50
- 4.2 Specifications for the RIEGL VZ-2000 scanner utilized for the 3D long-range data acquisition in Kruger National Park, 2016 51
- 4.3 The mean canopy height (m) values derived from reference plots (RP) and LR-TLS (LR). SD is the standard deviation. 57
- 4.4 The mean canopy cover (%) values derived from reference plots (RP) and LR-TLS (LR). SD is the standard deviation. 58
- 5.1 R^2 , RMSE and MAE of mapped AGB from ALOS-PALSAR-2 and Sentinel-1 83
- 6.1 Summary of the discussions on each scientific contributions 92

Chapter 1

State of the art and research questions

1.1 Background and motivation

“These steppes were principally covered with the grasses of the genera killingia, cenchurus, and paspalum, which at the season scarcely attain a height of nine or ten inches near Calabazo and St. Jerome der Pirital, although on the banks of the Apure and Portuguesa they rise to the length of four feet. Along with these were mingled some turnerae, malvaceae, and mimosae. The pastures are richest on the banks of the rivers and under the shades of corypha palms. These trees were singularly uniform in size; their height being from twenty-one to twenty-five feet, and their diameter from eight to ten inches.. A few clumps of a species of rhopala occur here and there”. (Travels and Researches of Alexander von Humboldt, 1833, Chapter 15, Journey across the Llanos from Aragua to San Fernando)

This quote from Humboldt’s writing wonderfully describes the existence of one of the complex vegetation structure ecosystem - *Savannas*. A variable tree cover which sprawls across continuous herbaceous layer, with diversity in stature and architecture defines the complex structure of savanna systems (Scholes & Archer, 1997; Ratnam et al., 2011). Savannas are geographically vast located in the wet-dry tropics of Africa, South America, Australia and Asia (Scholes & Archer, 1997), occupying roughly an eighth of the global land surface. Due to the extensive global distribution, savanna ecosystems contribute significant environmental and economic value to the world. For example, savanna ecosystems store 15% of Earth’s carbon and account for 30% of the global terrestrial net primary production, equivalent to that of tropical forests (Grace et al., 2006). Additionally, savannas are biodiverse systems, which harbor a range of tree species and fauna (Parr et al., 2014; Murphy et al., 2016). At present, one-fifth of world’s population live in and around savannas, and depend on a multitude of savanna goods and services including fuel wood, food and livestock grazing (Frost et al., 1986; Olsson & Ouattara, 2013).

As human population grows and expands, savanna habitats are increasingly threatened due to changing land tenure and land-use policies (Galvin & Reid, 2010; Bond & Parr, 2010). A global study by Goldewijk (2001), estimated that in the past three centuries savanna ecosystems have witnessed largest land-clearing. Furthermore, climatic extremes such as dry years (Hill & Hanan, 2010), and government driven afforestation initiatives for carbon sequestration (Ratnam et al., 2016) are a threat to the savanna ecosystems globally. These changes are likely to alter the vegetation structure and carbon sinks/strengths of savanna ecosystems. Therefore, to keep these systems sustainable, it is crucial to document accurate vegetation structure, carbon storage and long-term change trajectories. This information can assist better policy decisions, land holders and non-government organizations in the management of savanna lands. Consequently, systematic mapping approaches at suitable scale and frequency is a key to advance vegetation structure retrievals in savanna systems, and our ability to predict the future changes.

Motivated by the significance of savanna systems in mediating terrestrial ecosystem functioning and services, *this study is geared toward a better understanding of savanna struc-*

ture and function. More specifically this thesis unites two strands of knowledge - *method development* for characterizing savanna vegetation inventories from high resolution remote sensing data sources, and subsequently *realizing the power* of derived products in unravelling savanna vegetation dynamics and function. It presents the distribution of savanna vegetation structure from plot to regional scales, as well as the influence of changing land-use patterns, rainfall and soils on vegetation structure and their contribution to carbon cycle.

In the introduction, background information on biotic and abiotic factors controlling savanna vegetation structure is presented. Later, a short introduction on the estimation of savanna vegetation structure by remote sensing methods are discussed. The last part of the introduction presents the main objectives and structure of the whole thesis with a short overview of each chapter's contribution.

1.2 Biotic and abiotic determinants of savanna structure

Many who have glanced at savanna landscapes have wondered about their architecture and form. Why aren't savannas complete forest or grasslands? And why does heterogeneity vary between landscapes? Scientific interest in the vegetation heterogeneity of savannas dates back to Charles Darwin who wrote about the complexity of savanna structure while en route to South America-

“The general and entire absence of trees in Banda Oriental is remarkable. Some of the rocky hills are partly covered by thickets, and on the banks of the larger streams, especially to the north of Las Minas, willow trees are not uncommon. Extremely level countries, such as the Pampas, seldom appear favourable to the growth of trees. It has been inferred with much probability, that the presence of woodland is generally determined by the annual amount of moisture; yet in this province abundant and heavy rain falls during the winters; and the summers, though dry, is not so in any excessive degree. We see nearly the whole of Australia covered by lofty trees, yet that country possesses a far more arid climate. Hence, we must look to some other unknown causes.”(Charles Darwin, 1839, *Voyage of the Beagle, Chapter 3*)

As observed by Charles Darwin, vegetation assemblages in savanna ecosystems are dynamic and spatially heterogeneous (Jeltsch et al., 1998). Which factors, and to what extent vegetation structure is constrained, has long been debated. It has been shown that multiple interacting factors such as climate, fire, herbivory, hydrology and topographic factors govern the spatio-temporal variability and dynamics in savannas (Tinley, 1982; Bond, 2008). These factors dominate vegetation structure at multiple spatial scales (Figure 1.1), and result in varying vegetation patterns at micro, landscape and regional scale (Gillson, 2004).

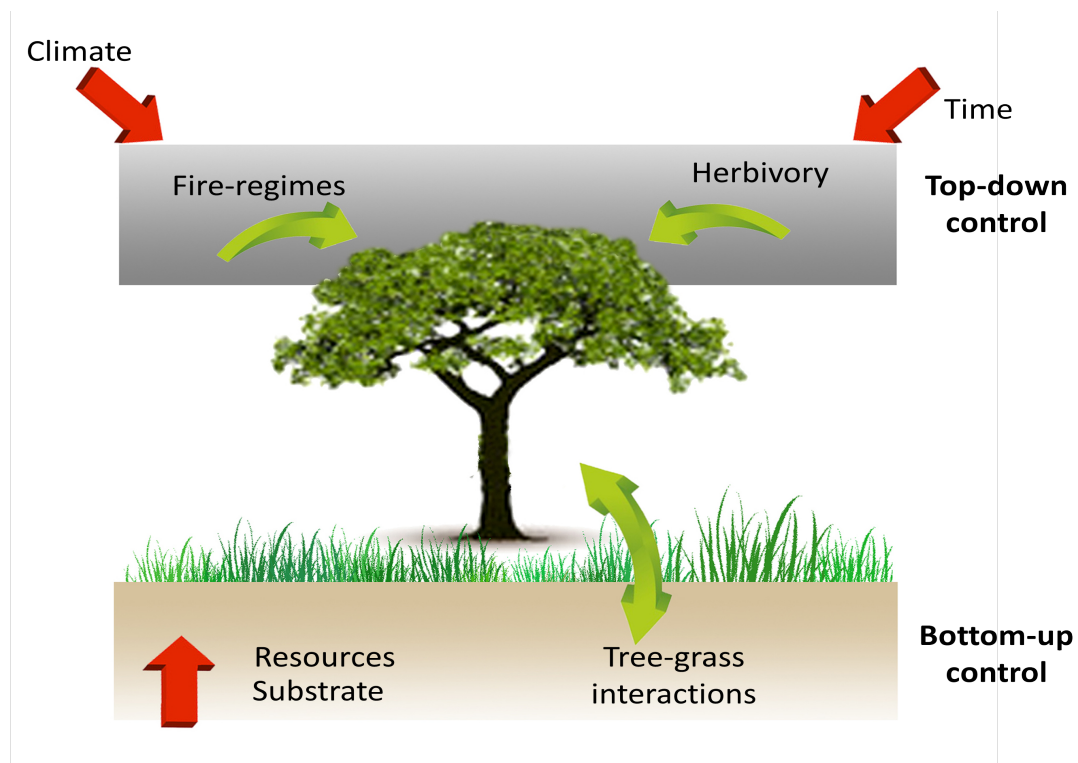


Figure 1.1: Conceptual chart of biotic and abiotic factors influencing savanna vegetation structure at various scales. The outer box represents the boundary of savanna ecosystems, with climate, topography and substrate controlling ecosystem structure at larger scales, while interactive controls depicted inside the box act at smaller spatial scales.

1.2.1 Climate

In the arid and semi-arid regions, where savanna ecosystems mostly occur, climate and vegetation links are governed through the dynamics of rainfall. Rainfall events regulate the availability of soil moisture, growth of woody vegetation, and determine the maximum carrying potential of tree cover at a given site (Woodward et al., 2004). A broad continuum of rainfall range supports the existence of mixed tree-grass compositions (Lehmann et al., 2011), spanning from low canopy cover in dry Serengeti grasslands of Africa (300 mmyr^{-1}) and intermediate canopy cover Oak savannas of northern California (605 mmyr^{-1}) to high canopy cover in wet mixed tree-grass communities of the *cerrado* in South America (1500 mmyr^{-1}).

Analogous to the occurrence of savannas in diverse rainfall regimes, one could question whether there is a rainfall threshold which determines the mixed tree-grass composition existence. Sankaran et al. (2005), drawing on information from sites across Africa, spanning a broad rainfall gradient, identified savanna regions receiving a rainfall in the range of $150\text{-}650 \text{ mm yr}^{-1}$ support a stable mixture of trees and grass layer, as water limitation prevents occurrence of closed canopies. Within this range, tree cover increases linearly with the rainfall (Figure 1.2a), and attains maximum canopy cover at 650 mmyr^{-1} . In contrast, savannas residing in regions with rainfall greater than 650 mm yr^{-1} , become

unstable systems and are likely to have closed canopies. A similar recent observation by Staver et al. (2011), highlighted the variations of tree cover across sub-Saharan Africa, where a bimodal distribution along the rainfall gradient was observed, with presence of savanna in the regions that received rainfall less than 1000 mm yr^{-1} , while regions receiving 2000 mm yr^{-1} were forest systems (Figure 1.2b).

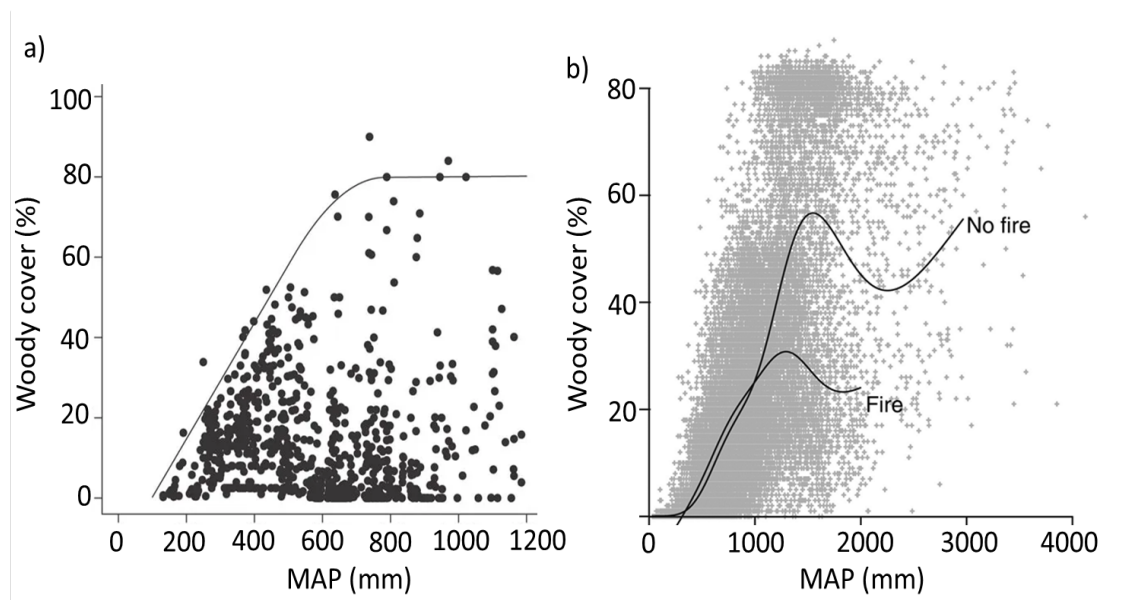


Figure 1.2: (a) Derived relationship between woody cover and mean annual precipitation (MAP) at African savanna sites (Sankaran et al., 2005) (b) Woody cover estimates for Africa showing a bifurcated distribution with fewer sites in the 50-70% (Staver et al., 2011).

1.2.2 Fire regimes

How do savanna ecosystems attain stable mixed tree-grass compositions in a high rainfall region? The disturbance based models, proposed by Higgins et al. (2000) and Sankaran et al. (2005), explain the positive disturbance feedback mechanism for the bi-modality (Figure 1.2b) and suppression of closed canopies across high rainfall regions. Herbivory, severe wind-storms and fire regimes are key disturbances which frequently affect the vegetation structure in savannas, while at the same time maintaining stable mixtures of trees and grasses (Levick & Asner, 2013; Bond & Keeley, 2005; Platt et al., 2002).

Fire is one of a suite of drivers which is indelibly etched in savanna ecosystems for billions of years (Brain & Sillert, 1988), occurring naturally by lightning or more recently through human activities for fuel wood and livestock grazing (Scott, 2000). The high flammability of savannas emanate from prolonged dry seasons combined with dead fuel accumulation which forms conditions conducive to the initiation and spread of fires. In the last 100 years, fires have been used as a management tool in savannas, for maintaining vegetation in a more open state than otherwise would occur (Parr & Andersen, 2006). From studies in different savanna systems around the world, we know that fires affect plant communities by influencing the size-class structure, woody vegetation biomass, and composition. Some

studies have shown that fire regime effects are minimal (1% decrease in canopy cover) in arid savannas, while fires in mesic savannas result in a 23% decrease in cover (Bucini & Hanan, 2007). This suggests that fire effects on vegetation structure can not be considered in isolation, and are rather governed by climatic context (Lehmann et al., 2011). The fire-rainfall synergistic effect on vegetation observed in these studies emerge from coarse scale analysis of vegetation patterns. Hence, quantitative analyses that take into account fire frequency manipulation over longer time periods are needed to thoroughly characterize the influence of fire on savanna vegetation heterogeneity.

The consequences of fire for vegetation structure at micro to landscape scales are regulated by the intensity, season and frequency of fire (Gill, 1975). For example, savanna fires are fuelled by grass biomass, so rainfall conditions and soil fertility favorable to grass growth could increase the fire intensity, thus limiting tree populations (Archibald et al., 2010). Conversely, rainfall conditions may increase the moisture level of fuel-load, which inhibits fire intensity and allows more trees to escape the fire (Bond, 2008; Staver & Levin, 2012). Similarly, effects of fires on vegetation structure of savanna ecosystems vary with the frequency of occurrence. Fires of high frequency limit the transition of tree saplings to adult size classes through a “fire-trap” mechanism, where tree saplings are forced to smaller height class woody re-sprouts (Higgins et al., 2000). Fires occurring at longer time intervals can be more intense, causing a direct decline in the canopy cover of woody vegetation, and are accompanied by slow demographic changes. Clumping in form of multi-stem trees and shrubs is one such demographic change (Grady & Hoffmann, 2012), which is hypothesized as a defence mechanism against fire (Scholes & Archer, 1997). Whether longer fire return intervals pave the way for increased woody biomass or modify the structure to more denser canopies needs deeper exploration.

Despite the general acceptance of fire regimes in stabilizing the tree-grass ratio, the emissions resulting from fire regimes remain a major concern. Approximately 85% of the global savanna lands burn annually (Andela et al., 2017), releasing 1341 *Tg* of carbon annually in the atmosphere (Van Der Werf et al., 2017). These emissions are strongly influenced by the season of burning. For instance, mean monthly fire emissions for 15 year time period (2000-15) were 40% higher in the late dry season than early dry season burning (Lipsett-Moore et al., 2018). Currently, although there is a considerable effort in shifting the burning period to the early dry season in some systems, which can help to abate carbon emissions (Russell-Smith et al., 2013), there is limited evidence to the effects of modulating fire frequencies in late dry season.

1.2.3 Substrate and topography

Tree-grass mixtures are also driven by the variability in soil texture, which mediates the hydraulics - run-off, infiltration, water retention and evaporation of the rainfall water (Rodríguez-Iturbe & Porporato, 2007; Fernandez-Illescas et al., 2001; Colgan et al., 2012). The inverse texture hypothesis proposed by Noy-Meir (1973), relates the effect of soil texture in arid and semi-arid systems on woody cover. This hypothesis suggests that

a dry region with coarse sandy soil will support more canopy cover. One belief for the hypothesis is that coarse sandy soils allow for deeper percolation of soil water due to capillary movement, which can be accessed by the trees during the period of dry season (Holdo, 2013). Conversely, fine textured soils have higher water retention capability, but when they dry out, moisture clings to the tightly bound clay particles, exacerbating water stress for the vegetation, and keeping the woody cover low (Fensham et al., 2015). On the contrary, in wet regions, coarse soils are more vulnerable to run-off and leakage due to low infiltration (Xu et al., 2018). The inverse texture hypothesis thus postulates that in wet regions, more woody trees persist in the fine textured soil landscapes.

Substrate properties in combination with topography such as hillslopes further amplify the savanna vegetation patterns by modifying the nutrient availability across the slopes (Colgan et al., 2012). For instance, during rainfall events on sandy soils, downslope movement of rainwater can carry salts and clay at the foot-slope. This accumulation of salts at the foot-slope, result in the formation of impervious sodic B horizons and seasonal water-logging, which keeps the woody cover low (Venter and Scholes, 2003). Regardless of the mechanism, tree-grass mixtures differ depending on edaphic conditions.

1.2.4 Tree-grass interactions

Another avenue by which vegetation pattern and composition in savannas emerges is through tree-grass interactions. The nature of tree-grass interactions can either facilitate or suppress plant growth forms, depending on ecophysiological characteristics of tree and grasses and resource requirements (light, water and nutrients). Water is a limiting factor in savannas, influencing subsistence mechanism for tree and grasses to coexist together. The success of tree-grass coexistence results from spatial partitioning of soil water by rooting depth i.e. utilization of top surface water by grasses, while trees persist by accessing water in the deeper soil layers (Walter & Burnett, 1971; Ward et al., 2013). Even though rooting depths of trees and grasses are spatially separated, grass layer can still compete with trees by up-taking a significant amount of water from upper soil, resulting in a reduced flow of water to deeper layers (Xu et al., 2015; February et al., 2013). This below ground competition in tree strata can be lessened by the large spatial expanse of lateral roots (Schenk & Jackson, 2002). Furthermore, grasses can reduce the growth and survival of woody seedlings, due to below and above ground competition for light, water and nutrients. In addition to below and above ground competition, tree-grass interactions can facilitate each other. For instance, trees may stimulate herbaceous layer growth by amelioration of harsh environmental conditions, nutrient enrichment, or increased resource availability (Pugnaire et al., 1996; Ludwig et al., 2004).

This overview indicates the wide range of biotic and abiotic conditions which shape the savanna vegetation structure. The strong interconnection between the factors is one of the main reasons why deciphering the extent to which different factors influence the ecosystem is so complex. Hence, studies which not only consider the isolated effects of these factors, but also examine the interactive effects, are required.

1.3 Woody encroachment and homogenization in savanna landscapes

Woody encroachment is a pervasive phenomenon occurring in savannas worldwide over the last century. It can be defined as proliferation of stem densities and biomass of woody plants, resulting in open canopy systems switching to impenetrable thickets. Increases in woody plant cover has been observed in savanna ecosystems of Africa, Australia, North and South America, Australia, Africa and southeast Asia (Stevens et al., 2017; Murphy et al., 2014; O'Connor et al., 2014). Expansion of woody thickets create homogeneous landscapes, which jeopardises the habitat suitability and biodiversity (Parr & Andersen, 2006). For example, in a study across cerrado savannas of South America that has been experiencing woody expansion for over 30 years, Abreu et al. (2017) reported a decline of 27% in plant species and a 67% loss of endemic species. An increase of woody vegetation globally across the savannas could be advantageous from a carbon sequestration perspective, but it may threaten the grazing potential of savanna landscapes, thereby affecting pastorals and subsistence farmers, and impact on biodiversity conservation.

The underlying causes of woody encroachment are the subject of considerable debate. Land-use changes via agriculture, urban development, suppression of fire and heavy grazing have been implicated as potential contributing factors (Wigley et al., 2010; Roques et al., 2001). The classic two-layer root niche separation Walter Hypothesis Walter & Burnett (1971) gives one possible explanation to this occurrence, suggesting that if the grass layer is removed e.g. from heavy grazing, it allows more water to percolate into deeper soil layers, which is preferentially used by woody plants. The spatial rooting niche separation is not ubiquitous at all the sites. For instance, there was no significant influence of changing herbaceous density on recruitment of *Acacia karoo* seedlings in an arid savanna (Du Toit, 1972). While, at some savanna sites, recruitment of the heavily encroaching species *Acacia mellifera* was found to be much more sensitive to rainfall than to grazing (Kraaij & Ward, 2006).

An alternate hypothesis proposes global drivers such as increasing atmospheric CO₂ concentrations as a possible explanation responsible for expansion of woody plants in savannas (Bond & Midgley, 2012). Rising CO₂ can drive woody expansion in savannas, through a number of mechanisms (i) elevated CO₂ preferentially favours C₃ synthesis relative to C₄ grass layer, thus increasing the growth of woody plants, (ii) rising CO₂ reduces the transpiration rate of grasses, causing more water to percolate in deeper soil layers for the woody plant growth and (iii) faster escape of juvenile trees from the fire-trap.

A fire regime of higher frequency and intensity is a potent agent in combating woody encroachment. Late dry season infrequent fires, which are intense and much larger in spatial extent could be viewed as an opportunity to lessen the woody proliferation. Consequences can be seen as positive or detrimental depending on the view point. For example, Higgins et al. (2012), showed that the effects of fire intensity were greatest for intermediate sized woody vegetation (1-5 m canopy height), while larger trees (>5 m height) faced negli-

ble probability of topkill. There is, however, also a view that because of the interactive effects of highly intense fire regimes and herbivory, savanna landscapes may experience a homogenization of the vegetation structure (Smit et al., 2016). Solutions to woody plant encroachment can not be contemplated from the fire regimes alone, but it should also incorporate rainfall and topography of the region, and how interactions between these factors retain the vertical structure of the vegetation.

1.4 Savanna vegetation structure estimation

The aforementioned sections briefly elucidate the dynamics and functioning of savanna ecosystems, and how climate and land-use changes accelerate the strong biophysical feedback. Appraising these changes rely on the accurate and detailed information about savanna vegetation structure and biophysical parameters at various scales.

Plot and transect scale manual vegetation measurements have been the foundation for vegetation surveys in savanna ecosystems for over 60 years (Herrick et al., 2005), which include measurement of vegetation height, fractional cover, biomass and plant species. With increasing recognition of carbon sequestration potential of savannas, vegetation surveys in savannas have expanded to long-term plot networks. Long-term plot scale inventories established in mixed tree-grass communities of South Africa (Biggs et al., 2003; Siebert & Eckhardt, 2008), northern Australia (Edwards et al., 2003), Brazilian cerrados (Moreira, 2000) and India (<https://lemonindia.weebly.com/research.html>) have enabled to study vegetation dynamics in response to drivers such as fire regimes, grazing and geology. Though long-term dataset are a valued asset for underpinning many land-management and policy decisions, vegetation biophysical metrics are constrained to much smaller spatial scales (<1 ha).

Remote sensing images are a key method to spatially characterize vegetation structure because of their synoptic view and recurrent mapping capabilities. Optical images are commonly available remote sensing data, consisting of multiple bands of data, which can offer different information on vegetation structure characteristics based on its spectral reflectance. Moderate to coarse resolution multi-spectral optical dataset from Landsat and MODIS sensors have been successfully used as a consolidated tool for estimating woody cover extent and changes (Gaughan et al., 2013; Gessner et al., 2013) in savanna ecosystems. Optical reflectances and their tree cover proxies such as EVI (Enhanced Vegetation Index) and NDVI (Normalized Difference Vegetation Index) are highly sensitive to the photosynthetic parts of vegetation, however in heterogeneous systems, it is difficult to separate woody cover from the grass layer due to spectral similarities between tree and herbaceous layer. It is possible to minimize this spectral ambiguity by utilizing multi-seasonal proxies that can capture the phenological differences between the two plant forms (Higginbottom et al., 2018; Lu et al., 2003; Roderick et al., 1999). In savannas, most woody vegetation shed their leaves in dry season, which decreases temporal variation in optical data derived proxies, as shrubs maintain leaves throughout the dry season

(Bucini et al., 2010). Besides this, capturing the phenological contrast between the two plant forms may be impeded by the rainfall and soil variability.

A number of fine resolution vegetation maps have also been generated from optical images at regional to global scales, such as the global vegetation continuous field product from Landsat sensor (Hansen et al., 2013). Often derived with less explicit local site information, these global Landsat resolution data are unable to provide accurate representation of vegetation metrics. Furthermore, these global products have limited use in savannas as the calibration procedure omits smaller trees ($<5\text{ m}$) and shrubs, thereby underestimating woody cover.

In contrast to optical dataset, Synthetic Aperture Radar (SAR) sensors, which operate in the microwave region ($1\text{mm}-1\text{m}$) of the electromagnetic spectrum, are not saddled by the mixed reflectances from trees and grasses, are instead sensitive to the vegetation structure including low biomass savanna systems (Santos et al., 2002). SAR systems actively transmit microwave energy at different wavelengths and measure the amount of energy that is returned to the sensor by the underlying vegetation and surface, also known as backscatter. In the microwave region, a combination of factors such as wavelength, dielectric constant and geometrical properties of vegetation elements permit such an interaction by SAR backscatter (Woodhouse, 2006). Moreover, in savanna systems, greater diversity in backscatter interactions are observed due to large variability in size, density and spatial distribution of vegetation. Previous studies on microwave backscattering at various frequencies and polarizations were found to be sensitive to savanna vegetation structure (Ryan et al., 2012; Mitchard et al., 2011; Lucas & Armston, 2007). In terms of wavelength, it is generally understood that longer wavelengths at L and P bands are more suitable for quantifying woody vegetation structure as the backscatter occurs mostly from branching elements and stems of the woody vegetation (Le Toan et al., 1992; Mitchard et al., 2009). However, at shorter wavelengths particularly X- band, radar energy attenuates quickly in the canopy, before interacting with stems and large branches.

Recent developments in open access SAR data streams from C-band Sentinel-1 (Torres et al., 2012) and L-band ALOS-PALSAR mosaics (Shimada et al., 2016) have made a step change in our understanding of savanna vegetation structure gradients across large scale. Both sensors have the capability of acquiring cross polarized (HV, horizontal sent-vertical received or VH, vertical sent-horizontal received) backscatter in addition to co-polarized (HH- horizontal sent-horizontal received, VV- vertical sent-vertical received) data. The enhanced data collection capabilities resolve trees and grasses distinctly, thus deciphering the conundrums of actual carbon storage potential of savannas.

SAR backscatter is not a direct measure of carbon storage or aboveground biomass of a system, but is governed by accurate and sub-optimal acquisition of reference vegetation biophysical parameters (canopy cover, height), that may be related to it. Most evidence for savanna biomass at larger scales stem from relating remote sensing proxies to plot-scale measured vegetation biophysical parameters. However, Staver (2018) points out predictions at plot scale ($<1\text{ ha}$), suffer from sample size limitations, due to variability in

vegetation cover and thereby are not representative of inherent heterogeneity in savannas. Apart from sample size limitations, several fundamental barriers, for instance, sparse, non-repeatable and biased site selection measurements preclude plot inventories to be an avenue for ascertaining savanna vegetation structure and trajectory at larger spatial scales. More objective validation and calibration methods at plot and landscape scale level can potentially increase the accuracy of remote sensing based products.

The current endeavours to accurately map vegetation structure at plot to regional scale are on the brink of technology revolution with the advent of LiDAR (light detection and ranging) (Lefsky et al., 2002; Dubayah & Drake, 2000). LiDAR is an active remote sensing technology that acquires high resolution 3D data by measurement of light scattering from vegetation layers. It therefore has the potential to curtail the uncertainties of in-situ measurements (Mascaro et al., 2011). 3D data acquired from LiDAR sensors consist of collection of spatially distributed points illuminated along the path of the laser, with each point representing the distance (range) between sensor and target. Current LiDAR systems measure distance by using time of flight mechanism, where elapsed time between emission of laser pulse from the sensor and time of detection at the sensor is measured. Another way of calculating distances is by estimating the phase difference between transmitted and received signal. These distance measurement are converted to a three-dimensional co-ordinate by using the location and orientation of the LiDAR sensor. In most of the vegetation mapping applications, pulse ranging LiDAR are employed, while CW LiDAR are seldom utilized. Additionally, LiDAR systems can also be classified based on return energy, namely discrete return, which records few returns from each laser pulse, and full waveform LiDAR, which captures the whole backscatter energy distribution (Wagner, 2010).

LiDAR focused studies have also exploited the use of intensity and shape of incoming laser pulses to identify target characteristics. For instance, at 1064 *nm* wavelength, in a vegetated landscape, it is possible to differentiate between green and brown biomass as high intensity laser pulses are retrieved from tree trunks, while clusters of leaves reflect lower intensity (Yao et al., 2011) laser pulses. This variation in intensity of returns allows for quantifying distribution and density of canopy elements (Moffiet et al., 2005), which gives LiDAR remote sensing an edge over other mapping capabilities. While LiDAR has a demonstrated capacity to support vegetation inventory and monitoring, most work has been focused on temperate conifer and tropical forest ecosystems, with limited research in savanna ecosystems.

LiDAR data utilization for savanna vegetation structure mapping date back to early 2000s, with most 3D measurements acquired from large footprint (>10 *m*) spaceborne and airborne platforms. Height metrics from large footprint sensors have proven to be significantly correlated with basal area, aboveground biomass and carbon density of savannas, owing to the volumetric nature of 3D measurements. Examples include, Gwenzi & Lefsky (2014), showed the capability of waveform LiDAR to assess vegetation heights in Oak savannas from large footprint GLAS (Geoscience Laser Altimeter System) on-board

ICESat (Ice, Cloud, and land elevation satellite). Goldbergs et al. (2018), demonstrated that canopy height metrics derived from Riegl LMS-Q560, a full waveform airborne LiDAR sensor, correlated to estimates of aboveground biomass across a tropical savanna. Yet, vegetation in savannas vary widely in structure, composition and architecture, large footprint LiDAR are unable to resolve the structure of shrubs beneath the canopy.

Terrestrial LiDAR or Terrestrial laser scanner (TLS) is a ground based LiDAR technique which produces highly dense uninterrupted 3D point cloud within millimetres of accuracy (Disney et al., 2018). Figure 1.3 shows an example of TLS data from a South African savanna, acquired during the late dry season. TLS has revolutionized the measurement capacities from three-dimensional vegetation structure - mean we are now able to identify and measure the vegetation dimensions unbiased from vegetation structure, distribution and composition. Therefore, TLS estimates can potentially reduce the uncertainties in terrestrial carbon stocks of savannas and enable improved calibration and validation of satellite biomass products.

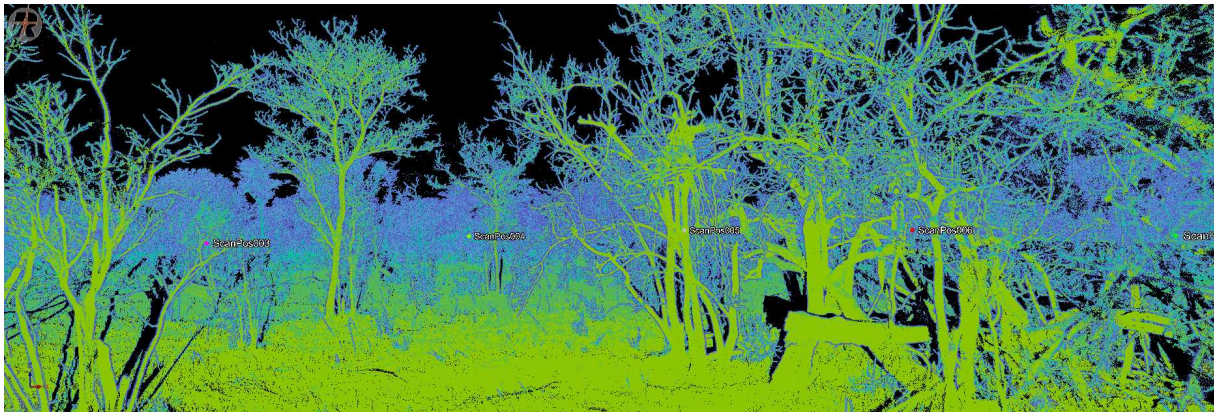


Figure 1.3: Illustration of terrestrial LiDAR data captured in South African savanna and coloured according to amplitude. Amplitude is higher for the woody component than the photosynthetic part of the vegetation.

For application of TLS in the field, it is placed 1-2 *m* above ground and vegetation is scanned from multiple locations to capture hectare scale, consistent and greater point clouds (Wilkes et al., 2017). As the 3D dataset are very large, converting to tree and plot scale biophysical properties is a major challenge. Several approaches have aimed to measure key structural metrics at plot scale in forest ecosystems, such as canopy cover, tree locations, stem density and canopy height (Côté et al., 2012; Dassot et al., 2012; Pueschel, 2013). Tree level structural attributes can be inferred by reconstructing detailed structure of trees, which provides more accurate estimation of volume and biomass (Raumonen et al., 2013; Hackenberg et al., 2015). For heterogeneous savanna vegetation, such reference dataset from TLS are currently unavailable. Few studies in dryland sagebrush steppe ecosystem of western United States have demonstrated the potential of TLS in quantifying shrub canopy volume using 3-D convex hull approach (Olsoy et al., 2014).

It is clear from this review that remote sensing imagery acquired from terrestrial, air-borne or spaceborne platforms have emerged as a vital tool for monitoring and mapping vegetation structure across ecosystems. The complexity, and consequent difficulty with mapping of savanna vegetation structure demands that we establish a better synergy of these available dataset, their spatial scales and at the same time reducing the known uncertainties.

1.5 Aims and research questions

The main objective of this thesis is to examine woody vegetation structure subject to land-management and environmental controls in the semi-arid savannas of South Africa. This thesis also showcases the utility of high resolution 3D data from TLS and Radar remote sensing dataset in the context of mapping and monitoring savanna vegetation. Three broad research questions with sub-research questions are addressed in this thesis and are outlined below. Figure 1.4 describes key topics covered in each research objective and dataset requirements.

(i) Objective 1 - Analyzing vegetation structure and spatial organization across fire-regimes

The role of fires as the main driver of vegetation dynamics in savannas, maintaining the equilibrium between grasses and trees has been documented in several previous studies. However, studies of the variation in vegetation structure by fire occurrence have been limited to transect scale analysis, with a limited reliability in documenting whole horizontal and vertical vegetation structural change. My research uses high resolution 3D point cloud data from TLS across South African savannas for more enhanced understanding of vegetation structure change subjected to long-term fire-treatments. The use of TLS data, further enabled the derivation of vertical plant profiles, documenting the level of landscape homogenization in savannas. By linking variation in woody cover, height, biomass and vertical profiles to fire management strategies across climatic and geologically different sites in *Chapter-3*, we expand our understanding of the role of fires in shaping woody communities and carbon sequestration potential of savanna systems. In particular, the following research questions are addressed in *Chapter-3* of this thesis:

- *How vegetation structure and above-ground carbon storage respond to increasing fire frequency?*
- *How does the effect of fire-regimes vary across plot and landscape scale?*
- *Do differences in rainfall and geology interact with fire-regimes in altering vegetation structure?*

The results and discussions on the above mentioned research questions can be found in section 3.3 and 3.4.

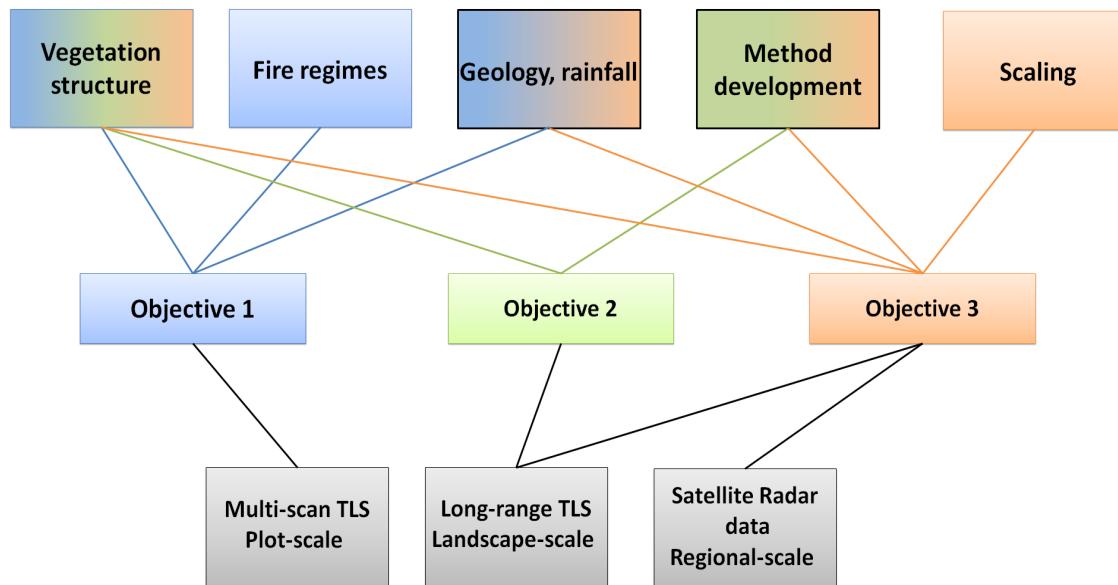


Figure 1.4: Framework demonstrating the link between the objectives resulting from this dissertation. Upper boxes show the different topics and links studied in this dissertation. Colored boxes in the middle indicate objectives in this dissertation. Grey boxes in the bottom row indicate different data types and methodologies applied in the different objectives.

(ii) Objective 2 - Characterizing savanna vegetation structural attributes at landscape scale - method development

Chapter-4 analysis was performed at plot scale (7 ha), with 3D dataset generated from multiple TLS scanning locations. However, the heterogeneity in woody vegetation structure also varies along hillslopes to landscape scales. At present, most landscape to regional scale savanna vegetation mapping rely on extrapolating limited field inventory data comprising of height, canopy cover and diameter. The often very limited availability of field inventory data in savannas lead to errors related to the landscape scale representation of these sampling plots. In general, field inventory data should meet the following demands: (i) minimal effort, and (ii) Capture several hectares of vegetation structure with high precision.

While TLS data provides detailed representation of the vegetation structure, TLS does not provide regional or landscape scale 3D data. The development and availability of high precision, long-range TLS (LR-TLS) can provide 3D data at much larger scales. This can lead to the easy deployment and overcome sample size limitations that primitive TLS scanning suffers from. Such a method suggests for application in savannas, where there are sparse records of accurate vegetation inventory data. The specific issues to the application of LR-TLS in extracting savanna vegetation structure are dealt in *Chapter-4*:

- How do structural measurements from LR-TLS degrade with distance from scanner?
- What are the distances over which LR-TLS can reliably extract 3D structural char-

acterization?

- *What are the implications of LR-TLS approach in vegetation monitoring?*

The results and discussions on the above mentioned research questions can be found in section 4.3 and 4.4.

Objective 3 - Assessing spatial patterns of woody structure in a savanna system with earth observation data

To date studies investigating woody vegetation structure at regional and landscape scale in savanna ecosystems, have been limited by the accurate ground data for the calibration and validation of satellite derived AGB datasets. The ground reference data are collected at different height thresholds over sparsely distributed small size plots (<1 ha), from which estimations of aboveground biomass and carbon are based. This leads to the following problems: (i) No meaningful validation- due to sparse distribution of sampling plots, (ii) vegetation products from different field data sources are hard to compare, and (iii) uncertainties are not well defined. Therefore, the aim of *Chapter-5* is to improve the estimates of woody vegetation structure at regional scales using the thoroughly investigated LR-TLS for calibration and validation of Radar satellite data. In this part of the thesis, the following research questions are addressed:

- *What is the sensitivity of Radar backscatter at two wavelengths (C and L band) to long-range scan derived biomass and canopy cover?*
- *How do differences in height thresholds impact the accuracy of woody vegetation structure estimations?*
- *What is the spatial variability of vegetation structure across the landscapes?*

The results and discussions on the above mentioned research questions can be found in section 5.3 and 5.4.

1.6 Outline of the thesis

The thesis consist of six chapters, including this introductory chapter and a brief study site and instrumentation description (Chapter 2). Chapters 3 to 5 provide answers to the research questions presented in section 1.5, and outline of chapters with their overarching goal is presented in Figure 1.5

Chapter 3 examines the effect of sixty-three years of experimental burning on woody cover, height, carbon storage and vertical vegetation structure across savanna sites embedded in a rainfall and geological gradient. The central aim of this chapter is to disentangle the vegetation responses to increased late-dry season fire-regimes. Understanding vegetation, fire and climate dynamics is important for the effective carbon management in savanna landscapes. Thus, this chapter recommends fire regime strategies according to the climate of the site.

Chapter 4 introduces an approach to estimate savanna woody vegetation at landscape to hillslope scale from Long-range TLS. This approach was tested on two distinct savanna sites and validated with thirteen reference measurements.

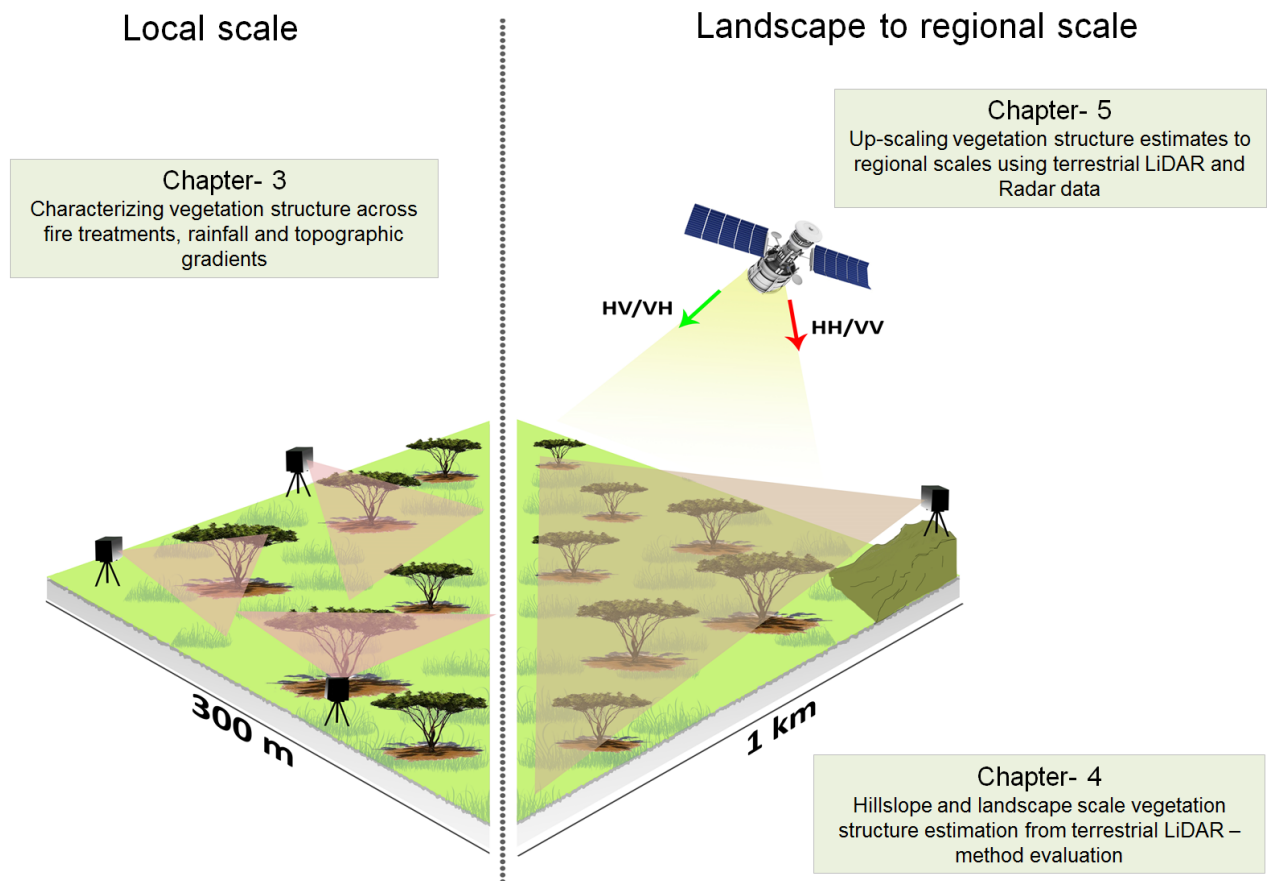


Figure 1.5: Conceptual representation for the chapters of this thesis in relation to the main objectives and research questions across various spatial scales. Figure style adapted from Schimel et al. (2019).

Chapter 5 adapts the methodology from Chapter-4 to estimate the landscape scale vegetation estimates from point clouds. With vegetation metrics extracted from 900 *ha* data, extrapolation to regional scale was achieved by using Radar data.

Chapter 6 summarizes the major findings of this thesis and later these findings are discussed in relation to the research questions. This chapter also gives a brief overview of the future directions in the savanna ecology with the 3D dataset acquired during this PhD work.

Each thesis aim chapter (3 to 5) consist of it's own introduction as well as method section, as these chapters have different research objectives. Also, these chapters correspond to complete manuscripts for submission to peer-reviewed journals. This might lead to some repetitions of the introductory material.

Chapter 3 was published in *Ecosphere*¹, chapter 4 was published in the *International*

Journal of Applied Earth Observation and Geoinformation², and chapter 5 will soon be submitted for publication³.

¹Singh, J., Levick, S. R., Guderle, M., Schmulius, C., & Trumbore, S. E. (2018). Variability in fire-induced change to vegetation physiognomy and biomass in semi-arid savanna. *Ecosphere*, 9(12), e02514.

²Singh, J., Levick, S. R., Guderle, M., & Schmulius, C. (2020). Moving from plot-based to hillslope-scale assessments of savanna vegetation structure with long-range terrestrial laser scanning (LR-TLS). *International Journal of Applied Earth Observation and Geoinformation*, 90, 102070.

³Singh, J., Saatchi, S. S., Levick, S. R., Guderle, M., Berger, C & Schmulius, C. Explicit woody canopy characterisation for improved remotely sensed observations of above-ground biomass in semi-arid savanna. (*In preparation*)

Chapter 2

Study site and instrumentation

2.1 Study Area

The study area of this thesis work is the semi-arid savanna landscapes of Kruger National Park (KNP), South Africa (23°98'S, 31°55'E) (Figure 2.1). KNP is a national reserve located in north-eastern South Africa that covers an area of almost 2 million ha. The park encompasses broad ecological gradients, from semi-arid semi-arid north (400 mm mean annual rainfall) to the mesic south (750 mm mean annual rainfall) (MacFadyen et al. 2018). The long-term MAP is 506.6 mm, where rain occurs mostly between October and March. Along with the rainfall gradient, KNP has a longitudinal geological gradient, with granites being dominant in the west which weathers to sandy soils while soils in the east are clay rich derived from basalt geology (Venter, 1986). The terrain in KNP is fairly flat (average slope $1.6 \pm 2.5^\circ$) with few geological formations in the southwestern corner and eastern border.

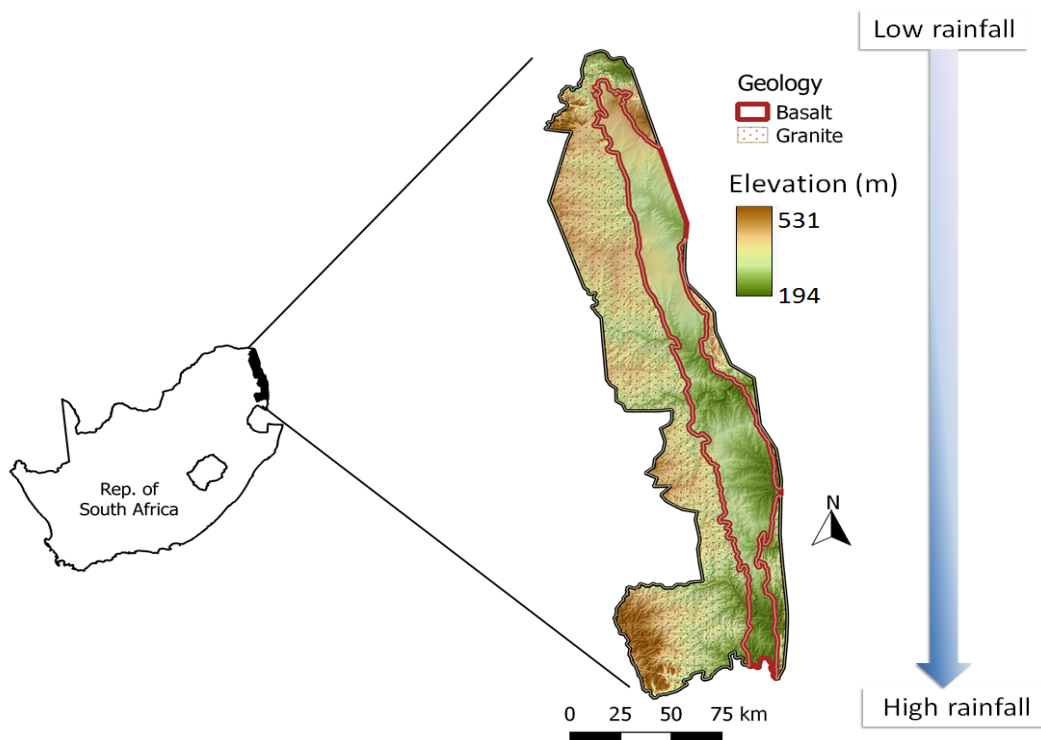


Figure 2.1: Location of the KNP with longitudinal geomorphological division and north-south rainfall gradient.

KNP is comprised primarily of sub-tropical wooded savannas, and consist of diverse range of vegetation namely, mopane (*Colophospermum mopane*), knobthorn (*Acacia nigrescens*), marula (*Sclerocarya bierra*), *Combretum* species, sicklebush (*Dichrostachys cinerria*) and silver cluster-leaf (*Terminalia sericea*) (Gertenbach, 1983). Vegetation height falls in the 2-8 m range, with vegetation taking up the form of single or multi-stemmed physiognomy.

This work is comprised by three subprojects that were conducted in distinct sites of KNP:

Analyzing vegetation structure and spatial organization across fire-regimes (Chapter 3), characterizing savanna vegetation structural attributes at landscape scale - method development (Chapter 4) and assessing spatial patterns of woody structure in a savanna system (Chapter 5). Detailed site, data descriptions and processing are found in the research objectives chapters.

2.2 Woody vegetation data

2.2.1 Terrestrial laser scanning-3D data

Woody vegetation data for KNP was acquired using Riegl VZ-2000 terrestrial laser scanner (TLS) during the dry season period of October 2016 (Figure 2.2). Riegl VZ-2000 scanner covers a vertical field of view of 100° ($+60^\circ/-40^\circ$) and a 360° horizontal frame scan, with a measurement rate up to 400000 points per second (Table 2.1) at 1 *MHz* pulse repetition rate. At the study site, two scanning mechanisms were adopted (i) multiple scanning consisting of 15 scans, to achieve a complete and objective coverage of all trees and shrubs (explained in detail in Chapter 3 section 3.2), and (ii) long-range single scans, to map landscape scale vegetation structure (explained in detail in Chapter 4 section 4.2). Instead of relying on the reflectors for the co-registration of 3D scans, the work in this thesis utilises dead trees, branch nodes and tips as tie points for merging the scans together. Normally, a set of 6 tie points were matched in every scan. Afterwards, the multi scans were registered using Riegl's proprietary software RiSCAN PRO (<http://www.riegl.com>). The overall registration accuracy between the merged scans was 0.01 *m*. Subsequently, all acquired data were further georeferenced to the coordinate system UTM 36S. Such transformation was useful for calibrating and validating spaceborne data with the derived vegetation metrics from TLS.

Table 2.1: Specifications of Riegl VZ-2000 laser scanner (Data source Riegl VZ-2000 data sheet).

Specifications	Riegl VZ-2000
Max. vertical field of view ($^\circ$)	100
Max. horizontal field of view ($^\circ$)	360
Accuracy (mm) at 150m range	8
Points per sec (max)	396000
Beam divergence (mrad)	0.3
Max. resolution ($^\circ$)	0.0015

2.2.2 Earth observation data

The work in this thesis relies on earth observation dataset from L-band ALOS-2 PALSAR-2 and C-band Sentinel-1 SAR sensors. These dataset were mostly utilized to extrapolate the patterns of savanna vegetation from landscape to regional scale, and to determine how varying height thresholds can impact the accuracy of mapping. More details can be found in Chapter 5 section 5.2. The following text gives a brief introduction of the SAR



Figure 2.2: Riegl VZ-2000 terrestrial laser scanner at a terrestrial vantage point in KNP.

dataset.

ALOS-2 PALSAR-2

ALOS-2 PALSAR-2¹ is acronymed for Advanced Land Observing Satellite, which is a L-band (23.5 cm) SAR wavelength sensor on-board Japanese Aerospace Exploration Agency (JAXA). PALSAR-2 is a successor of PALSAR sensor and became operational in the year 2014. PALSAR-2 provides data in a dual (HH and HV) and full (HH,HV,VH and VV) polarizations in scanSAR (swath width: 250-300 km), fine beam single polarization (FBS) (swath width: 40-70 km), fine beam dual polarization (FBD) (swath width: 40-70 km) and full polarimetric (swath width: 20-60 km). The revisit period for PALSAR-2 is 14 days. For the work in this thesis, dual pol FBD scenes in HH and HV polarization with an incidence angle between 28.6 ° to 32.9 ° were acquired. The study area is covered by four scenes: two from November 8, 2015, and two from December 1, 2015. All images were acquired in ascending mode and SLC (Single look complex) data form. Since the cumulative precipitation for November and December in year 2015 was below the average rainfall in previous years, we assume SAR data will have minimum influence of soil moisture. Five processing steps were performed on SLC SAR data- (i) multi-looking, for achieving square pixels on ground (1 look Range x 5 Azimuth), and derive backscatter intensity, (ii) radiometric calibration with a sensor specific calibration factor of -83 dB, (iii) geocoding using 20m digital elevation model (DEM), and (v) topographic normalization.

¹In some sections of the thesis ALOS-2 PALSAR-2 SAR sensor has been written as PALSAR-2 or ALOS PALSAR-2.

Sentinel-1A

Sentinel-1 is a C-band (5.5 cm) SAR system consisting of two satellite system, which orbit 180°, launched in 2014 and 2016 respectively. Sentinel-1 acquires data in four different modes namely stripmap (SM), interferometric wide swath (IW), extra wide swath (EW) and wave mode (WV). SM, IW and EW modes acquire data in dual polarization (<https://directory.eoportal.org/web/eoportal/satellite-missions/c-missions/copernicus-sentinel-1>). For this study, SAR data acquired in IW mode in dual polarization (VV and VH) are used. Altogether, 5 scenes in October 2015 were used in this study. Scenes were downloaded and post-processed in Google Earth Engine (<https://developers.google.com/earth-engine>). Google earth engine uses pre-processing steps implemented by the Sentinel-1 toolbox (<https://step.esa.int/main/toolboxes/sentinel-1-toolbox>) to derive backscatter coefficient. The processing steps were - (i) border and thermal noise removal, (ii) radiometric correction, and (iii) terrain correction. The final products were resampled to a resolution of 20 m.

This chapter briefly introduced the data requirements for the research objectives performed in this thesis work. Detailed 3D and spaceborne data processing methods can be found in the respective research objective chapter, where different scanning mechanisms, statistical analysis and calibration and validation of spaceborne data are explained in detail.

Chapter 3

Effects of fire regimes on savanna vegetation structure - A local scale analysis

This chapter is originally published as:

Singh, J., Levick, S. R., Guderle, M., Schullius, C., & Trumbore, S. E. (2018). Variability in fire-induced change to vegetation physiognomy and biomass in semi-arid savanna. *Ecosphere*, 9(12), e02514. The publication is available at <https://esajournals.onlinelibrary.wiley.com/doi/epdf/10.1002/ecs2.2514>. **Copyright** ©2018 The Authors. This is an open access article under the terms of the Creative Commons Attribution License, which permits use, distribution and reproduction in any medium, provided the original work is properly cited.

Abstract

Fire plays an intrinsic role in shaping the biophysical attributes of savanna ecosystems. Savanna fires limit vegetation biomass below their climatically determined potential, but the magnitude of this effect and how it varies across heterogeneous landscapes is poorly understood. In this study, we explore woody tree structure and canopy characteristics across a fire manipulation experiment that has been maintained for 63 years in South Africa's Kruger National Park (KNP). Our study design assessed three late dry-season fire regimes (biennial, triennial and unburnt) across a precipitation gradient (737 - 496 mm yr^{-1}) spanning four different landscapes with a mixture of sandy and clay soils. We used terrestrial laser scanning (TLS) to quantify tree height, canopy cover, and above-ground carbon storage across the experimental treatments. Vegetation physiognomy was influenced by the interaction between landscape and fire frequency. In the absence of fire, woody height, cover and biomass increased with increasing rainfall. The presence of fire acted to reduce structure and biomass as expected, but the magnitude of this effect increased with increasing rainfall. We found minimal difference between the effects of biennial or triennial burning - except at the wettest site where the triennial fire plots had half the biomass of those burnt biennially. The rainfall dependent fire-vegetation relationships shown here provide empirical quantification of top-down constraint by fire and highlight the challenges of predicting responses to disturbances in these inherently heterogeneous ecosystems. Robust quantification of 3D structure and dynamics through terrestrial laser scanning will be useful for constraining carbon stock models and predicting trajectories of change under future climate and land-use conditions.

3.1 Introduction

Savannas cover roughly 20% of the world's dry tropical landscapes (Scholes & Archer, 1997; Murphy et al., 2015). They are critical to the regulation of the terrestrial carbon cycle and contribute 30% of global net primary production (Grace et al. 2006). Savanna ecosystems are characterized by a mixed physiognomy that includes a continuous grass layer mixed with variable amounts of woody cover (Sankaran et al. 2008). Because of the contrasting response of the two coexisting plant guilds (trees and grasses) to environmental and climatic variables such as water and light availability, and rising CO₂ concentration and temperature, it is challenging to isolate the effects influencing the relative abundance of these co-occurring life forms. Classical ecological theory such as Walter two-layer hypothesis, predicts the equilibrium coexistence of trees and grasses due to spatial niche separation, and assumes that grasses use subsurface water while, trees have access to deeper water reserves (Walter & Burnett 1971; Ward et al. 2013). In addition to water availability, tree-grass co-existence has been ascribed to the stochastic interactions between edaphic conditions and consumer control (herbivores and fires) (Coughenour & Ellis, 1993; Scholes & Archer, 1997; Bond & Keeley, 2005; Levick & Rogers, 2011), however an ecological explanation for the observed savanna structural intricacy that unites the characteristics of these factors in space and time is still not available.

Fire exerts strong control on savanna structure, and modification of fire regimes influences the functioning of savanna vegetation communities (Moreira 2000; Bond et al. 2005; Govender et al. 2006; Higgins et al. 2007; Smit et al. 2010; Levick et al. 2012). Fire driven structural changes occur at multiple scales, altering vertical canopy height distributions and plant basal area at the local scale, and changing the tree-grass balance at landscape scales. These hierarchically nested structural variations have important implications for ecological processes, including changes in carbon stocks (Bond et al. 2005; Higgins et al. 2007), nutrient cycling (Pellegrini et al. 2015), hydrology, (Asner et al. 2004; Savadogo et al. 2007) and wildlife habitat availability (Parr & Andersen 2006). Therefore, studying the effects of prevailing fire regimes on vegetation structure is integral to understanding the current changes occurring in these ecosystems, such as loss of large trees and increased shrub thickening (Levick & Asner, 2013), and for forecasting ecosystem response under changing climate and land-use scenarios.

Natural and anthropogenic fires in savanna ecosystem account for the vast majority of global burned areas, with 20% burnt annually (Dwyer et al. 2000; Lehmann et al. 2014), thus reducing the substantial dry matter (Scholes et al. 1996). Numerous studies corroborate that fire mostly reduces woody biomass and the absence of fire could potentially transform these landscapes into closed woodlands (Van Wyk 1971; Bond et al. 2005). A four decade fire manipulation study across the savannas of Kruger National Park, South Africa, showed that total fire suppression allowed significant increases in woody biomass; lower fire frequency regime caused smaller increases, but more frequent fires resulted in greater losses of woody biomass (Higgins et al. 2007). Similarly, Australian estimates suggest that while the net ecosystem productivity in savannas without fire is 3 MgC

$ha^{-1}yr^{-1}$, it is only $1 MgC ha^{-1}yr^{-1}$ with fire (Williams et al. 2004), as well as tree diversity of mesic savannas in Australia increases where fire is excluded (Lawes et al. 2011), with few species typically associated with rainforest (Williams et al. 2003). Significant changes in fire regimes could therefore potentially lead to a biome switch.

Fire limits woody plant demography through its impact on seedling recruitment, growth and topkill (Higgins et al. 2000; Bond & Keeley 2005; Hanan et al. 2008). Topkill in tree saplings prevents them from escaping the zone of influence of grass fuelled fires, thus causing multi-stemmed morphology and reducing the number of larger size classed individuals (Enslin et al. 2000; Jacobs & Biggs 2001). Similarly, even with some large individuals topkill can cause considerable loss of biomass, which can not be quickly regained (Hoffmann & Solbrig, 2003). The capacity to resprout depends on the interactive effect of characteristics of the fire regime i.e. frequency, season and intensity (Gill, 1975), bud availability and their level of protection, and availability of resources (nutrients and water) (Clarke et al., 2012). Resprouting increases with increasing soil fertility and moisture gradient which causes canopy and understorey closure rapidly after fire events (Clarke et al. 2005). In wet (high-rainfall) savannas, where tree-grass competition is reduced due to water availability, trees can potentially escape the flame zone and gain taller canopies despite high fire frequency (Levick et al. 2012; Lawes et al. 2011). On the other hand, lower fire frequencies can result in more intense, destructive burns due to greater accumulation of fuel load (Govender et al. 2006).

Burn intensity can be experimentally manipulated by selecting the season of the fire, as well as the return frequency. Early dry season fires are of low intensity and less extensive, while late dry season burns often produce high intensity fires (van Wilgen, 2009). High intensity fires can be very effective at reducing encroachment by woody shrubs in the wet savannas, which opens up the landscape but at the same time such practices result in the loss of large trees (Smit et al. 2016). Further, the effects of fire regimes on vegetation structure can vary with geological substrates, through the differential soil and vegetation patterns that they give rise to (Levick et al. 2012; Smit et al. 2010). In addition, the vegetation-fire dynamics can be regulated by herbivory which alters the fuel loads, thereby collectively shifting savanna landscapes towards either grassland or woodland (Asner & Levick 2012; Pellegrini et al. 2017). However, it is often difficult to characterize the relative effects of herbivory from other ecological processes, leading to uncertainty about its relative importance as a driver of vegetation structure across landscapes (Levick & Rogers 2008; Asner et al. 2015; Davies et al. 2018).

Monitoring with traditional field-based techniques has provided insights into the role of fire regimes in shaping woody vegetation structure (Enslin et al. 2000; O'Regan 2005; Higgins et al. 2007; Devine et al. 2015). However, field inventory studies are restricted to specific plots and rely on sampling strategies such as belt transects or quadrats, which may not adequately describe the spatial variability of vegetation structure within a landscape. In recent years, airborne light-detection and ranging (LiDAR) techniques have emerged as a key remote sensing technology for advancing the knowledge of vegetation

structural changes in savannas due to fire (Smit et al. 2010; Levick et al. 2012; Smit et al. 2016). These approaches have enabled the characterization of vegetation organization in space and time, including canopy position, extent and connectivity (Lefsky et al. 2002). Nevertheless, in a mixed tree-grass system significant proportion of the vegetation occurs in short size-classes and resides beneath the overstory canopy. Airborne instruments often fail to detect the shrub stratum canopy and stem architecture. The effect of the arrangement of fine-scale vegetation elements becomes more critical when examining the effect of fires on vegetation communities at small and local scales. As such, there is a need to capture and describe these complex vegetation structures in greater detail.

Terrestrial LiDAR, also referred to as terrestrial laser scanning (TLS), characterizes the three dimensional (3D) distribution of vegetation structure at high resolution and accuracy (Dassot et al. 2011). In doing so, it enables measurement of conventional woody biophysical parameters with less uncertainties (Calders et al. 2015), and allows for the creation of new metrics such as canopy density and base height which capture additional aspects of woody vegetation structure (Newnham et al. 2015). Cuni-Sanchez et al. (2016) demonstrated the potential of one such new metric i.e vertical plant profiles across a Central African savanna-forest mosaic for assessing long-term structural differences among the vegetation types. These new metrics have provided fresh insights into the distribution, abundance and diversity of vegetation species. TLS data can therefore be used to inform conservation managers as to the impacts of fire policies on fine scale changes in savanna structure.

In this study, we employ advances in TLS technology to capture the 3D structure of woody vegetation across a long-term fire experiment in Kruger National Park, South Africa. Our specific research questions (as defined in section 1.5 at page 13) are to explore: (1) how vegetation structure (average and maximum height, canopy cover) and above-ground carbon storage respond to varying fire frequencies; (2) does the effect of fire regimes vary across plot and landscape scale; and (3) how differences in rainfall across the landscapes interact with fire frequency in altering vegetation structure.

3.2 Study site and experimental design

Our study focused on the Experimental Burn Plots (EBPs) of Kruger National Park (KNP), a national reserve covering *1.9 million ha* in north-eastern South Africa (Figure 3.1). KNP is comprised primarily of sub-tropical wooded savannas, and consist of mopane (*Colophospermum mopane*), knobthorn (*Acacia nigrescens*), marula (*Sclerocarya bierra*), *Combretum* species, sicklebush (*Dichrostachys cinerra*) and silver cluster-leaf (*Terminalia sericea*) (Gertenbach 1983).

The park encompasses a gradient of increasing rainfall from the semi-arid north (400 *mm* mean annual rainfall) to the mesic south (750 *mm* mean annual rainfall) (MacFadyen et al. 2018). Soils are heterogeneous and are related to the geomorphological division between granites in the west, weathering to sandy soils, and clay soils derived from basalt

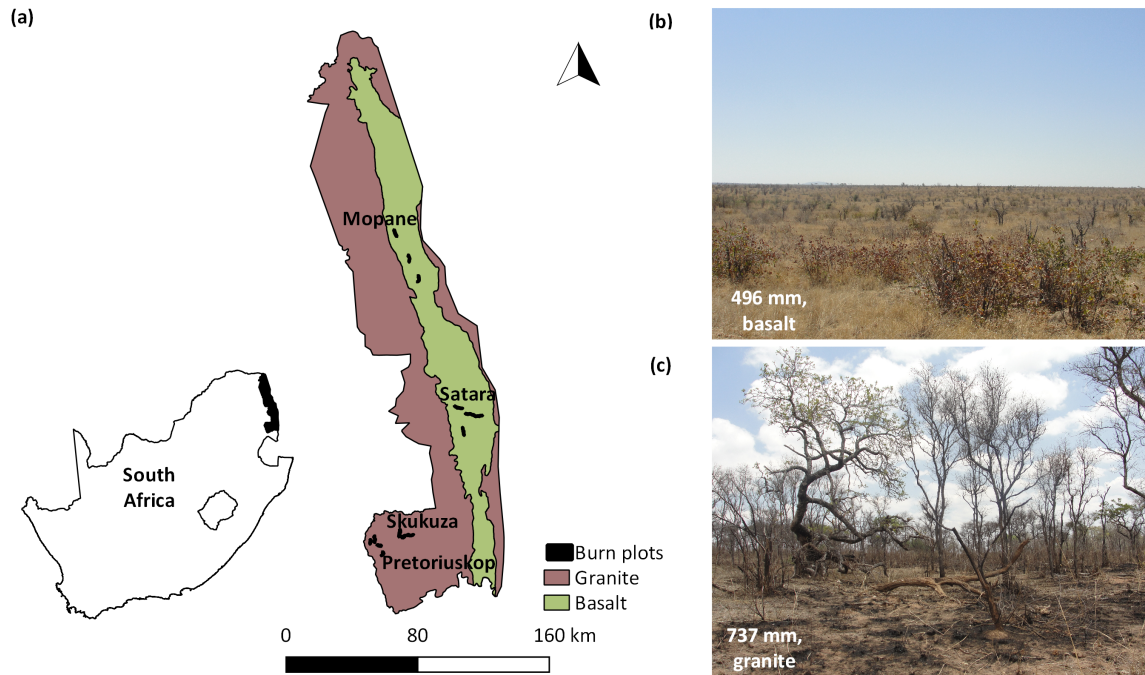


Figure 3.1: (a) Location of the four experimental burn plots within Kruger National Park, South Africa. Differences in vegetation structure along the precipitation gradient. (b) Upper photograph is from Mopane EBP receiving 496-mm mean annual precipitation (MAP) on basaltic soils. (c) Lower photograph is from Pretoriuskop EBP receiving 737-mm MAP on granitic soils.

erosion in the east. The EBPs were set up in the KNP in 1954 to study the effects of fire on vegetation under grazing pressure from herbivores (van Wilgen et al. 2007). The experiment consists of application of controlled fires at varying frequencies (annual, biennial and triennial), and seasons (Dry: August and October; Wet: February, April, and December), on a set of 7 ha plots with four replicates across the four major vegetation landscapes (Mopani, Satara, Skukuza and Pretoriuskop) of the KNP.

Our study focused on all four EBP regions, stretching from Mopani and Satara in the north to Skukuza and Pretoriuskop in the south. We investigated two burn strings at each site, and the selected EBPs spanned 168 ha with differing plant productivity and physiognomies, caused by the gradients in mean annual precipitation (Mopane: 496 mm, Satara: 544 mm, Skukuza: 650 mm and Pretoriuskop: 737 mm), geology and soil types (fertile in Mopani and Satara, infertile in Skukuza and Pretoriuskop) (Biggs et al. 2003). Within each EBP, we evaluated three late dry-season treatments: (i) fire exclusion (unburnt), (ii) October triennial burn, and (iii) October biennial burn. The late dry-season fires were considered due to their effect on demographic legacies of current tree populations (Levick et al. 2015), since between 1941-1996, most management fires in KNP and surrounding savanna landscapes were concentrated in the late dry season (Govender et al., 2006).

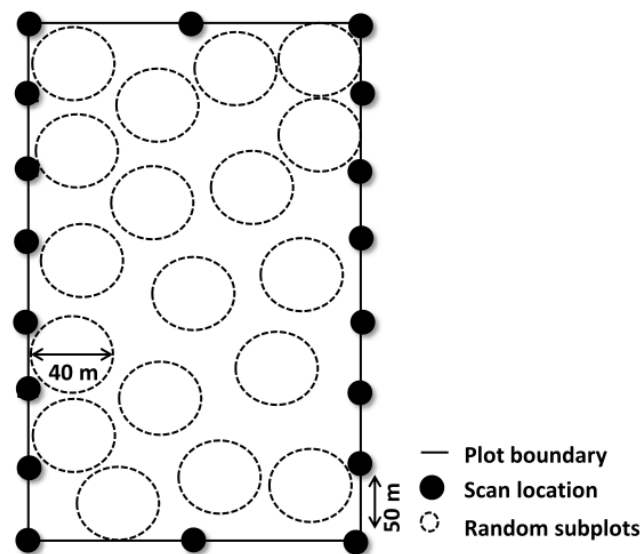


Figure 3.2: The TLS scanning setup of the EBPs with solid black dots indicating the scan locations. Sampling of the EBPs was achieved by placing random circles of 40 m radii depicted with dotted circles.

3.2.1 Woody vegetation data

We mapped EBPs across four landscapes in October 2016 using the RIEGL VZ-2000 terrestrial laser scanner (RIEGL Laser measurement systems GmbH). The RIEGL VZ-2000 is a multiple return LiDAR scanner which operates in the near infrared spectrum (wavelength 1500 nm) with a beam divergence of 0.30 mrad. The laser ranging data were combined with an external differential GPS (accuracy 3 cm), to determine the 3D location of each laser return. Inertial measurements (roll, yaw and pitch) of the scanner were collected through an internal compass and inclination sensors. We used a systematic scanning design, by placing the scanner at 50 m intervals along each EBP, giving a minimum of 15 scans per EBP (Figure 3.2). These multiple single scans ensured complete coverage of the vegetation structure within the EBP. However, to reduce the time and effort required for multi-scan approach (see Liang et al. 2016), we utilized a vehicle rooftop mount for operating the scanner, with a scanner height of 2.5 m. The LiDAR data for all the scan positions were collected at 1010 kHz pulse repetition rate and an angular sampling of 0.02° in both azimuth and zenith direction, ensuring sufficient point density to enable fine scale description of even smaller woody vegetation.

3.2.2 Point cloud processing

Multiple LiDAR scans of each EBP were first co-registered using the RiSCAN PRO package (RIEGL GmbH). A coarse registration between the scans was achieved using large woody trees (branch tips and nodes) as tie points, which were present in all the scans. Since the LiDAR survey took place in the leaf-off stage at the end of the dry season, the occlusion of woody trees by bushes and understory from different scan positions was minimised. The coarsely merged scans were fine tuned by eliminating the translation and

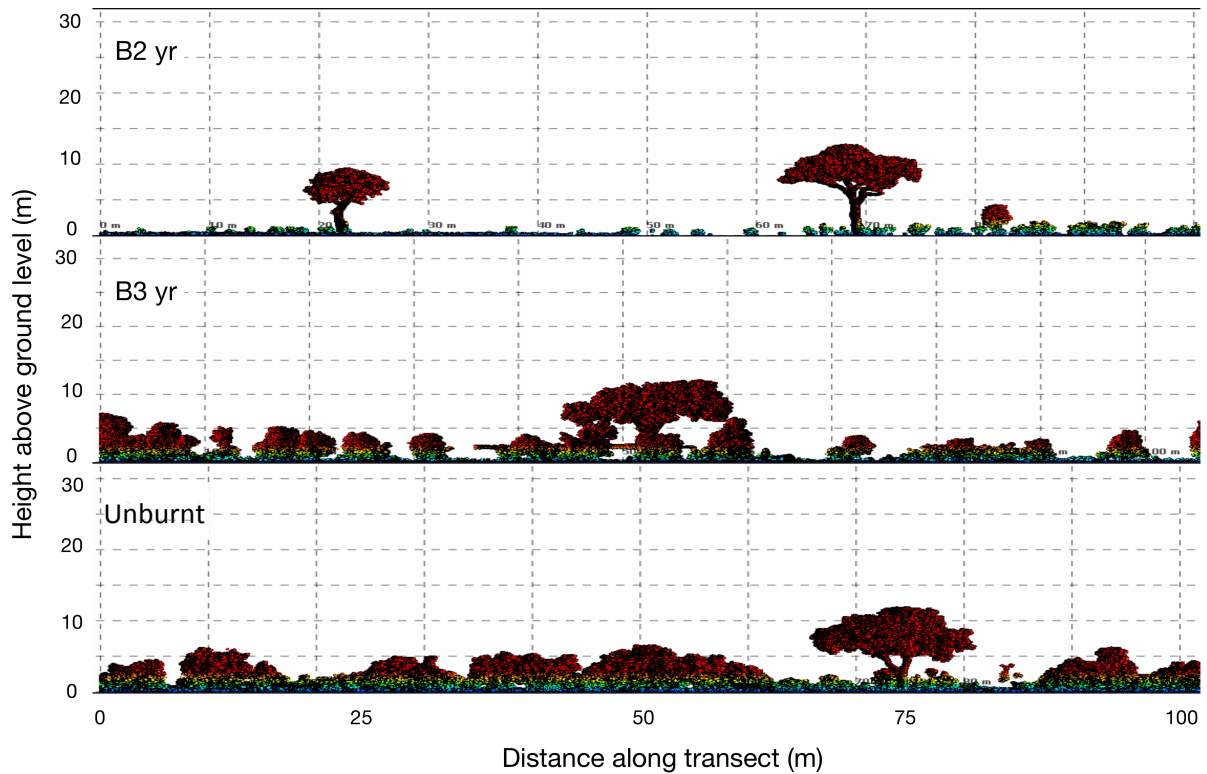


Figure 3.3: Normalized height distribution of vegetation within a 100 x 30 m transect of the laser footprint, represented at 5 m height increments. The colour scale from green through red indicates increasing vegetation height. The panel shows data from biennially (B2-yr) and triennially (B3-yr) burnt plots, and fire exclusion (unburnt) from the Satara site, with maximum height of 12 m.

rotation errors with a multi-station adjustment (MSA) approach. MSA iteratively adjusts the position and orientation of each point-cloud by least square error optimization. Once the best fit between the scans is completed, the calculated transformation matrix is applied to all the raw point clouds, to associate them into a common coordinate system. The standard deviation of the registered scans for all EBPs ranged from 0.01 to 0.02 *m*. Registered point clouds were then filtered to remove noisy isolated points or those with low reflectance using the default reflectance filters in RiSCAN PRO. The presence of noise was often attributed to dust in the atmosphere, wind or edges of the bushes close to the scanner. Point clouds were then trimmed to include only 3D data within the EBP region.

The pre-processed LiDAR data were used to derive height normalized point clouds (Figure 3.3), which were subsequently used to produce count frequency rasters by batch scripting several modules of LASTools (rapidlasso GmbH, 2014; Isenburg (2014)). We computed height count rasters from 0 *m*, at every 0.5 *m* interval of the LiDAR data, and scaled them to percentage canopy profiles. Woody canopy height was estimated at a step size of 0.05 *m* to create approximately 8000 X 9000 pixel rasters using the highest ‘z’ coordinate

among all the LiDAR returns in the corresponding pixel area. The resulting canopy height grids were hard classified in SAGA GIS (SAGA GIS,2016; www.saga-gis.org), assuming the LiDAR data between 0.0-0.5 *m* as ground points, while the points between 0.5-30 *m* were categorized as woody vegetation. The reclassified grids were then expressed as the percentage canopy cover.

3.2.3 Statistical analyses

We distributed eighteen 0.12 *ha* plots (20 *m* radius) randomly within the TLS 3D data of each EBP treatment, totalling 432 sample plots (Figure 3.2), to assess differences in vertical canopy profiles, cover and height comparisons. The 20 *m* radius size of the subplots enabled us to sample large area of the plots and subsequently minimizing the edge effect. Percentage canopy cover and mean height of each sample plot were computed for all pixels higher than 0.5 *m*. We used a one way ANOVA and a Tukey's *post hoc* ($P < 0.05$) test to compare the differences in mean canopy cover and mean canopy height between areas of fire and fire exclusion (unburnt) in different landscapes. The relationship between fire frequency and landscape and their effect on woody cover, average and maximum height were analyzed using linear mixed effects models in R (Team-RCORE, 2016), with the package NLME (Pinheiro et al., 2014). Explanatory variables in the model were fire frequency and landscape (Mopani, Satara, Skukuza and Pretoriuskop), while the subplots nested within each treatment replication and landscape were specified as the random variable. Models with all possible combinations were fitted using maximum likelihood (ML) method, and were evaluated using Akaike's information criterion (AIC), a model selection index, which favours both model fit and simplicity (Burnham & Anderson, 2002). From the AICs, the Δ AIC score for each model was calculated by comparing them to the least AIC score model, for assessing the probability of the best-fitting model, where for the best model Δ AIC = 0. For each model, we calculated Akaike weights (w_i), a normalized relative likelihoods of the models (Wagenmakers & Farrell, 2004). Next, Akaike weights were used to calculate the weight of evidence (w_+) for each of the explanatory variable by adding the Akaike weights for all the models in which the explanatory variable was present (Burnham & Anderson, 2002).

Aboveground biomass at the plot level was estimated from the TLS-data-derived single predictor variable 'HXCC' (Colgan et al. 2013) (Equation (3.1)). This equation was preferred as it is derived from actual weighing of the harvested tree samples and considers the specific wood density. Furthermore, many of the tree species sampled in this study are commonly found in KNP.

$$AGB_{plot} = -11.5 + 25.8H_{plot}XCC_{plot} \quad (3.1)$$

where H is the mean top-of-canopy height of a plot and CC is the mean canopy cover of a plot.

3.3 Results

3.3.1 Shifts in vegetation structure across fire frequencies and landscapes

At the regional scale fire frequency did not significantly influence the average height of woody plants ($F(2, 432) = 0.154, p = 0.85$). Analysis of change in maximum height over all landscapes also revealed a non-significant effect of fire frequency ($F(2, 432) = 0.72, p = 0.48$). However, the response of woody cover to fire treatments differed markedly across the no-fire (unburnt) vs. fire treatments ($F(2, 432) = 45.75, p < 0.001$), with the highest woody cover observed in the unburnt plots. At the regional scale the effect of triennial fire treatments was more pronounced in reducing woody cover (11.18%, $p < 0.001$) than the biennial fires, which led to a decrease of canopy cover by 8.5% per 0.12 ha ($p < 0.001$).

Landscapes varied in average vegetation height from 1.5 m in northern dry Mopani EBPs to 4.5 m in southern wet Pretoriuskop EBPs. At the landscape scale, fire frequency had a divergent effect on average vegetation height. In the southern wet savanna sites, average height was higher in the biennially burnt plots, whereas in the northern dry savanna unburnt plots had taller vegetation. Triennial and biennial fire treatments in Mopani EBP strings led to a significant decrease in average height by 0.34 m and 0.32 m respectively ($F(2, 105) = 9.53, p < 0.001$) (Figure 3.4). In contrast, fire regimes did not significantly influence the average height in Satara and Pretoriuskop burn plots (Satara: $F(2, 105) = 0.419, p = 0.65$; Pretoriuskop: $F(2, 105) = 0.917, p = 0.40$). However, for Skukuza, the unburnt plot had 0.40 m less average height than the biennially and triennially burnt plots ($F(2, 105) = 3.298, p = 0.040$) (Figure 3.4). The variation in average height across the burn plots was best explained by the linear mixed model when only landscape variable ($w_I = 0.7, w_+ = 0.71$) was taken into account (Table 3.1, 3.2).

Maximum vegetation height exhibited a varied response to differences in fire frequency regimes, with taller canopies present in the the annually burnt plots of the wetter southern EBPs of Pretoriuskop and Skukuza (Figure 3.4). However, the maximum heights observed in the northern Mopane EBPs were similar across the fire treatments and unburnt plots (Figure 3.4 b). In common with the linear mixed models for average height, landscape rather than fire frequency, had its most considerable effect on the maximum height of the woody vegetation ($w_I = 0.7, w_+ = 0.71$) (Table 3.1, 3.2). In the Pretoriuskop and Skukuza wet savannas, the maximum height was 13.89 m and 8.61 m higher than the drier Mopani EBP strings.

The magnitude of effects of fire frequency on woody canopy cover differed across the sites and across the productivity gradient. In all the EBPs across the park, woody cover was at a maximum in the unburnt plots compared to the burnt plots (Figure 3.4). Although both the northern EBPs lie in the same geological substrate and have similar fire treatments, woody canopy cover response to different fire frequency varied significantly across the two regions (Figure 3.4). A Tukey post hoc test revealed that triennial fires were more effective

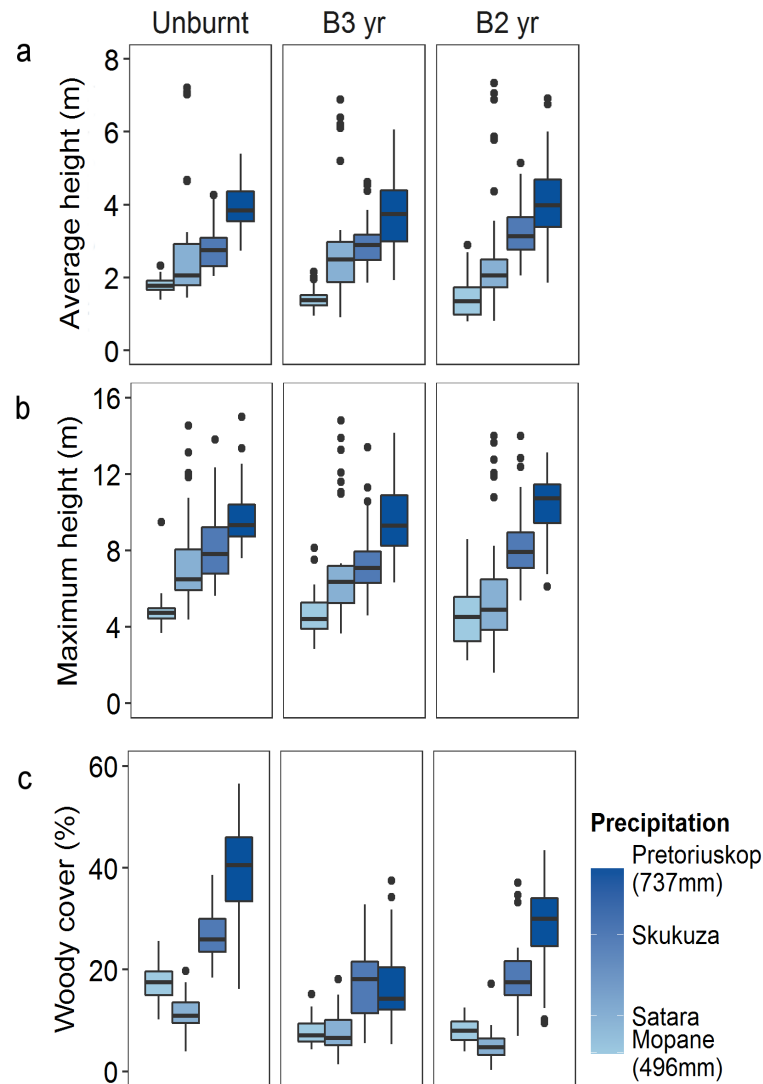


Figure 3.4: Average height (a), maximum height (b), and canopy cover (c) in plots subjected to different burn treatments. B2= biennial, B3= triennial and Unburnt= fire exclusion. Colour shading indicates the increasing MAP from Pretoriuskop to Mopane.

in reducing the woody cover by 10% in Mopani EBPs, whereas triennial fires in Satara EBPs reduced the woody cover only by 3.5% as compared to the biennial fires, which had the effect of decreasing the Satara canopy cover by 6.3%. In Southern EBPs triennial fire was associated with less canopy, which reduced the canopy cover by 9.29% and 21.9% for Skukuza and Pretoriuskop respectively. The best model explaining the woody cover heterogeneity was obtained by fitting the fire frequency and landscape ($w_I = 0.54$) (Table 3.1). Fire frequency ($w_+ = 0.91$) proves to be an important predictor in determining the woody cover across the different landscapes (Table 3.2). The woody cover in Pretoriuskop and Skukuza was 13.6% and 7.12% higher than the woody cover observed in northern dry EBP strings. A contrasting feature observed is that Satara has 6.45% lower woody cover

Table 3.1: Results from an analysis of the effects of fire frequency and landscape upon three-dimensional vegetation characteristics at the EBPs in Kruger National Park, South Africa. Results are the Akaike's Information Criterion for linear mixed effect models, with * referring to the most parsimonious model.

Structural parameters Model Terms	Avg height			Max height			Woody cover		
	AIC	Δ AIC	w_I	AIC	Δ AIC	w_I	AIC	Δ AIC	w_I
Fire Frequency*landscape	314.08	29.22	0	174.23	30.25	0	421.86	6.43	0.02
Fire frequency+landscape	297.21	12.34	0.01	156.68	12.71	0.001	415.43	*	0.54
Fire frequency	295.43	10.56	0.003	153.95	9.97	0.005	416.30	0.87	0.35
Landscape	248.86	*	0.7	143.97	*	0.7	419.31	3.87	0.07
Null model	286.65	1.78	0.2	146.71	2.73	0.2	420.18	4.75	0.04

Table 3.2: The importance of two variables (landscape and fire frequency) examined as predictors of average and maximum vegetation height, and woody cover, with * referring to the variables with reasonable level of support as predictors.

Variable	w_+
Average vegetation height	
Fire frequency	0.004
Landscape	0.71*
Maximum vegetation height	
Fire frequency	0.006
Landscape	0.70*
Woody cover	
Fire frequency	0.91*
Landscape	0.63

than Mopani strings. High woody cover is reduced by the triennial fire than the biennial fire at wet sites (Pretoriuskop), whereas fire frequency has a relatively lower effect at dry sites (Satara) (Figure 3.4).

3.3.2 Vertical vegetation profiles

The structural height distinction between burnt and unburnt plots is demonstrated by their vertical height distribution profiles (Figure 3.5). In the unburnt treatments, all the plots except for Satara contained higher frequencies of LiDAR returns from the shrub layer (0.5 m - 2 m) (Mopani: 10.83%, Satara: 5.535%, Skukuza: 7.49%, and Pretoriuskop: 6.43%). In contrast, plots subjected to fire treatments exhibited a different pattern, with a reduced percentage of LiDAR returns from the shrub layer.

The response of the vegetation to different fire frequencies was heterogeneous across the landscapes with higher fire frequencies associated with lower canopy height in the drier northern EBPs (0.057% LiDAR returns at 5m canopy height in unburnt plot), but with taller canopies in the wetter southern EBPs (5.8% LiDAR returns at 5 m in unburnt plot) (Figure 3.5). Finer scale exploration of the vegetation canopy height distributions

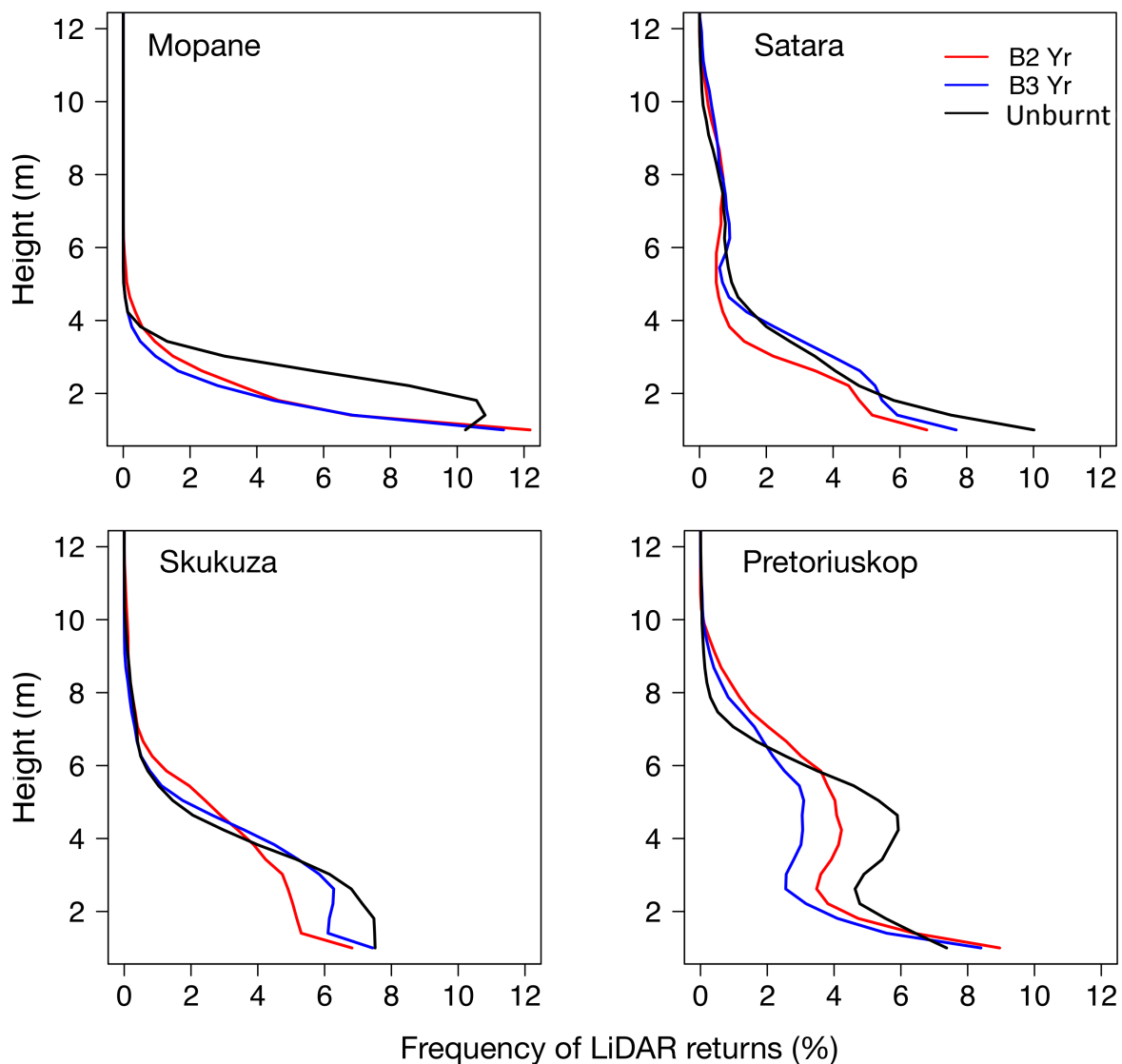


Figure 3.5: Structural responses of woody vegetation height to different fire frequencies as a function of landscape type.

at the four landscapes revealed contrasting physiognomies, with northern EBP (Mopani and Satara) displaying an inverse-J distribution, while that of the southern EBP (Pretoriuskop) exhibiting a bi-modal height class structure. In all landscapes, the slope of the vertical distribution profiles decreased with increasing fire frequencies and the shift in the slope was stronger in the triennial fire regimes than the biennial fires. The two Southern EBP sites (Skukuza and Pretoriuskop) have the same underlying granite geology and geographic proximity, but the 3D vertical canopy profiles for the two sites were entirely different due to difference in MAP ($>100\text{ mm}$) and vegetation species composition. A greater proportion of the LiDAR returns from the 4-6 m height class were observed in the triennial fire regime of Skukuza site, while at Pretoriuskop triennial fires were associated with less LiDAR returns from the taller canopies. The transition from overstorey height

class to reduced canopy (shrubs) due to fire varied across the landscapes. The natural break (inflection) occurred at heights of 1.5 m (Mopani), 1 m (Satara), 1 m (Skukuza) and 2.8 m (Pretoriuskop). The changes in the shape of the canopy height profiles reflect a complex dynamic relationship between woody vegetation structure and fire frequency under different climatic and edaphic conditions.

3.3.3 Aboveground biomass across the sites

The importance of fire regimes versus resources (climate and soil) in shaping the vegetation was evaluated with woody plant biomass. Fire suppression allowed woody biomass to accumulate at substantial rates (7-33 tha^{-1}), which increased along the MAP gradient from north to south (Figure 3.6).

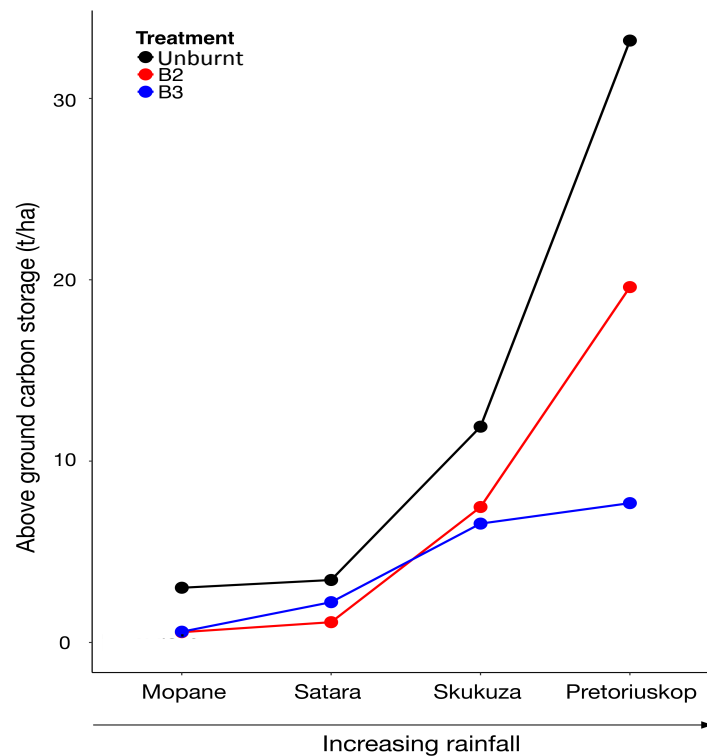


Figure 3.6: Woody biomass in plots subjected to different burn treatments estimated from the terrestrial LiDAR point cloud data. Results are shown for the long-term experimental burn plots at Mopani and Satara, the dry savanna and Skukuza and Pretoriuskop, the wet savanna subjected to a burn frequency of B2= biennial, B3= triennial and Unburnt= fire exclusion.

The difference between the potential biomass (unburnt plots) and actual biomass (burnt plots) for the rainfall deficit landscapes was very small. At the two dry sites on basalt geology, annual burning resulted in a loss of woody-biomass carbon (0.5 tha^{-1}). In contrast, the wettest sites on granite substrate continued to accumulate woody biomass up to 20 tha^{-1} under the increased fire frequency regime. However, the wettest sites experienced the greatest aboveground biomass losses during less frequent fire events. Also, for the Skukuza landscape, which receives 100 mm less MAP than Pretoriuskop, the difference

between the woody plant biomass generated by the biennial and triennial fires is much less, while at Pretoriuskop the woody plant biomass in the fire treatments differs by 15 tha^{-1} .

3.4 Discussion

3.4.1 Regional variation in vegetation structure in the absence of fire

At a regional scale the spatial pattern of woody vegetation structure appears to be driven by the interplay of multiple environmental gradients. In KNP, the east-west geological and north-south rainfall gradient have been hypothesized to be largely responsible for variation in woody vegetation structure. While this assumption was true for all 3D vegetation structure metrics, the differences in their magnitudes were distinct. When we consider the fire excluded plots of our study, we observe that the northern basaltic regions have shorter and sparser canopies than the woody canopies of the southern granite substrate (Figure 3.5). The basalt landscapes are characterised by clay soil, which tightly binds moisture during dry season, resulting in a low water availability (Colgan et al. 2012). Low water availability has the potential to increase competition between grasses and juvenile trees, thereby keeping the woody vegetation short. Conversely, granite substrates support taller woody vegetation because of the competitive edge of trees over grass in terms of deeper rooting systems with access to more stable moisture reserves (Walter & Burnett, 1971; Alizai & Hulbert, 1970). Consistent with this observation, the southern granite plots, which receive 737 $mm\text{yr}^{-1}$ MAP, have 23% more woody cover (Figure 3.4) than the dry basaltic control plots. The woody cover in savannas increases linearly with MAP, and a MAP of 650 $mm\text{yr}^{-1}$ and above is sufficient for canopy closure, thus local disturbance such as fire regimes becomes a key factor in constraining the spatial expansion of the woody vegetation (Sankaran et al., 2005).

3.4.2 Top-down control by fire in savanna system

The 63 years of prescribed burning across the EBPs of the KNP have led to marked differences in woody vegetation structure, and our results indicate that the patterns and processes of vegetation structural change vary at different spatial scales. When averaged across the four experimental sites (Mopane, Satara, Skukuza and Pretoriuskop), fire frequency had no significant effect on average height. At the landscape scale, however, average canopy height declined in the northern Mopane plots, and increased in the Skukuza plots, with increasing fire frequency. Differences in average canopy height across the northern low MAP regions of the park may be due to the confounding effects of water stress, arising from the increased tree-grass competition, whereby trees produce shorter multiple stems rather than a single taller stem. It is also possible that different species respond differently to the fire regimes. For instance, in the Skukuza landscape, fire treated plots were associated with a greater proportion of LiDAR returns in the 4 - 8 m height classes, and a lower LiDAR returns above 4 m in the fire excluded plots (Figure

3.4 b and Figure 3.5). Similar findings are reported by Levick et al. (2015), who showed that the Skukuza fire exclusion regions were associated with shorter vegetation, while a greater proportion of the taller vegetation was observed in the higher fire frequency. The vegetation communities in the Skukuza are dominated by *Combretum apiculatum*, which Higgins et al. (2007) hypothesized regenerates poorly under low fire frequencies and that saplings are shade intolerant.

Our study has shown that the effect of fire frequency on woody vegetation structure differs by region, in relation to rainfall and soil type. For the EBPs in the drier regions (MAP= 544 mm yr^{-1}) of the park, the maximum height of the woody vegetation was usually reduced under higher fire frequency conditions, while the wetter southern region of the park supported taller vegetation canopy under high fire frequency (Figure 3.4 b). Moreover, the wetter sites of KNP possessed much higher canopy cover under a high frequency burning regime. In the regions of high fire occurrence, fire stimulates the growth of the plant, in an effort to exceed the flame zone (Bond & Keeley, 2005; Archibald & Bond, 2003). Also, the highest fire frequency considered in our study is burning every 2 years, which is a sufficient time frame in a wet region to stabilize competition among the trees and grasses, leading to greater growth and survival of trees (Archibald & Bond, 2003). However, deriving an understanding from this explanation is not simple as fire intensity is a linear function of fuel load which increases with increasing MAP (Govender et al. 2006). For instance, frequent fires lead to a reduction in fire intensity by preventing the buildup of grass fuel load, thereby facilitating more individuals into the upper height classes and more canopy expansion. However an additional year in between the successive fires at a wet site will cause large reductions in the woody canopy cover due to high intensity fires arising from greater accumulation of the fuel load between the fire events (Figure 3.4 c).

As the rainfall increases from north to south across the reserve, there is a gradual transition of distribution of vegetation communities. The response of vegetation communities to fire regimes differs with their adaptation capabilities, in relation to environmental stresses and herbivory. The complex interactions associated with the plant species and environmental stresses are evident from the vertical vegetation profiles (Figure 3.5). The vegetation structure in the northern basalt region is depicted by a flat height class distributions. The flattened height class distribution or inverse J shaped indicates a strong top-down control on vegetation structure in the basalts. Basalts weather to nutrient rich soil and support high herbivory density, which keeps the juvenile trees within the fire-trap and weakens the larger trees by girdling, increasing their vulnerability to future fire events (Helm et al. 2011; Moncrieff et al. 2011). Presence of inflection points at 0.5 m and 2 m in the EBPs distributed across Satara landscape indicate a feedback from the selective foraging activities of the herbivores, resulting in a patchy distribution of vegetation damage by fire (Figure 3.5). As such the influence of fire on vegetation structure is sensitive to the herbivory density (Pellegrini et al. 2017). However, the high nutrient concentration in basalts leads to increased grass production, high fire intensity and, reduced vegetation

height (Bond & Keeley, 2005).

3.4.3 Empirical evidence of ‘consumer control’

Our exploration of woody biomass across the experimental treatments contributes to a more comprehensive understanding of consumer control by fire, which was conceptualized previously by Bond & Keeley (2005). Our results provide the first quantitative test of this conceptual model (Figure 3.6). At dry sites, woody biomass was found to be less sensitive to fire frequency, instead presence of fire alone was more influential in lowering the biomass. The effect of fire frequency on woody biomass are greater in the wetter sites, where woody biomass in biennial and triennial burnt plots differed by 10 tha^{-1} . Notable here is the mesic site Pretoriuskop on granites, where unburnt plots supported up to 33 tha^{-1} of the woody biomass and those burned every 2 years retained more woody biomass than those burned every 3 years. This was unexpected given the role of fire in limiting woody vegetation in more mesic savannas. Multiple mechanisms may influence the increase in woody biomass in spite of frequent burning, including growth of fire-resistant trees, and the plausible increase in atmospheric CO_2 concentrations could increase the chances of trees escaping fires (Bond et al. 2003; Buitenwerf et al. 2012). Still the large differences between potential (unburnt plot) and actual (burnt plots) woody biomass at wet sites suggest significant consumer control on savanna ecosystems.

3.4.4 Limitations and future directions

Recently there have been many vegetation structure models derived from airborne LiDAR and spaceborne datasets, to explain the role of fire in shaping savanna systems and tree-grass balance (Smit et al. 2010; Bucini et al. 2010; Levick et al. 2012, 2015). Given the KNP’s low to medium woody cover, present remote sensing models cannot account for impacts of fire on the structure and dynamics of dual layering or sub-canopy woody vegetation. In turn, TLS measurements provided dense 3D point clouds, capturing the high degree of heterogeneity inherent across the EBPs and enabled us to quantify the structural features accurately. Savannas exhibit complex vegetation structure with substantial seasonal variations between trees and grasses (Archibald & Scholes, 2007), so TLS mapping should ideally be conducted in leaf-off periods to prevent occlusion by grasses and shrubs. Our use of TLS point cloud data and high resolution canopy height profiles has provided some useful insight into savanna woody vegetation spatial patterns emerging from fire regimes and landscape interaction at the plot scale. However, there is much more to be learned from the 3D metrics in terms of woody canopy architecture and biomass allometry.

We have focused heavily on the effect of fire frequency at small and site-specific scales, and acknowledged the interaction of fire with a single determinant landscape as a function of rainfall. It is likely that the interactive effects of fire regimes and herbivory abundance may vary the woody biomass significantly. Also, despite the large spatial extent of each burn treatment, plot-based experiments fail to depict the stochastic relationship between

disturbance regimes, and environmental and topographic processes (Levick et al. 2012; Staver 2018). Therefore, we recommend the integration of 3D inventory metrics with broader-scale remote sensing analyses to achieve a comprehensive model that accounts for the productivity of savanna systems under a wide range of topographic and bio-climatic conditions. However, a single regional model can not adequately represent savanna woody vegetation characteristics at a global scale. In our study, relationship between moisture, fire regimes and woody vegetation structure vary across the four landscapes of KNP (Figure 3.5). Differences in these relationships reflect the greater role of region specific climate, phenology, growth rates, canopy architecture, and biomass allometry of woody taxa in determining the structure of savanna vegetation. Similarly, Lehmann et al. (2014), predicted net decrease in African woody biomass from a single global model, whereas the regional model predicted a net increase. Thus any such extrapolation to a global scale must incorporate the evolutionary and environmental differences of each regional ecological setting, to underpin the trajectories of change in vegetation to future climate, with implications for global carbon stocks.

3.4.5 Implications for management

The fire induced changes reported here in both the vertical and horizontal components of the woody layer highlight the large influence that land managers can exert on savanna vegetation through alteration of fire frequency. Our findings show that through long-term biennial and triennial burning in the Mopane landscape, diverse woody structures are being transformed to short homogenized communities together with significant changes in canopy cover and aboveground carbon storage (Figure 3.5). Frequent fires in combination with browsing will lead to higher abundance of short height class individuals by preventing woody tree recruitment. Longer fire return intervals could be beneficial to woody recruitment, but at the same time may serve to suppress canopy height because of high intensity fires.

A broad spectrum of fixed fire treatments are applied across KNP as a whole, but deeper investigation is needed to ensure that there is enough variability for trees to escape the flame zone and attain the upper height class and canopy expansion. Presence of large trees substantially influences the carbon sequestration potential (Levick & Asner, 2013) and faunal diversity (Cumming et al. 1997) of the system. Fire managers have been encouraged to introduce spatio-temporal variability in the fire regime through landscape scale patch mosaic burning (Parr & Andersen, 2006), but managers have less control over the total area of the park burnt annually due to the occurrence of unplanned fires (van Wilgen et al. 2014). Increased woody cover of the mesic Pretoriuskop sections of the southern granitic substrate is of growing concern, yet it is an area with one of the highest fire frequencies in the park. Importantly, it is not just variation in frequency that is needed, but variation in fire intensity, with infrequent hot fires needed to combat thickening (Smit et al. 2016). Stratifying ignition locations by catchment and hillslope position could result in a more diverse spatial pattern of fires over time (Levick et al.

2012).

Lastly, our findings here provide useful quantification of the degree to which different fire regimes can suppress above ground carbon storage, and how this changes with spatial context. These trends are of global significance, at a time when many countries hosting the savanna biome are contemplating carbon sequestration initiatives (Russell-Smith et al. 2013; Bradshaw et al. 2013; Lipsett-Moore et al. 2018).

3.5 Conclusions

This study highlights the variable effects of fire-frequencies on vegetation structure across rainfall and topographic gradient of a savanna system. Though presence of frequent fires constrained the vegetation structure at dry sites, in wetter savanna sites, fire occurring every 3 years reduced the woody vegetation more than frequent fires. Fire-regime effects varied across the landscapes, with stronger influence at granite sites due to presence of more fuel load than basalt sites. Additionally, varying fire frequencies were required to maintain an open tree-grass coexistence at wet sites, while at dry sites the presence of fire rather than fire frequency was a stronger explanatory factor in altering woody vegetation.

Chapter 4

Mapping savanna landscapes - A long-range terrestrial laser scanning approach

This chapter is originally published as:

Singh, J., Levick, S. R., Guderle, M., & Schullius, C. (2020). Moving from plot-based to hillslope-scale assessments of savanna vegetation structure with long-range terrestrial laser scanning (LR-TLS). *International Journal of Applied Earth Observation and Geoinformation*, 90, 102070. **Copyright** ©2020 The Authors. Published by Elsevier B.V.

Abstract

Reliable quantification of savanna vegetation structure is critical for accurate carbon accounting and biodiversity assessment under changing climate and land-use conditions. Inventories of fine-scale vegetation structural attributes are typically conducted from field-based plots or transects, while large-area monitoring relies on a combination of airborne and satellite remote sensing. Both of these approaches have their strengths and limitations, but terrestrial laser scanning (TLS) has emerged as the benchmark for vegetation structural parameterization - recording and quantifying 3D structural detail that is not possible from manual field-based or airborne/spaceborne methods. However, traditional TLS approaches suffer from similar spatial constraints as field-based inventories. Given their small areal coverage, standard TLS plots may fail to capture the heterogeneity of landscapes in which they are embedded. Here we test the potential of long-range (>2000 m) terrestrial laser scanning (LR-TLS) to provide rapid and robust assessment of savanna vegetation 3D structure at hillslope scales. We used LR-TLS to sample entire savanna hillslopes from topographic vantage points and collected coincident plot-scale (1 ha) TLS scans at increasing distances from the LR-TLS station. We merged multiple TLS scans at the plot scale to provide the reference structure, and evaluated how 3D metrics derived from LR-TLS deviated from this baseline with increasing distance. Our results show that despite diluted point density and increased beam divergence with distance, LR-TLS can reliably characterize tree height (RMSE = 0.25 - 1.45 m) and canopy cover (RMSE = 5.67 - 15.91 %) at distances of up to 500 m in open savanna woodlands. When aggregated to the same sampling grain as leading spaceborne vegetation products (10-30 m), our findings show potential for LR-TLS play a role in constraining satellite-based structural estimates in savannas over larger areas than traditional TLS sampling can provide.

4.1 Introduction

Savannas are heterogeneous ecosystems composed of mixed-tree grass communities that cover 20 % of the global vegetated land surface (Scholes & Archer, 1997). Given their significant contribution to terrestrial net primary production (1-12 Mgha⁻¹yr⁻¹), savannas are important for the regulation of the global carbon cycle (Grace et al., 2006). However, understanding of savanna structural dynamics and their carbon sequestration potential remains limited in the face of global environmental (Williams et al., 2004; Wigley et al., 2010; Buitenwerf et al., 2012; Stevens et al., 2017) and land-use changes (Archibald et al., 2013). To effectively implement sustainable land management practices, while at the same time maintaining a range of tree-grass mixtures for biodiversity conservation, savanna ecosystems warrant comprehensive and timely inventory efforts. Structural information is not only fundamental to advancing savanna ecological process understanding, but also assists in the development of baseline information required for global carbon emission agreements (e.g., REDD+). Therefore, regular monitoring campaigns are necessary to characterize and map savanna vegetation structure under diverse land-use conditions.

Mapping savanna vegetation structure is challenging due to heterogeneity at hillslope and regional scales that arises from the interaction of topography, soils, climate and biological factors (Meyer et al., 2007; Levick & Rogers, 2011; Sankaran et al., 2008; Vaughn et al., 2015). Most of our current understanding of savanna vegetation structure derives from field-based measurements using either plots or transects. While such field data can be scaled to larger extents with remote sensing imagery (Lucas & Armston, 2007; Boggs, 2010), their limited spatial coverage means they may fail to account for variable vegetation structure across the landscape (Asner et al., 2009; Mathieu et al., 2013). In response, there has been growing interest in the use of Light Detection and Ranging (LiDAR) to augment traditional field measurements (Dubayah & Drake, 2000; Lefsky et al., 2002; Asner et al., 2007) with high-resolution 3D data of vegetation canopies. LiDAR data can be acquired from spaceborne, airborne or terrestrial sensors, with each sensor meeting different vegetation mapping needs (Urbazaev et al., 2015; Levick & Rogers, 2008; Staben et al., 2018), improving predictions and minimizing extrapolation errors (Frazer et al., 2011). A key advantage of airborne LiDAR is wide geographic coverage but detection of smaller trees and shrubs, which are important components of savanna ecosystem functioning, is still challenging.

The last decade has witnessed a growing interest in ground-based LiDAR, or terrestrial laser scanning (TLS), for high precision 3D quantification of vegetation structure. TLS instruments facilitate unprecedented spatial structure and reflective representation of vegetation components, right down to individual branch and leaf scales (Dassot et al., 2012; Newnham et al., 2015). 3D data collected from TLS is considered to capture a much more holistic representation of vegetation structure than can possibly be achieved through manual fieldwork, and has successfully been applied as an effective and accurate approach to calibrate vegetation models (Dittmann et al., 2017; Calders et al., 2018), and define stand structural diversity (Ehbrecht et al., 2017). Also, metaproperties from TLS such as laser

returns, intensity and distance can reflect the underlying conditions of the ecosystem (Paynter et al., 2018). Key geometrical attributes including tree height (Hopkinson et al., 2004; Strahler et al., 2008), vertical height profiles (Singh et al., 2018) and canopy structure (Hardiman et al., 2018) can be reconstructed and measured with high accuracy from TLS data. Besides basic vegetation attributes, TLS point clouds enable non-destructive approaches to quantify canopy and stem volume, which reduces uncertainties in biomass estimations that arise from conventional inventory methods. (Calders et al., 2015; Disney et al., 2018; Stovall et al., 2018; Gonzalez de Tanago et al., 2018).

Realisation of the ecological importance of the 3D information that TLS provides has led to optimisations in data acquisition and processing. The acquisition of single scan TLS measurements offers a rapid and efficient means of characterizing vegetation structure (Liang et al., 2016), due to reduced field effort and faster post-processing, thereby enabling data acquisition at a greater number of sampling points. Single scan approaches have been successfully used for the estimation of canopy cover (Muir et al., 2018), wood volume (Astrup et al., 2014), basal area measurement (Seidel & Ammer, 2014) and vertical plant profiles (Calders et al., 2014). However single scan approaches can physically only sample one side of a tree and are more prone to occlusion of distant vegetation by the foreground elements (Strahler et al., 2008; Hilker et al., 2010; Wilkes et al., 2017). The degree of occlusion within a single scan is influenced directly by the vegetation structure, tree stand density and plot size (Olofsson & Olsson, 2018). A systematic multiple scanning approach with subsequent co-registration of scans reduces this occlusion effect (Wilkes et al., 2017), and has been shown to produce improved accuracy of vegetation structural metrics (Calders et al., 2015; Saarinen et al., 2017). The additional setup time and logistics associated with multiple position scanning (Wilkes et al., 2017) can lead to similar to that required for manual field inventories of vegetation structure (Newnham et al., 2015), and this often constrains the TLS measurements to plot-scales (<1 *ha*).

Much of the progress to date in TLS measurement of vegetation structure has taken place in temperate and tropical forested systems. As such, the sampling range of common TLS sensors has not been considered a limiting factor, since field of view seldom exceeds sensor range. In open systems like savannas, field of view can greatly exceed the sampling range of common TLS sensors. However recent break-throughs in time-of-flight LiDAR sensor technology have dramatically increased the usable sampling range of TLS sensors, with some providers now offering ranges of up to 6000 *m* (e.g. Riegl VZ-6000). These instruments have the potential to map entire hillslopes from a suitable vantage point with a single scan approach, allowing capture of data at 10-100's *ha* scales. Long-range terrestrial laser scanning (LR-TLS) necessitates trade-offs between laser energy and pulse frequency, where increasing pulse energy subsequently reduces the laser pulse frequency and increases scanning time. Although laser beams are coherent light energy, most sensors are subject to a degree of beam divergence, meaning that the width of the beam (footprint) increases with distance from the scanner. Over the short distances typical of plot-based TLS approaches this is of little consequence, but understanding the effects of beam diverge

on retrieval of vegetation structure parameter becomes important when considering long-range scanning.

In this study, we aimed to assess the potential of LR-TLS scans for extracting key structural attributes of savanna woody vegetation at hillslope scales. Specifically, we explore how structural measurements from LR-TLS degrade with distance from the scanner, and identify the distances over which LR-TLS can be reliably used for 3D structural characterization. Also this study highlights the implications of long-range scanning.

4.2 Methods

4.2.1 Study area

This study was conducted in the semi-arid savanna landscapes of Kruger National Park (KNP), South Africa (23°98'S, 31°55'E) (Figure 4.1). KNP is a national reserve located in north-eastern South Africa that encompasses an area of almost 2 million ha. We focused on two sites in the south-western part of the park, using natural vantage points at Mathekenyani and Stevenson Hamilton lookouts (Figure 4.1). The areas around these vantage points comprise of flat and low slope terrain that are dominated by the short height class and broad canopies of semi-deciduous *Combretums* and *Accacia nigrescens*, which occur in a matrix of evergreen *Euclea divinorum* (Gertenbach, 1983). Woody canopy cover ranges from as low as 20% to near closed canopy cover of 50% across dispersed trees and shrubs, and closed woodlands of more than 80% cover in riparian areas (Table 4.1). The region has a mean annual rainfall of 550 mm yr^{-1} , most of which falls between October and March (MacFadyen et al., 2018). Soils in most of the south-western KNP are derived from granite substrates which are nutrient-poor, and exhibit significant catenal variations from deep sand and loam on upland to duplex sodic soil on bottomlands (Venter, 1986).

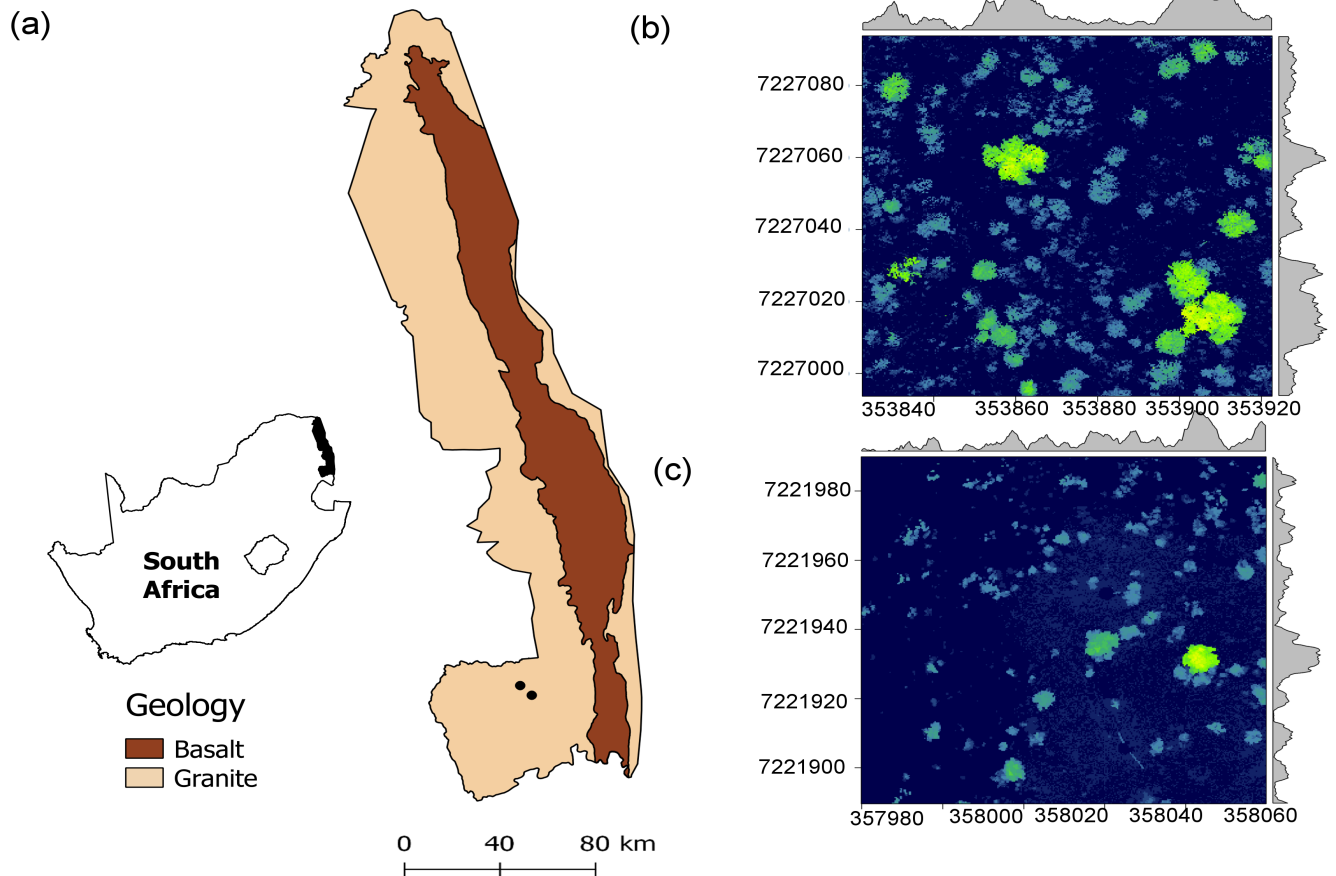


Figure 4.1: (a) Location of the two sampling landscapes (shown with black circles) in Kruger National Park, South Africa. The rightmost panels show examples of 2D LiDAR data from the two sites, with the level-plots describing vegetation heterogeneity. Mathekenyani and Stevenson sites are shown in (b) and (c) respectively.

Table 4.1: Characteristics of two study landscapes located in Kruger National Park, South Africa. Canopy cover and slope are calculated from the multi-scan TLS data.

Site	Plot	Canopy cover(%)	Elevation (m)	Understorey	Slope (°)
KNP	Mathekenyani	52.21	12	Little	1.95
KNP	Stevenson	37.7	25	Little	3.13

4.2.2 Terrestrial LiDAR sampling at landscape and plot-scales

Both sites were mapped in October 2016 (late dry season) using a Riegl VZ-2000 terrestrial laser scanning system (RIEGL Laser Measurement Systems GmbH). The RIEGL VZ-2000 is a multiple return long-range 3D scanner, which operates in the near-infrared spectrum (1550 nm) and produces a beam divergence of 0.35 mrad. The instrument provides the 3D information at a rate of 400,000 measurements sec⁻¹, and the measurements can be

obtained up to a distance of 2500 *m* on a natural surface. The inclination sensor provides rotation matrices (roll, yaw and pitch) of the scanner, allowing for accurate projection of the laser pulses. To improve the accuracy of the 3D positioning, LiDAR laser ranges were combined with an external differential Leica GS14 GNSS GPS (accuracy <3 *cm*).

The landscape scanning design consisted of acquiring single long-range scans from elevated vantage points. Scans were taken with an azimuth and zenith range of 180° and 100° respectively. The scanner settings were the same at both sites and are summarised in Table 4.2. This scanning setup resulted in a mean point density of 158.6 per *m*² at 100 *m* to 6.02 laser returns per *m*² at a distance of 600 *m*.

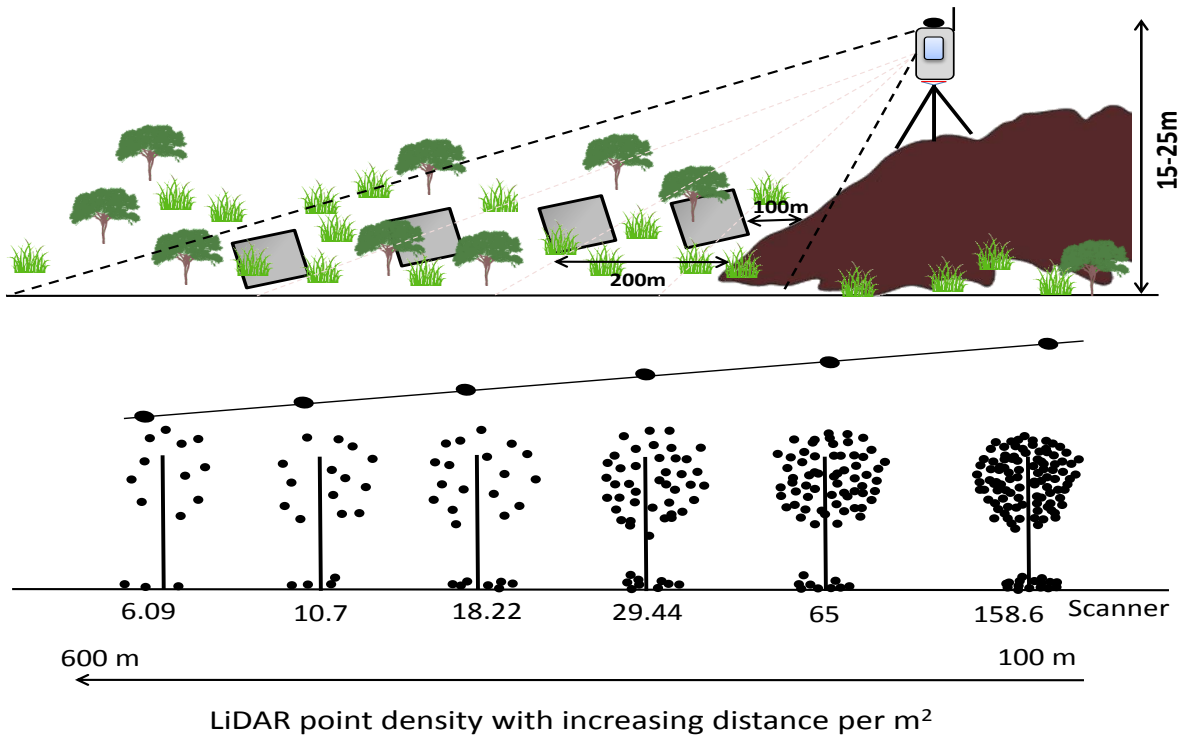


Figure 4.2: Conceptual representation of the long-range scanning set-up adopted in this study. The black outlined squares indicate the multi-scan reference plots positioned 100 *m* apart from each other, and overlaid in the long-range scan footprint up to 600 *m*, with an associated decreases in point density.

Table 4.2: Specifications for the RIEGL VZ-2000 scanner utilized for the 3D long-range data acquisition in Kruger National Park, 2016

Beam divergence	0.35 mrad
Pulse repetition rate	50 kHz
Angular sampling	0.02 degrees
Maximum range	1500 m
Acquisition time	35 minutes

In each landscape, we collected reference plots using a multi-scan set-up within equidistant 1 *ha* areas. Each reference plot was located within the footprint of the LR-TLS scans

(Figure 4.2). We placed six reference-plots in 100 *m* intervals up to a distance of 600 *m* from the vantage point. The reference-plots were scanned from the four cardinal directions at 550 *kHz*, with an angular resolution of 0.02°. The multi-scan approach captured the full 3D structure of the plots, providing a level of structural detail that cannot be achieved through manual field-measurement. As such, we treated these plots as ground-truth data against which to assess the LR-TLS (Figure 4.3).

4.2.3 Point cloud processing

LR-TLS and reference-plot scans for each respective landscape were co-registered using the RiSCAN PRO package (RIEGL GmbH), to eliminate the rotation errors between different scans. A coarse registration between the scans was achieved by using large woody trees (branch tips and nodes) as the tie points. Fine tuning of translation and rotation errors within the scans was done by using multi-station adjustment (MSA) approach. MSA uses iterative closest point (ICP) algorithm to adjust the orientation and position of each 3D dataset, and calculates the best overall fit. The best fit transformation and rotation matrix are applied to each raw point cloud to associate them to a common coordinate system. The standard deviation for the distances between merged point clouds ranged from 0.01 to 0.02 *m*. The point clouds were post-processed to remove noise occurring due to partial or false returns from the sky or dust by using the range and deviation default filters in RiSCAN PRO.

The co-registered LiDAR data points from reference-plots and LR-TLS scans were then ground classified, and height normalized. Canopy height models (CHM) from normalized point clouds were generated by selecting the highest ‘z’ coordinate 3D point among all LiDAR returns within a ‘1 x 1 m’ grid cell, thus converting the 3D data to raster for further analysis. The resulting canopy height grids were classified in SAGA GIS (www.saga-gis.org). LiDAR data between 0.0 and 0.5 m was classified as ground points, while all points above 0.5 m were categorized as vegetation. These classified grids were aggregated to percentage canopy cover at ‘30 x 30 m’ for every reference and LR-TLS plots. The number of ‘1x1’ m pixels in every ‘30 x 30 m’ grid with height greater than 0.5 m were then divided by the total number of ‘1 x 1’ pixels in that grid, yielding the percentage of canopy cover present in each grid cell. For the comparison between LR-TLS and the reference-plots, difference values were derived by subtracting the value of each pixel of the LR-TLS raster from the corresponding pixel of the reference-plot raster.

Normalized point clouds were used to produce the LiDAR return counts from 0 m at every 0.5 m interval of the LiDAR data in LAStools (rapidlasso GmbH, 2014;Isenburg (2014)). These LiDAR counts were converted to percentage of frequency, and plotted against canopy height to visualize the vertical vegetation profiles of the landscapes.

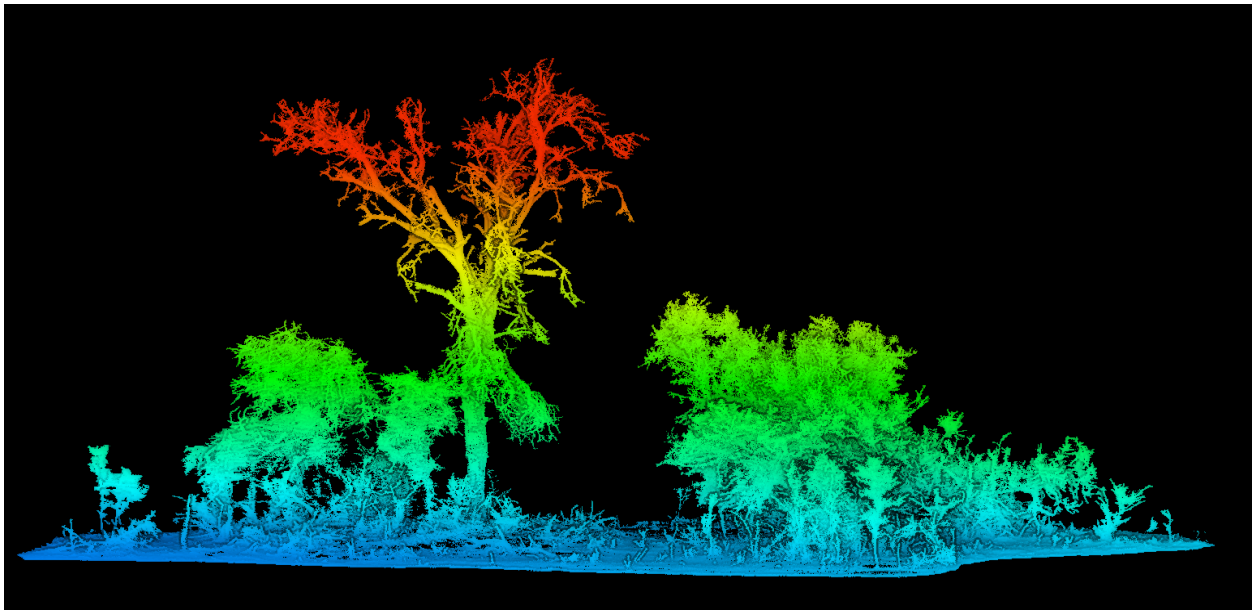


Figure 4.3: Reference-plot example, derived from multi-scan TLS and shown in oblique view with colour scale representing height above ground level. TLS instruments capture vegetation 3D structural detail in a holistic manner that cannot be recorded manually in the field.

4.2.4 TLS derived indicators for validation at individual tree scales

3D data collected from LR-TLS and reference-plots were used to estimate structural parameters for individual trees, such as the plant height (m) and ground projected area of the canopy (m^2). The individual trees and shrubs were extracted from the normalized LR-TLS and reference-plot scans, using Quick Terrain Modeler (www.appliedimagery.com). In each segmented tree and shrub, LiDAR measured plant height was determined as the vertical distance between the highest point and stem base at the ground. The segmented trees and shrubs were converted to raster form by generating the individual canopy height models (described in section 4.2.3). Gaussian filtering with varying parameters were implemented on the individual trees and shrubs to smooth the canopy surface. A standard deviation of 1 and search radius ranging from 2-5 m was used in the Gaussian filter. The next step was applying the watershed segmentation, which assumes the presence of dark pixels in between tree crowns, where dark pixels represent ground surface while bright pixels represent tree canopies. To reduce the high degree of over-segmentation within a tree crown, threshold based region merging was implemented to amalgamate the segments. These segments were later converted to polygons and area geometry was calculated to extract canopy area. An individual watershed segmentation approach over plot-scale segmentation was implemented to overcome the high degree of segmentation within individual trees due to presence of multiple stem allometry.

4.2.5 Statistical analyses

To evaluate the effect of increasing distance on LR-TLS performance, we distributed 30 x 30 *m* grid within overlapping footprints of the LR-TLS scans and the reference-plots and extracted the height and canopy cover metrics. Statistically significant differences among canopy metrics from LR-TLS and reference plots were determined with a paired-sample t-test ($p < 0.05$). A linear regression between reference and long-range LiDAR woody cover and height at plot and individual scale was calculated and model performance was assessed with coefficient of determination (R^2). To account for the error propagation in the two sites, root mean square error (RMSE) and bias between LR-TLS and reference-plots was calculated.

Vertical height distribution profiles from the LR-TLS and reference-plots at increasing distance from the scanner were compared with respect to distribution patterns. To test whether increasing distance from the scanner had a significant effect on the vegetation vertical profiles, a two-tailed Mann Whitney U test was performed with a confidence interval of 0.05. The statistical significance was evaluated at 3 height classes - (i) 0 – 2.5 *m* (understorey and shrub), (ii) 2.5–5.5 *m* (midstorey) and (iii) 5–8 *m* (overstorey).

4.3 Results

4.3.1 Vegetation height-class characterisation with LR-TLS

Comparison of the proportional distribution of LiDAR returns by height class showed that LR-TLS scans were capable of closely replicating the vegetation vertical profile structure of the savanna landscapes, despite their lower point density (Figure 4.4 and 4.5). A general trend of increasing divergence between LR-TLS and reference-plot data was observed with increasing distance of laser ranging.

With a mean woody canopy cover of 52.21 % within the 1 *ha* reference plots at the Mathekenyani site, the overall distribution of LiDAR returns at a distance of 100 *m* from the LR-TLS was analogous to the reference ($t = -1.84, df = 14, p = 0.08$) (Figure 4.4). In general, up to a distance of 400 *m*, the LR-TLS derived vertical profiles represent a symmetric distribution with those of the reference-plots ($p > 0.05$, for the 3 height classes). At 500 *m* distance, significant differences in point distribution arose in the shortest height class ($p = 0.04, t = -2.92, df = 4$), while the relative distribution of points for the two taller classes was similar between LR-TLS and reference-plots ($t = 1.8331, df = 4, p = 0.14$).

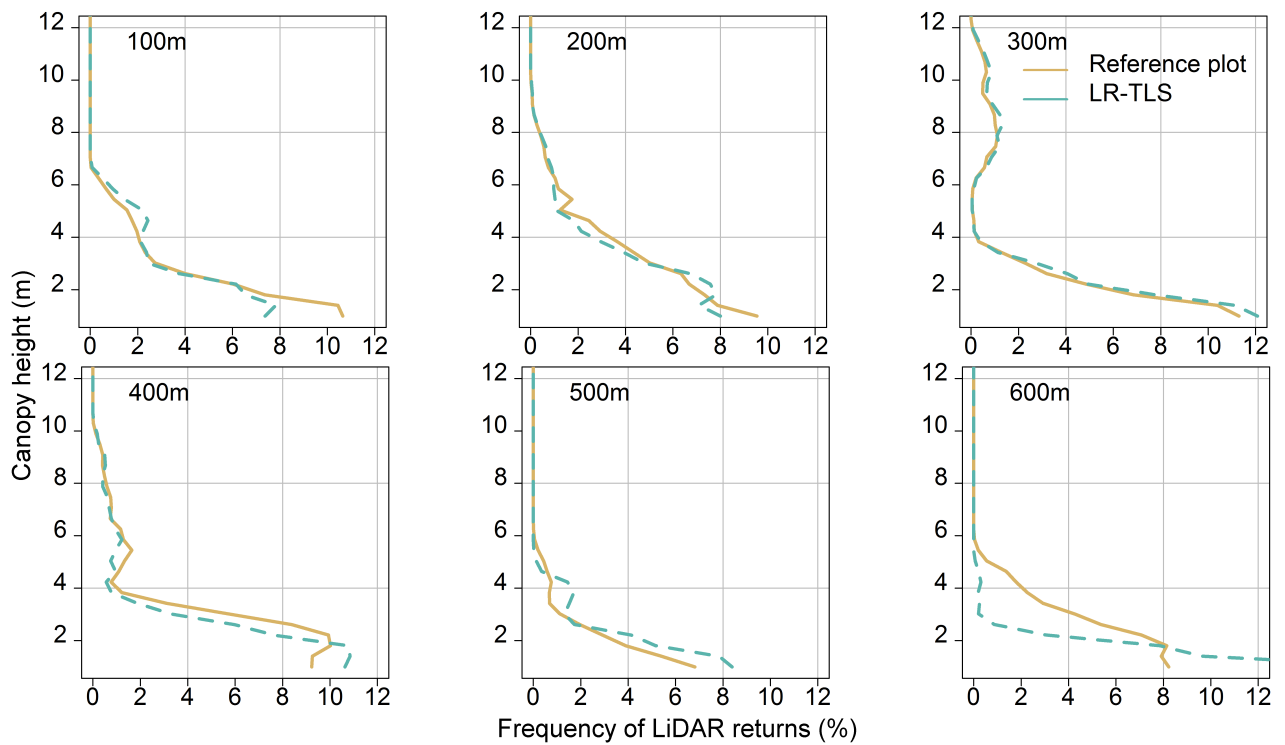


Figure 4.4: Comparison of vertical height distribution derived from LR-TLS and reference-plots in vertical intervals of 0.5 m at increasing distances in the Mathekenyani landscape.

Differences in vertical vegetation profiles in the Stevenson-Hamilton landscape were more variable across the range of distances explored. Vertical profiles shape was very similar up to 400 m distance ($p > 0.05$) (Figure 4.5). However, some individual plots showed large discrepancy between the LR-TLS and reference profiles. For example, at 100 m distance there was a relatively greater proportion of returns from the mid-storey vegetation in the LR-TLS profiles than the reference-plot profiles, and deviated across the height range at distances of 500 m and 600 m (Figure 4.5).

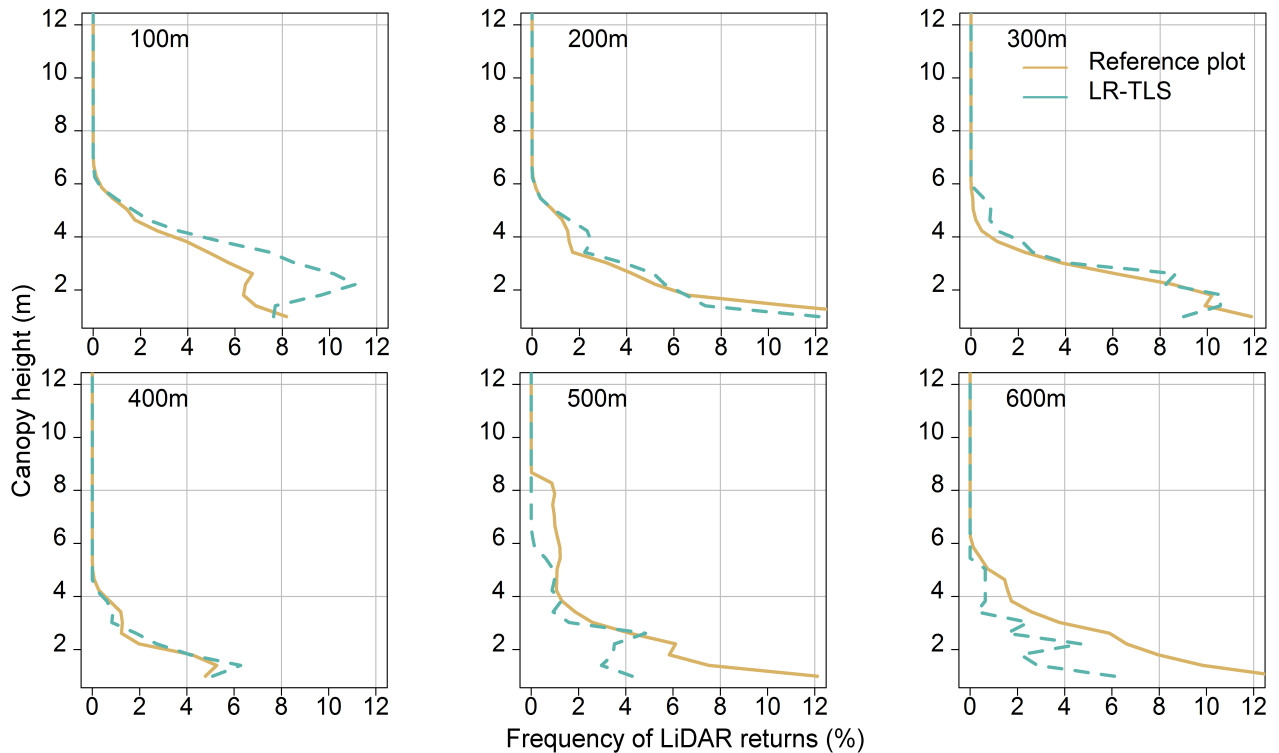


Figure 4.5: Comparison of vertical height distribution derived from LR-TLS and reference plots in vertical intervals of 0.5 m with increasing distances in the Stevenson-Hamilton landscape.

4.3.2 Canopy height and cover differences

The overall distribution of canopy heights within the three defined height classes measured with LR-TLS correlated well with reference-plot metrics, performing better at Mathekenyani ($R^2 = 0.80$) than at Stevenson-Hamilton ($R^2 = 0.54$) (Table 4.3) and (Figure 4.6).

The performance of LR-TLS in the estimation of mean canopy height was similar among the two landscapes, and tended to slightly overestimate canopy height. Mean canopy height differences between LR-TLS reference-plot values were not statistically different up to a distance range of 600 m in either landscape (Mathekenyani: $p = 0.79$, Stevenson: $p = 0.26$). Underestimation of canopy height was greater (1.62 m difference) where undulating hillslopes and denser canopy was present, such as at the 500 m plot in Stevenson-Hamilton landscape, and negligible (0.10 m) on flatter more open sites.

Table 4.3: The mean canopy height (m) values derived from reference plots (RP) and LR-TLS (LR). SD is the standard deviation.

Ranging distance (m)	Mathekenyani				Stevenson					
	RP _{mean}	RP _{SD}	LR _{mean}	LR _{SD}	p	RP _{mean}	RP _{SD}	LR _{mean}	LR _{SD}	p
100	1.49	0.26	1.31	0.25	0.33	2.92	0.58	2.61	0.45	0.14
200	1.50	2.19	1.78	0.51	0.38	1.95	0.37	1.33	0.41	0.02
300	2.25	1.10	2.51	0.62	0.54	3.08	1.02	2.10	0.64	0.08
400	1.53	0.51	1.97	0.54	0.11	0.98	0.37	0.70	0.51	0.47
500	1.35	0.58	1.45	1.05	0.12	3.17	2.12	1.55	0.74	0.05
600	2.73	0.41	1.43	0.55	0.79	1.49	0.47	1.20	0.59	0.26

Table 4.4: The mean canopy cover (%) values derived from reference plots (RP) and LR-TLS (LR). SD is the standard deviation.

Ranging distance (m)	Mathekenyani				Stevenson					
	RP _{mean}	RP _{SD}	LR _{mean}	LR _{SD}	RP _{mean}	RP _{SD}	LR _{mean}	LR _{SD}	<i>p</i>	
100	24.82	6.07	28.65	5.32	0.17	34.59	11.64	35.59	9.71	0.84
200	25.80	7.40	26.30	4.85	0.86	22.73	13.00	17.72	5.75	0.29
300	24.71	7.76	23.55	4.25	0.70	26.77	11.98	23.53	5.83	0.48
400	26.63	7.98	19.78	9.23	0.11	8.32	4.42	4.09	2.07	0.02
500	25.25	5.35	26.98	12.02	0.70	13.92	7.86	9.53	5.16	0.18
600	26.97	7.72	16.81	7.10	0.01	20.96	9.99	5.53	2.22	0.01

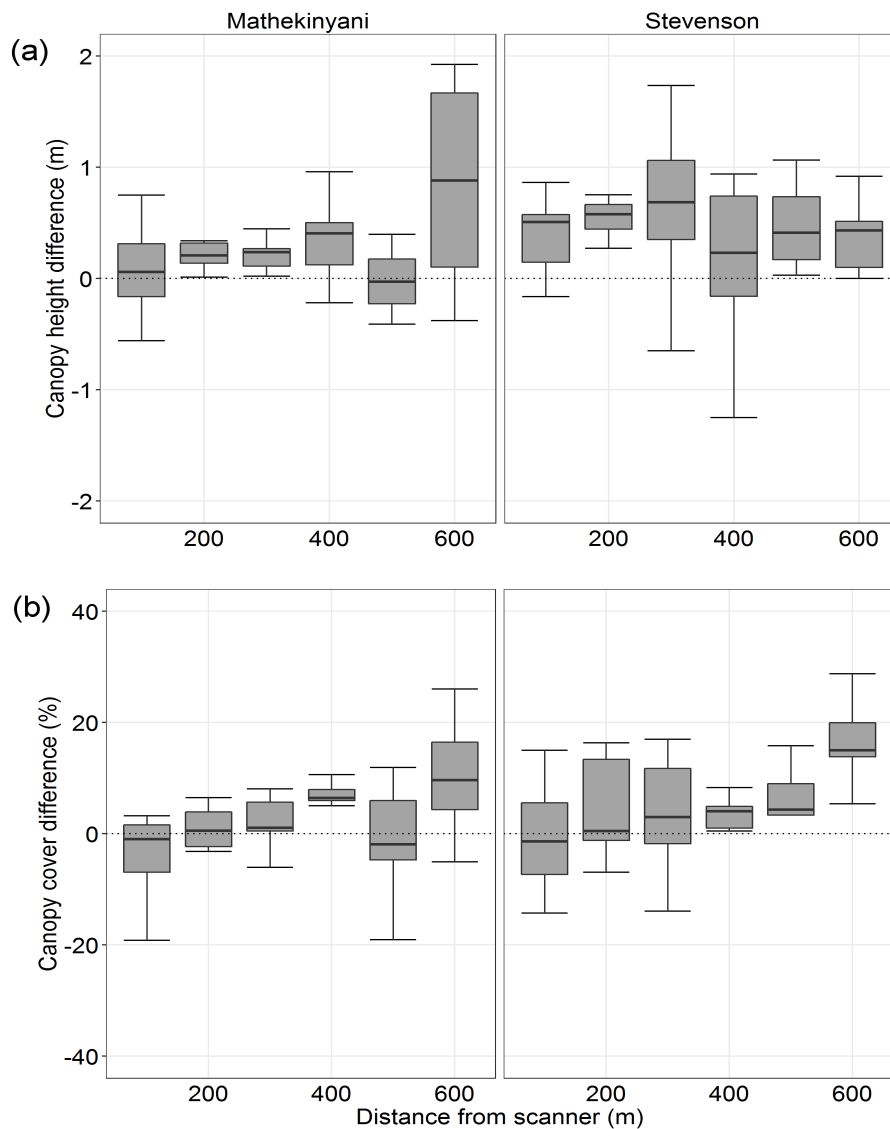


Figure 4.6: Canopy height (a) and canopy cover (b) differences between LR-TLS and reference-plots with increasing ranging distance.

Canopy cover estimates from LR-TLS demonstrated high correlation with the reference-plot data, with slight overestimation in both landscapes (Table 4.4). Differences in canopy cover estimates increased exponentially with ranging distance, varying from 1 % in the closer plots to a maximum of 15.43 % in the distant plots (Figure 4.6). Agreement between LR-TLS and reference-plots was best across plots on flatter terrain.

4.3.3 Individual tree metrics

For individual trees and shrubs, LR-TLS measured canopy heights were linearly correlated with the reference-plot data in both landscapes up to 400 m ranging distance ($R^2 = 0.99 - 0.87$, Figure 4.7 a,b). The detection of individual stems, especially shorter-statured shrubs, declined at distances greater than 500 m in both landscapes, resulting in an

underestimation of height. The RMSE for the canopy height at the furthest measured plots (600 m) were 2.44 m and 1.14 m respectively for Mathekinyani and Stevenson-Hamilton landscapes.

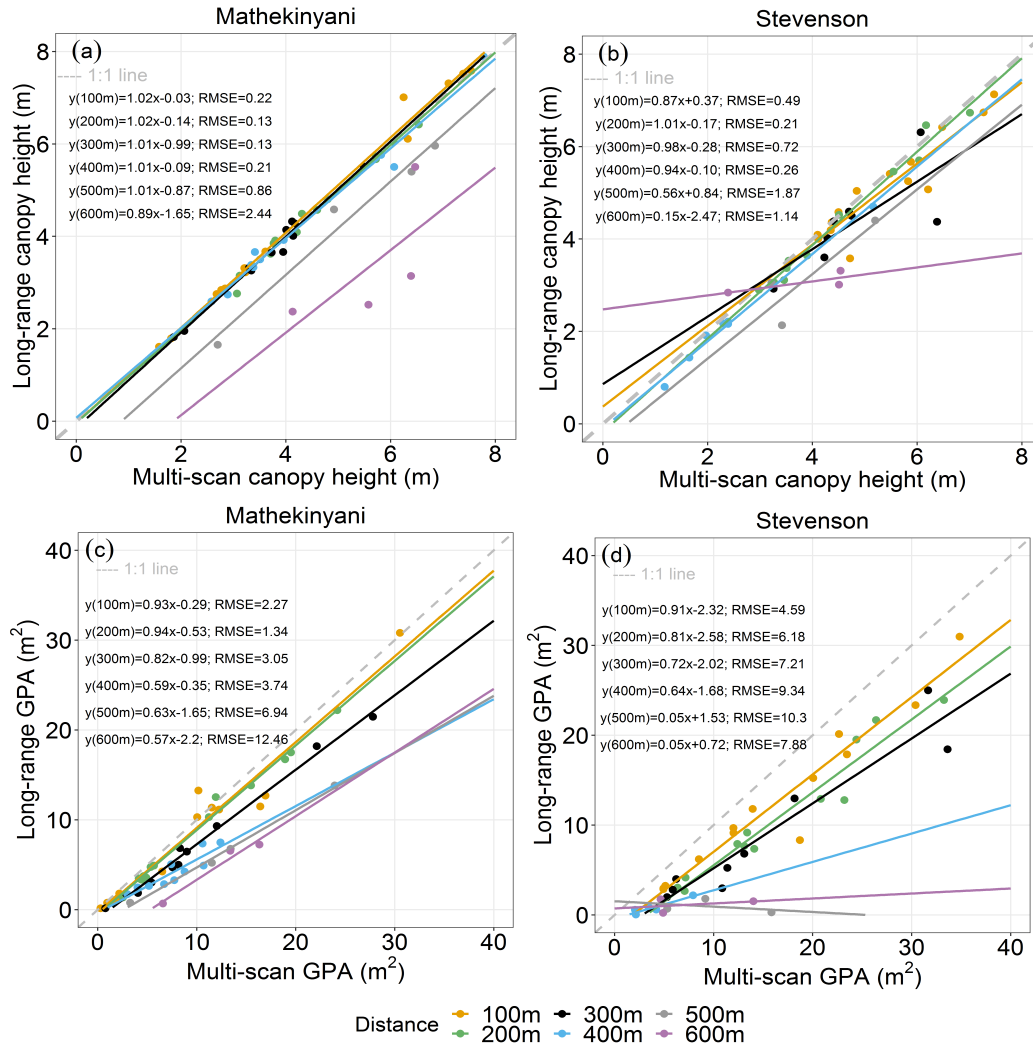


Figure 4.7: (a) Deviation in canopy height, and (b) canopy ground projected area (GPA) with increasing ranging distance in the two study landscapes. The colour coding represents the linear interpolation model at different laser ranging distances.

Canopy ground projected area for the individual trees can be determined with high confidence from the long-range scans up to 300 m of distance ($R^2 = 0.99 - 0.79$, Figure 4.7c,d). As canopy ground projected area is directly proportional to the point density, strong underestimation in the long-range scans is observed after a distance of 300 m ($RMSE > 3.05$). The linear regression model between reference and long-range scans differed at two sites, with the slopes of Stevenson site model diverging the most from the 1:1 reference line after a distance of 300 m (500 m: $R^2 = 0.16$, $RMSE = 10.3$; 600 m: $R^2 = 0.12$, $RMSE = 7.87$ Figure 4.7c,d).

4.4 Discussion

Our results demonstrate the utility of long-range terrestrial laser scanning (LR-TLS) for quantifying savanna vegetation structural metrics at hillslope-scales. Despite the trade-offs of long range scanning (reduced point density and increased beam divergence at longer ranging distances), we found that vegetation structural parameters can be reliably extracted up to 500 *m* away with LR-TLS in savanna landscapes, enabling structural sampling over broader areas that encompass the inherent heterogeneity.

4.4.1 The effect of increased ranging distance on the error propagation

LR-TLS and reference-plot vertical profiles were generally well matched, indicating that long-range scan observations can account for 3D vegetation structural patterns. The vegetation vertical profiles from LR-TLS mirrored the shape of the reference-plot profiles, with the relationships only degrading at ranging distances longer than 400 - 500 *m*. This effect arises from both the increased beam divergence, leading to reduced sensitivity to finer-scale vegetation elements, and a decrease in point density. We consider the decrease in point density to be a function of both the angular sampling resolution of the scanner, as well as site specific conditions which relate to increased occlusion from foreground vegetation and a loss of ground returns at lower incidence angles at longer ranging distances.

The reliable performance of height estimation from LR-TLS in our study landscapes was likely due in part to the presence of sparse canopies, and the clear lines of sight that characterize savanna landscapes. The accuracy of long-range scanning for vegetation metrics retrieval differed slightly among the two landscapes, reflecting differences in vegetation physiognomy and terrain morphology. Increased ranging distance from the scanner had less impact on canopy height retrieval in the Mathekenyani landscape, characterised by larger trees, than at the Stevenson-Hamilton landscape which was more shrub dominated. In addition to the distribution of taller trees, differences in canopy architecture due to leaf shape and branching angles, could have influenced these differences. For instance frequent crown openings in large tree dominated Mathekenyani landscape allowed deeper penetration of the laser pulses, and thereby resulting in a low RMSE of 0.32 *m* at 500 *m* distance. Srinivasan et al. (2015) also reported the underestimation of canopy height due to increasing canopy branching and distance from the scanner. Thus, when employing single scans for quantifying vegetation metrics, it is important to consider the laser pulse penetration through canopies to reduce the shadow effects and incomplete sampling of the vertical profiles. Also, some canopy height measurement error at the Stevenson-Hamilton landscape occurred as a result of topographic effects, where occlusion from catenal hillslope crests caused a reduction in ground returns. At the longer distances of 600 *m*, this shadowing by topography can misrepresent the true tree height in the normalisation phase of the processing chain. This potentially leads to canopy height bias because accurate representation of the terrain is crucial for calculating the canopy height models.

These factors discussed above are also relevant for canopy cover estimation, however as cover is an area based measure further considerations also apply. The high deviation and RMSE of canopy cover estimates after 400 *m* can be attributed to the occlusion of lower strata vegetation, the step size, at which 'z' value is interpolated for every output pixel of the CHM, and the window size for subsequent analysis. Decreased sensitivity to smaller vegetation individuals and components with ranging distance leads to a cumulative decline in canopy cover estimates. Usually a step size close to the laser spot size is recommended for resolving small vegetation individuals (Khosravipour et al., 2014), however we found that small vegetation elements and understorey plants can not be reliably identified by keeping the same step size with increasing distance from the LR-TLS. Laser spot size for Riegl VZ-2000 increases by 0.3 *mm* per 100 *m* of range (Riegl VZ-2000 datasheet), and as such the step size should therefore be adjusted at every 100 *m* range to account for the increasing beam diameter. The window size used for subsequent analyses also strongly influenced the accuracy of canopy cover estimates derived from LR-TLS. We found that the RMSE and linear regression model fits improved as window size increased from 0.09 *ha* to 1 *ha*. Though, Wilkes et al. (2017) describes 10 x 10 m sampling grid as an upper size limit for characterizing vegetation structure in a homogeneous and closed canopy sites. However, in heterogeneous savanna landscape, trees are non-uniform in size and widely spaced, providing enough laser pulse penetration through the sampled area. A lower perimeter to area ratio in large plot sizes results in fewer plot-edge effect, due to presence of tree crowns located outside the plot (Levick et al., 2016).

For individual large trees, LR-TLS accurately depicted the structure at ranging distances up to 400 *m*. Even small branches were documented at these distances, and the branching structure was retained in the LR-TLS data (Figure 4.8a). While LR-TLS could characterize the shrub height reliably, the internal canopy structure of shrubs in the farthest plots could not be differentiated (Figure 4.8b).

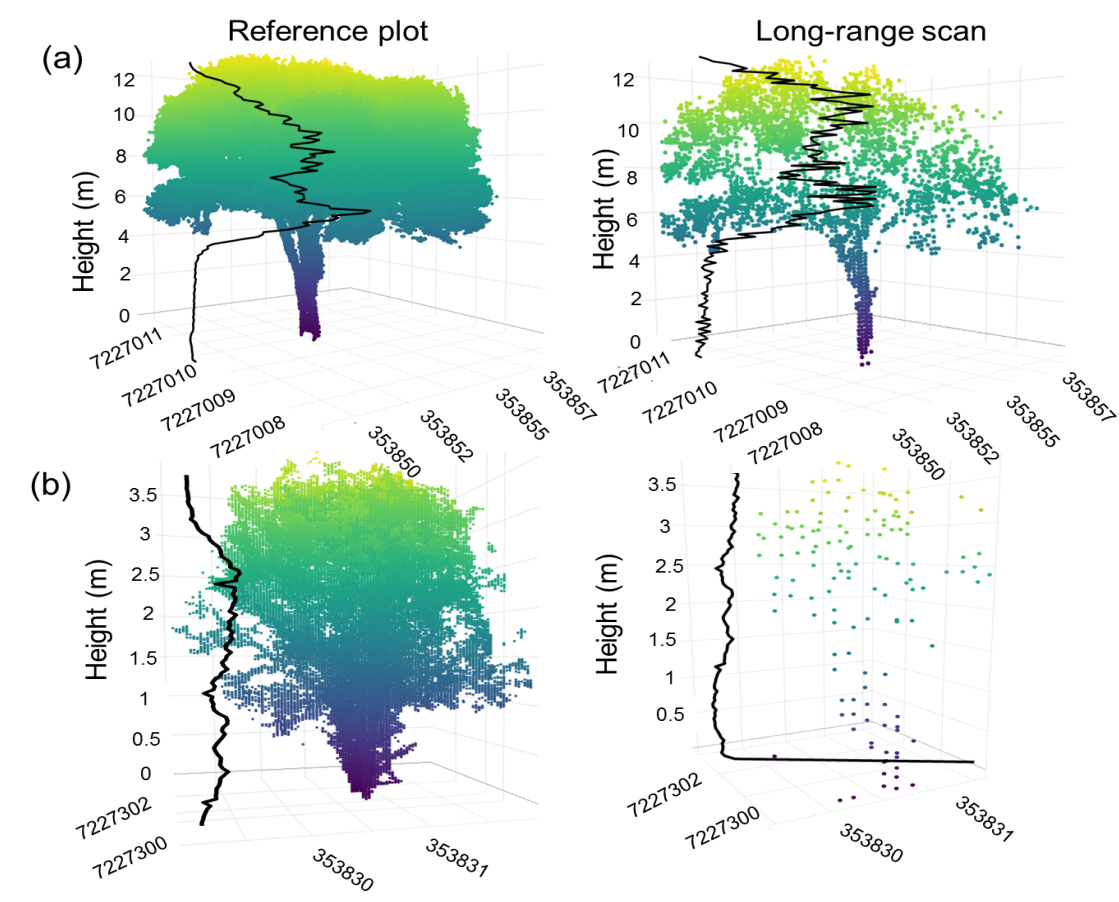


Figure 4.8: An example of height normalized LiDAR returns of a single tree (a) and shrub (b) from reference-plots and LR-TLS at a ranging distance of 400 m.

Underestimation of individual tree height with increased ranging distance was most often due to the loss of the lower stem architecture and ground points. Denser scan patterns, i.e. multi-scan approaches, increases the ability to resolve the stem architecture, particularly towards the ground, and therefore increases the fidelity of canopy height and projected area estimates. Larger differences in individual tree canopy height and ground projected area at distances further than 300 m were particularly evident in the Stevenson-Hamilton landscape, where presence of undulating terrain and a slope of 3.1° led to the attenuation of laser pulses and more occlusion.

4.4.2 Reliable quantification of 3D vegetation structure at hillslope-scales

LR-TLS suitably captured vegetation structural measures such as height, height profile distribution, and canopy cover at both plot and individual tree scales at distances of up to 400 m and 500 m in the two landscape we studied. Earlier studies demonstrate the utilization of TLS based vegetation metric estimation confined only to 0.01-1 ha spatial scale (Beland et al., 2019). In our study, if we consider 400 m as conservative range for reliable structural quantification, LR-TLS could theoretically be used to sample 50 ha of

landscape in a single scan - taking less than 1 hour with the settings used in this study. Of course this is assuming a full 360° scan from a point elevated above the canopy, which is not feasible in many situations. Nonetheless, even if only 180° or 90° scanning is possible - this approach still enables the acquisition of 3D structural data over 10's *ha* - scales that are required to adequately represent the heterogeneity of savanna ecosystems. Even larger areas can potentially be reliably mapped with the proposed method, if the vegetation is not obscured by occlusion and if the survey position can be elevated higher above the canopy. Topographic occlusion in the sampled areas was lowest at the Mathekenyani landscape, while the 3D point cloud at Stevenson-Hamilton displayed greater occlusion. The amount of occlusion also varied with vegetation physiognomy and distribution, as well as the height of the sensor in relation to the landscape. A sparse canopy and a mean nearest difference of 2 - 3 *m* between individuals was sufficient to prevent the attenuation of laser pulses in the Mathekenyani landscape. Also, the wider beam diameter at increasing distance (beam diameter = 0.3 *m* at 1000 *m*) from the scanner reduced the penetration through the understorey. Ducey et al. (2013), suggested that a small beam diameter leads to a better penetration through low branches and understorey vegetation. Raising the scanner higher above the canopy layer is the best option for reduce the occlusion effect, but statistical methods can also be employed to adjust the effects of occlusion (Strahler et al., 2008; Lovell et al., 2011).

With a high angular resolution of 0.02 degrees, 3D point clouds with a density of $>5/m^2$, at distances up to 600 *m* was produced, allowing long-distance scans to capture a large proportion of the target canopies and tree individuals. Point density diluted exponentially as the distance to the scanner increased, resulting in a heterogeneous point density. Many studies have reported that heterogeneous point density from single scanning mode has no adverse effect on the retrieval of physical attributes such as canopy height and cover (Thies & Spiecker, 2004; Maas et al., 2008; Moskal & Zheng, 2011), but ours is the first to explore the consequences over such long distances. Uniform point density is often required for clustering and classification of 3D points clouds with semi-automatic approaches (Olofsson et al., 2014), but this could be achieved by sub-sampling the point clouds if needed.

4.4.3 Limitations and future direction for large scale monitoring of savanna vegetation

Our use of LR-TLS has provided an alternative method for characterizing savanna vegetation structure at hillslope scales. However, we acknowledge a few limitations of this approach, which should direct new research and method development in this direction. First, our results may not extrapolate well from open savanna to other vegetation communities. For example, at riparian sites occlusion by dense understorey layers will inhibit deep laser pulse penetration up to 400 *m*. Also, performance of the LR-TLS will differ among flat and undulating terrain, with more bias in canopy height measurements in landscapes with undulating morphology. In general, occlusion could be reduced by acquiring multiple LR-TLS scans from different positions. Second, our study explored the efficiency of LR-TLS over two landscapes in open savanna, and a larger sample size will

be required to ascertain the generality of this method in different systems. Third, our use of LR-TLS is unique in that the scanner was positioned above the canopy to capture hillslope-scale 3D data. We had the advantage of the elevated vantage points, but at other sites alternatives such as elevating tripods or vehicle roof top mounts can be explored. Lastly, the individual plant scale analysis required a high degree of manual processing to extract single trees from the point cloud data. Although much progress has been made on automating these tasks in forested systems (Burt et al., 2018), these techniques need further development before they can be successfully applied to savanna tree structures which are more complex. This opens up the possibility of testing various automatic segmentation approaches for single tree extraction from LR-TLS, and subsequently realizing the potential of open access tools such as ForestR (Atkins et al., 2018) in defining the vegetation complexity.

In the next few years, vegetation structural information will be available from a number of satellite missions, including L - and S-band SAR (NISAR), P-band SAR (BIOMASS), spaceborne ISS-mounted LiDAR (GEDI) and ICESat-2. These products will facilitate mapping at regional and global scales, and will compliment the availability of open-access and high spatio-temporal resolution imagery from the Sentinel platforms - providing very valuable opportunity for fine characterization of savanna vegetation at landscape to regional scales. While the data collection capabilities can always be enhanced, the real challenges for applying these sensors to large area monitoring are calibration and validation. Field-based plot inventory data are not suitable in isolation, and while airborne LiDAR currently plays a key role and will continue to do so, we also need to explore new ways for reducing uncertainty in biomass allometries and upscaling models. For open tree-grass systems and shrublands, the LR-TLS approach presented in this paper can provide the continuum of ground reference data that can also encompass stand variation. This has the potential to improve the spatial extrapolation of vegetation structure from remote sensing proxies, which is a key to reducing uncertainties in the global carbon budget. Furthermore, the fixed scanning position of LR-TLS will enable repeat measurements of higher precision than what is possible from aircraft or UAV platforms, opening the door for examining fine-scale dynamics in vegetation canopies over hillslope scales. This is particularly relevant in savanna ecosystems, where future research should explore the potential of repeat LR-TLS to analyze structural changes over time for understanding the loss of big trees and patterns of woody encroachment (Levick & Asner, 2013; Lindenmayer et al., 2012).

4.5 Conclusions

Our exploration of long-range terrestrial scanning (LR-TLS) shows great promise for the reliable extraction of savanna woody vegetation inventory parameters including canopy height, vertical profile distribution, and canopy cover at hillslope scales. Plot and individual tree level metrics can be accurately retrieved from ranging distances of 400 *m*, meaning that 10-50 *ha* can be sampled in under one hour depending on the landscape. The use of

66 Mapping savanna landscapes - A long-range terrestrial laser scanning approach

LR-TLS for vegetation mapping in savanna will help overcome a key limitation of TLS in terms of limited spatial extent, enabling measurement and monitoring at hillslope-scales. LR-TLS will provide a useful tool to compliment field and airborne surveys in the direct calibration and validation of satellite derived biophysical attributes.

Chapter 5

Improved characterization of woody vegetation at regional scales using earth observation data

Abstract

Quantifying regional scale estimates of vegetation structure and aboveground biomass (AGB) is a major challenge in savanna landscapes due to their inherent heterogeneity. Most field-based measurements, and remote sensing calibration/validation exercises, occur at local plot scales that may not adequately represent the highly variable tree cover present in savannas. We reconstructed three-dimensional (3D) vegetation structure at broad landscape scales across a semi-arid savanna in South Africa, using long-range terrestrial laser scanning (LR-TLS). We sampled vegetation structure across hillslopes from topographic vantage points at multiple locations, covering more than 900 *ha* of diverse habitat. We used LR-TLS estimates of woody cover and canopy height to model AGB at landscape scales. Our high-resolution woody parameter layers were integrated with L - and C - band radar satellite imagery (ALOS-PALSAR-2 and Sentinel-1), to map woody properties over the broader savanna region that had gradients in rainfall as well as variable geology. We conducted a sensitivity analysis to assess the vegetation height threshold at which radar backscatter was most responsive to woody canopy. The correlation between radar backscatter and LR-TLS derived woody properties peaked at 2 *m* above ground level for the L-band data, and at 1.5 *m* for the C-band data (R^2 for HV ALOS-PALSAR-2 was 0.7 and R^2 of VH Sentinel-1 was 0.52). The root mean square error (RMSE) of the AGB estimation differed from 6.65 $Mgha^{-1}$ for the ALOS-PALSAR-2 to 8.04 $Mgha^{-1}$ for the Sentinel-1 backscatter data. These results highlight the need for explicit consideration of woody canopy height thresholds in regional scale biomass mapping. Furthermore, while current L- and C-band sensors capture larger vegetation structures well, they are not sensitive to the shrub layer - which is also missed in most airborne LiDAR surveys, and can make up a significant proportion of AGB in certain savannas. Understanding shrub layer dynamics is important for assessing trajectories of ecosystem change, and for moving beyond carbon accounting to more holistic measures of habitat condition. LR-TLS provides a robust means for assessing how well vegetation structures are represented from space, and could facilitate the refinement of AGB up-scaling equations in heterogeneous landscapes.

5.1 Introduction

Savanna ecosystems are a continuum of mixed physiognomies, defined by the patchy occurrence of woody and herbaceous plant communities in the landscape (Bond, 2008; Scholes & Archer, 1997). This coexistence of two plant guilds causes exceptional heterogeneity in ecosystem structure (Pickett et al., 2003), which varies from size class distribution (Rogers et al., 2003; Helm & Witkowski, 2012) at landscape scale to three-dimensional arrangement of vegetation elements from ground to top of canopy at plant scale (Archibald & Bond, 2003). Precipitation, fire regimes and herbivory maintain and amplify the growth rates and composition (Sankaran et al., 2005; Smit et al., 2010; Asner et al., 2009; February et al., 2013), and further exacerbate the spatial organization of savanna structure components. Due to the large spatio-temporal fluctuations in the vegetation structure, savanna carbon dynamics represent a large uncertainty (Ciais et al., 2011; Higgins et al., 2007). Therefore, accurate estimates of vegetation structure and biomass across savanna landscapes is vital to assess the absolute magnitude of carbon stocks and fluxes emerging from these dynamic systems. Such information is critical for refining the uncertainties in land-atmosphere carbon fluxes, due to fire, and to assist in predicting the trajectories of savanna vegetation dynamics under changing climate and land use practices (Wessels et al., 2011; Kgope et al., 2010; Wigley et al., 2010). While vegetation structure maps are of interest to international initiatives such as REDD+ and UNFCCC, the scope and scale of this opportunity remains unclear in savannas.

Our ability to quantify the spatial pattern of vegetation structure and biomass in savanna ecosystems are often based on plot-scale field inventories conducted in traditional ways (Higgins et al., 1999; Eckhardt et al., 2000; Cook et al., 2005). However, these field-based measurements are limited in their capacity to capture the multi-dimensional variability in savanna structure, due to their small sample sizes from sparse distribution and insufficient plot size (Staver, 2018). In addition, the measurements fail to account for allometry of multi-stemmed individuals, and the vertical distribution of woody structures from the ground to the top of canopy. Terrestrial laser scanning (TLS) also referred as Terrestrial LiDAR (light detection and ranging) offers an efficient solution to the problems of unrepresentative structure. TLS acquires the detailed three dimensional (3D) representation of the vegetation by transmitting coherent laser beams and measuring distances based on the time delay of the returned laser pulses (Newnham et al., 2015; Dassot et al., 2011). The returning laser signals characterize the spatial arrangement, size and radiometric attributes of woody and non-woody components. As a result, 3D data from TLS provides a non-destructive, repeatable and automated way to quantify the vegetation metrics within an ecosystem. The application of TLS technology to semi-arid landscapes is rapidly expanding, and has been used to estimate basic vegetation metrics such as canopy height, cover and vertical distribution of 3D points with high accuracies (Anderson et al., 2018; Olsoy et al., 2016; Muir et al., 2018; Singh et al., 2018). While strength of TLS data in replicating field measurements is evolving over the years (Calders et al., 2015), the measurements are normally confined to the same plot scales (<1 ha) that also

apply to regular inventory methods. Those spatial scales may miss regular variations with topography, rainfall or underlying geology that operate at broader spatial scales. Recent advancements in laser scanning has allowed TLS devices to be optimized for long-range (>100 *ha*) scanning by having a trade-off between the laser energy and pulse rate, which enables to spatial mapping of large areas. Singh et al. (2020), demonstrated the potential of long-range scanning for estimating savanna woodland vegetation structure in leaf-off condition. The authors acquired continuum of ground data, and reported a high retrieval accuracy of canopy height and cover, with a RMSE of 0.25 m and 5.67% respectively. In essence, long-range scans in savanna ecosystems present an opportunity to go beyond plot-scale inventories, and extrapolate the measurements to broader landscapes using satellite measurements.

The growing availability of satellite measurements particularly SAR (Synthetic Aperture RADAR) has helped to quantify the vegetation structure and biomass over much larger areas in savannas (Mermoz et al., 2014; Urbazaev et al., 2015). All-weather sensing, and sensitivity to density, orientation and geometrical features of vegetation constituents (e.g. canopy, stem, branches), makes radar data an efficient way to characterize vegetation structure (Woodhouse et al., 2012). As the density and size of the vegetation scatterers increase, there is an asymptotic increase in the received energy (backscatter intensity), thus SAR backscatter can identify variable canopy cover (sparse or closed), disturbance and regrowth in savannas (Mitchard et al., 2011). The degree to which vegetation structure can be resolved and signal attenuation depends on polarization, incidence angle and wavelength of the SAR system. For instance, Lucas et al. (2004) highlighted the sensitivity of cross-polarized data (HV, horizontal send, vertical receive, or VH, vertical send, horizontal received) to vegetation structure, as only those scatterers will be detected that change the orientation angle of incoming SAR signal, thus capturing the strong response from trees and shrubs. Generally, signal with shorter SAR wavelengths, such as X-band (2.5-4 *cm* wavelength) and C-band (4-8 *cm* wavelength), produce strong backscatter from top layer of canopy due to interaction with leaves and branches, but with thorough signal penetration in the grass stratum (Le Toan et al., 1992). While longer wavelengths, such as P-band (30-100 *cm* wavelength) and L-band (15-30 *cm* wavelength) perform better in extracting woody structural properties, as the backscatter results mostly from signal interactions with woody branches, trunks and ground surface and minimizes information from twigs and leaves (Saatchi & Moghaddam, 2000; Mitchard et al., 2009). It has been observed that in high biomass systems, C and L-band wavelength saturate at an AGB level of 75-150 $Mgha^{-1}$ (Saatchi et al., 2007a; Dobson et al., 1992). However, L and C-band wavelengths appear well adapted for the savanna ecosystems, where the canopy is seldom closed, and AGB is typically less than 100 $Mgha^{-1}$ (Carreiras et al., 2012; Urbazaev et al., 2015). The ability of different SAR wavelengths to estimate aspects of savanna vegetation structure, including woody canopy cover, volume and height was demonstrated (Bucini et al., 2010; Naidoo et al., 2015; Mathieu et al., 2013).

So far, savanna vegetation structure retrieval models from SAR have commonly used

range of airborne LiDAR measured landscapes for the calibration of SAR backscatter to biomass, height and canopy cover, with empirical relations (e.g. log relation and power law) and machine learning algorithm. Results of these studies are of immense importance for understanding the distribution of vegetation structure in savannas. However, the performance of SAR vegetation models in estimating vegetation structure depends on detailed measurements of vegetation dimensions, as variability in vegetation structure can have large impact on backscatter intensity. The uncertainty issues in LiDAR trained SAR models stem due to two reasons 1) distribution, amount and time-stamp of the LiDAR data, and 2) use of arbitrary height thresholds for canopy cover and biomass derivation. As a result, transferability of these relationships across different savanna structure is limited, and does not allow accurate estimations of woody cover and biomass. Further development towards relating backscatter to savanna structural properties, such as those readily measurable using terrestrial LiDAR, is hence still required. These LiDAR trained SAR models when derived over a range of vegetation landscapes can reveal the structural formations and spatial variations of vegetation structure, change, sink and source of carbon.

In this context, this study presents the first use of long-range TLS data as a potential approach to improving satellite-based woody canopy cover and biomass calibration and validation. This part of the thesis investigates the sensitivity of SAR backscatter at two wavelengths (C and L-band) to long-range scan derived biomass and canopy cover of a semi-arid savanna ecosystem of South Africa. Emphasis is laid on how differences in height thresholds impact the retrieval of woody canopy cover and biomass. The results are then discussed in the context of spatial variability of across topography and rainfall gradient.

5.2 Long-range scans acquisition sites and processing

5.2.1 Study site

The savanna vegetation structure was studied across Kruger National Park (KNP) (23°98'S, 31°55'E), a 20,000 km^2 national reserve located in the north-eastern South Africa (Fig. 5.1a). KNP is a sub-tropical wooded savannas, dominated by mopane (*Colophospermum mopane*) in the north, knobthorn (*Acacia nigrescens*) and marula (*Sclerocarya bierra*) in central part, and Combretum species and silver cluster-leaf (*Terminalia sericea*) in the southern part of the park (Gertenbach, 1983).

KNP is located in a low-lying (400 m above sea level) and gently undulating landscape, but has an east-west geologic gradient with granite in the west and basalt in the east (Venter, 1986), that strongly influences the soil and vegetation properties (Figure. 5.1a,b). Granitic substrates weather to nutrient-poor sandy soils and support a varying woody cover between 20% to near closed canopy woodlands of 60% canopy cover (Eckhardt et al., 2000). The soils on basalt substrates are more fertile (dark vertic clay soils) resulting in highly productive grasses. The high bulk of grass layer causes high intensity fires,

(Smit et al., 2013), which reduces woody plant density. Not only a geological gradient, KNP encompasses a north-south rainfall with the semi-arid north (400 mm mean annual rainfall) to the mesic south (750 mm mean annual rainfall) (MacFadyen et al., 2018) (Figure 5.1c). The rainfall gradient together with fire regimes (Govender et al., 2006), grazing (Donaldson et al., 2018) and mega-herbivore activity (Asner et al., 2015) regulates the plant productivity and physiognomies in the study site.

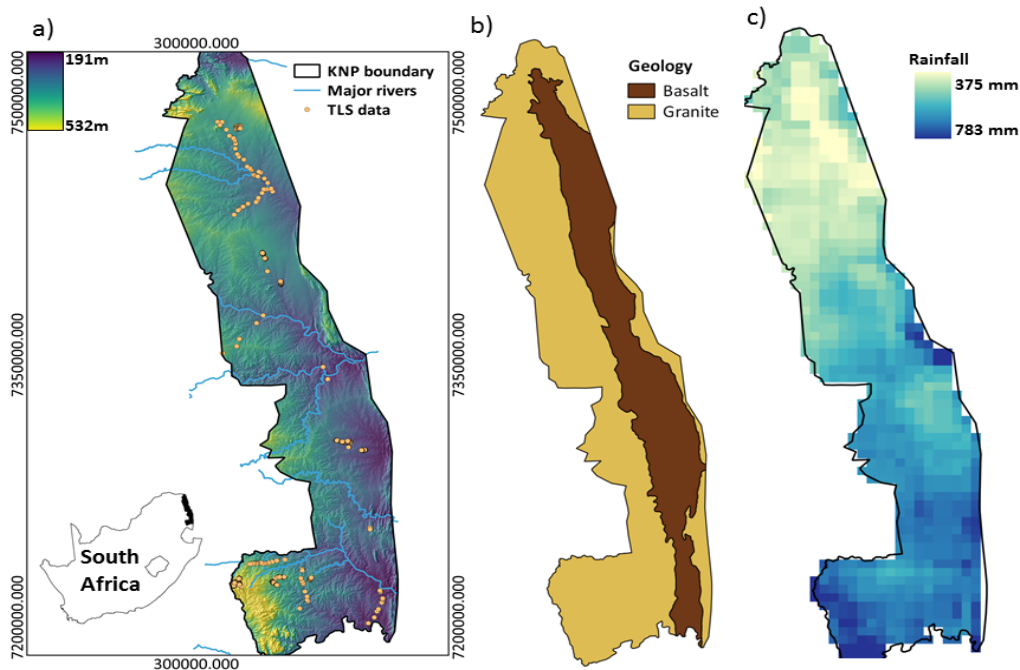


Figure 5.1: (a) Location of study site with LiDAR sampled plots within Kruger National Park, South Africa overlaid on elevation data, (b) major geology in the study site, and (c) mean annual precipitation of the park at 5° grid size.

5.2.2 Remote sensing data and processing

Terrestrial LiDAR data

Terrestrial LiDAR 3D data were collected by surveying across multiple vegetation landscapes within the KNP in 2016, using the Riegl VZ-2000 laser scanner (RIEGL Laser Measurement Systems GmbH) (Figure 5.1a). The terrestrial LiDAR survey was carried out in the late dry season (October), when vegetation was at leaf-off stage and grasses were diminished by grazing. A random sampling approach was utilized for acquiring 3D data across the park, and focus was to cover the wide spectrum of vegetation structure present in the park. The RIEGL VZ-2000 is a near-infrared (wavelength 1500 nm) multiple return LiDAR scanner which can scan objects upto 2000 m distance in a clean line of sight, with a beam divergence of 0.30 mrad. While scanning, an external differential global positioning system (GPS) (accuracy 3 cm) was utilized, to accurately determine

the geographic location of each LiDAR return. The orientation matrices (roll, yaw, and pitch) of the scanner were collected through an internal compass and inclination sensors of the Riegl VZ-2000 scanner. The landscape scanning design consisted of acquiring single long-range scans from elevated vantage points ($>15\text{ m}$ above ground level) or from a vehicle rooftop mount, with a scanner height of 2.5 m across the hill-slopes. For the topographic vantage points, the scanner was operated at 50 kHz , while a pulse repetition rate of 550 kHz was used for hillslope scanning. All the scans were taken at an angular sampling of 0.02° . Initially the scans were taken at full azimuth range of 360° at a coarse resolution, which were later trimmed to an azimuth and zenith range of 180° and 100° respectively. This trimming was performed to include only the region of interest, and reduce the noise from sky. This scanning setup resulted in a mean point density of 158.6 and 6.02 laser returns per m^2 at a distance of 100 m and 600 m respectively from the scanner location, enabling fine-scale description of even smaller woody vegetation. For this study, we collected LiDAR 3D data across 100 locations, widely distributed across the KNP, and capturing broad range of edhaptic conditions and vegetation physiognomies (Figure 5.1a). Maximum range of the scanner was 1500 m , that captured 7-150 *ha*, varying with vegetation structure at the sites.

ALOS PALSAR -2 SAR data

The Phased Array type L-band Synthetic Aperture Radar-2(PALSAR-2) operates at L-band wavelength (1.27 GHz ; 23.6 cm) which is on board the Japan Aerospace Exploration Agency's (JAXA) Advanced Land Observation Satellite 2 (ALOS). PALSAR-2 sensor is a polar, sun synchronous orbit sensor with a 14-day revisit time. Five scenes of ALOS PALSAR-2 fine beam dual polarized (FBD) (coherent *HH* and *HV*) imagery, acquired for path 180 and 181 on 1 December 2015 and 8 November 2015 respectively were used for this study. Each scene covers an area $59[\text{Az}] \times 70[\text{Rg}]\text{ km}$. The scenes were acquired in the ascending orbit, and were provided in single-look complex (SLC) level1.1 format. The cumulative rainfall on the date of acquisition was $56.9\text{-}100.4\text{ mm}$ (www.sanparks.org). We assume that this low precipitation during the acquisition of PALSAR-2 data will not increase the dielectric constant due to high evaporative rates.

The first processing step with the SLC data were - multi-looking intensity, where square pixel in ground range co-ordinates (azimuth resolution- 12.5m , multilook: 1 in range, 5 in azimuth) were obtained. Next, multilooked images were radiometrically corrected with a PALSAR-2 sensor specific calibration factor of -83dB . These multilooked and radiometrically calibrated scenes were geocoded and corrected for topographic artefacts by using a 20 m digital elevation model (DEM) from Shuttle Radar Topography Mission (SRTM). The next step included topographic normalization using the method reported by Santoro et al. (2006), for retrieving the final backscatter coefficient (σ°). After the geocoding process, all scenes were combined to create a mosaic. The geocoded and terrain corrected mosaics of *HH* and *HV* polarized data were converted to linear power of σ° .

These mosaics were converted to linear power intensity by using:

$$\sigma_{linearpower}^{\circ} = 10^{(\sigma_{dB}^{\circ}/10)} \quad (5.1)$$

All PALSAR-2 data pre-processing steps were performed in GAMMATM radar processing software (GAMMA Remote Sensing <http://gamma-rs.ch>).

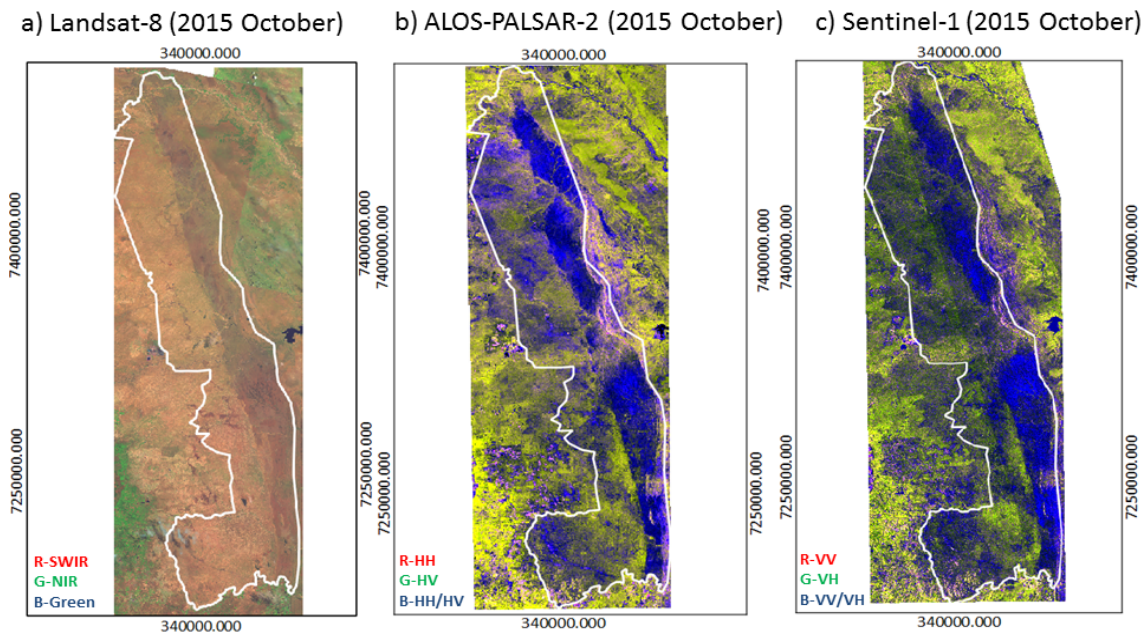


Figure 5.2: Landsat-8 and PALSAR-2 and Sentinel-1 SAR polarimetric imagery over the Kruger National Park in October 2015. The C and L band images are false colour composites.

Sentinel-1 SAR data

Sentinel-1A is a C band wavelength (5.5 cm) SAR sensor, imaging at 5.40 GHz with a 12 day temporal resolution. The level-1 Ground Range Detected (GRD) product in the Interferometric Wide (IW) swath mode, which has dual polarized VV and VH was used in this study. For this study, five Sentinel-1A images were acquired from Google Earth Engine during 25-26 October 2015 time period. The processing steps in Google Earth engine included (1) thermal noise removal using the look-up table within the meta-data, (2) radiometric correction by using sensor calibration parameters provided in the GRD metadata, and (3) terrain correction and normalization using 20 m DEM data from SRTM.

The backscatter coefficients in units of decibel power (dB) from the processed Sentinel-

1A data are converted to linear power (Equation 5.1), and then aggregated to a 100m resolution using simple averaging with a “4x4” window.

5.2.3 Estimation of woody cover and AGB from long-range terrestrial LiDAR

The LiDAR data points from long-range and hillslope scans were first ground classified, and height normalized. Normalized point clouds were utilized to generate the LiDAR return count for every site by utilizing several modules of LAStools (rapidlasso GmbH, 2014; Isenburg (2014)). The LiDAR counts were calculated from 0 m to 12 m (maximum canopy height in KNP), at a bin size of 0.5 m interval of the LiDAR data, and were plotted against canopy height to represent vegetation vertical profile structure. Woody canopy height models were prepared by selecting the highest 3D point within the ‘1 x1 m’ grid cell. The canopy height rasters were used to generate the canopy cover maps by reclassifying the canopy height grids in SAGA GIS (SAGA GIS, 2016; www.saga-gis.org) by varying the height threshold from 0.5-5 m, where LiDAR data between 0 m and threshold were marked as ground points, while all the points above height threshold were classified as woody vegetation. A percentage canopy cover map was prepared by calculating the number of pixels above the height threshold and then dividing by the number of pixels in that grid. The classified grids were scaled to percentage canopy cover for every scan data.

Aboveground biomass at the plot level was calculated from a single predictor variable ‘HxCC’ (Colgan et al., 2013) (Equation 5.2), where H is the mean top-of-canopy height of a plot and CC is the mean fractional canopy cover of a plot. This equation was preferred as it was derived by harvesting and weighing plot-scale major vegetation species occurring in KNP, against which airborne LiDAR methods estimations were compared.

$$AGB_{plot} = -11.5 + 25.8 \times H_{plot} \times CC_{plot} \quad (5.2)$$

5.2.4 Estimation of regional woody cover and AGB from SAR data

To establish the relationship between LiDAR derived vegetation metrics and SAR backscatter intensity, a regular spatial grid of 100 m resolution cells was created in QGIS 2.16.0 (<http://qgis.osgeo.org>), and applied over the dataset. A 100 m resolution was chosen mainly to reduce the issues of SAR speckle, and pixel level co-registration inaccuracy. Also, in the previous studies across savanna ecosystems, a grid size of 105 m was suggested to be providing strongest correlation between SAR backscatter and LiDAR derived woody variables (Mathieu et al., 2013). The strength of relationship between radar backscatter to woody cover and AGB was evaluated by using statistical regression. Backscatter from co-polarized (HH and VV) and cross-polarized (HV and VH) channels are tested to assess the relationship using Equation 5.3, 5.4, where σ° is the backscatter data from Sentinel and ALOS-PALSAR-2 sensor.

$$\sigma^\circ = a \times \text{biophysical parameter} + b \quad (5.3)$$

$$\sigma^\circ = a + b \times \ln(\text{biophysical parameter}) + c \times (\ln(\text{biophysical parameter}))^2 \quad (5.4)$$

An empirical relationship proposed by Saatchi et al. (2007a) was utilized to model AGB from SAR backscatter polarizations.

$$\ln(AGB) = a_0 + a_1(\text{copolar}) + a_2(\text{copolar})^2 + a_3(\text{cross-polar}) + a_4(\text{cross-polar})^2 \quad (5.5)$$

In this models AGB is the aboveground biomass ($Mgha^{-1}$), and a_0 , a_1 , a_2 , a_3 and a_4 are coefficients to be derived from the data.

5.2.5 Statistical analysis of the woody vegetation spatial pattern and mapping

The empirical model performance was analyzed with the coefficient of determination (R^2), root mean square error (RMSE) (Equation 5.6) and mean absolute error (MAE) (Equation 5.7). To assess the error distribution, we computed the residuals (Equation 5.8).

$$RMSE = \sqrt{\frac{1}{n} \sum_{i=1}^n e_i^2} \quad (5.6)$$

$$MAE = \frac{1}{n} \sum_{t=1}^n |e_t| \quad (5.7)$$

$$Residual = y_i - \bar{y}_i \quad (5.8)$$

A 10-fold cross-validation approach (Hastie et al., 2009) was utilized for the semi-empirical model evaluation, where 70% of data used for training the empirical model and 30% is used to evaluate model performance. The model predictability and accuracy was assessed by the coefficient of determination between observed and predicted (10-fold cross-validation) AGB.

5.3 Results

5.3.1 TLS derived vegetation metrics

Single long-range scans proved valuable for the detail spatial variability of vegetation structure, by capturing the physiognomy of large and small vegetation at landscape scale (Figure 5.3a). In total 500 *ha* of area was mapped representing vegetation along rainfall and topographical gradients. The first analysis was done by calculating the frequency distribution of LiDAR returns divided into two distinct geologies, and rainfall categories

of KNP. The more arid sites ($<500 \text{ mm yr}^{-1}$) at the basalt featured lower LiDAR returns typically due to presence of small and sparse vegetation, and higher levels of LiDAR returns from the taller vegetation in the wetter sites of granite substrate (Figure 5.3b,c). The peak in the upper canopy at granite site was larger than the plots on basalt geology. Plots on the granite substrate also showed a bimodal vertical plant profile, with an upper canopy peak at 7 m , and lower peak at 1 m , due to thick understorey. Also, the vegetation in two different rainfall regimes differ in terms of aggregation, with arid sites characterized by higher levels of aggregation in vegetation.

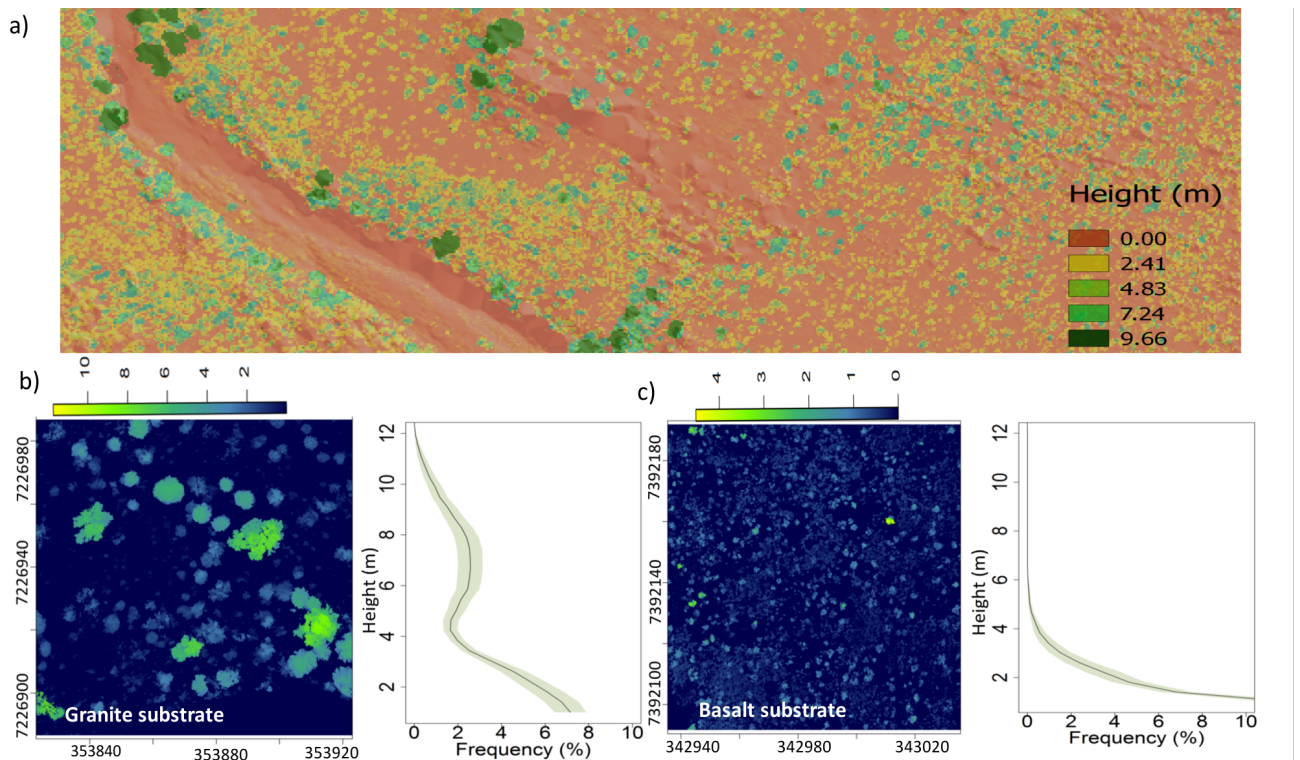


Figure 5.3: a) Normalized long-range scan from the southern Kruger National Park. Lower panel represents the frequency distribution of LiDAR returns calculated for two sites situated in granite (b) and basalt substrate (c) with a MAP of 747 mm and 353 mm respectively.

Across the study site, mean AGB measurements ranged from $11.8 - 76.8 \text{ Mgha}^{-1}$. The canopies within the inventoried sites had a cover ranging between 3.78 to 68.35% , and height of 2.22 to 6.52 m , with a mean of 34.21% and 3.65 m for canopy cover and height respectively. Box plots with woody properties divided into geology and MAP bins show that mean canopy height, woody cover and AGB increased steadily with increasing rainfall, and all three woody parameters were higher on the granite substrate (Figure 5.4). The box plots show a strong correspondence between woody canopy cover and AGB, as expected from the LiDAR-biomass model (Equation 5.2). Along the rainfall gradient from the driest ($<400 \text{ mm yr}^{-1}$) to the wettest (700 mm yr^{-1}) end, mean estimates of woody cover and AGB increased by 20% and 40% respectively.

There are clear AGB and woody cover transitions due to variability in topo-edaphic factor. The overall variation of AGB across two geologies ranges from values $11.86\text{-}28.28\text{ Mgha}^{-1}$ for basalt substrates to as high as $18.15\text{-}76.87\text{ Mgha}^{-1}$ for granite substrate. Within the hillslope catenas, there is spatial variation of carbon storage, where more woody cover is supported across high slope areas.

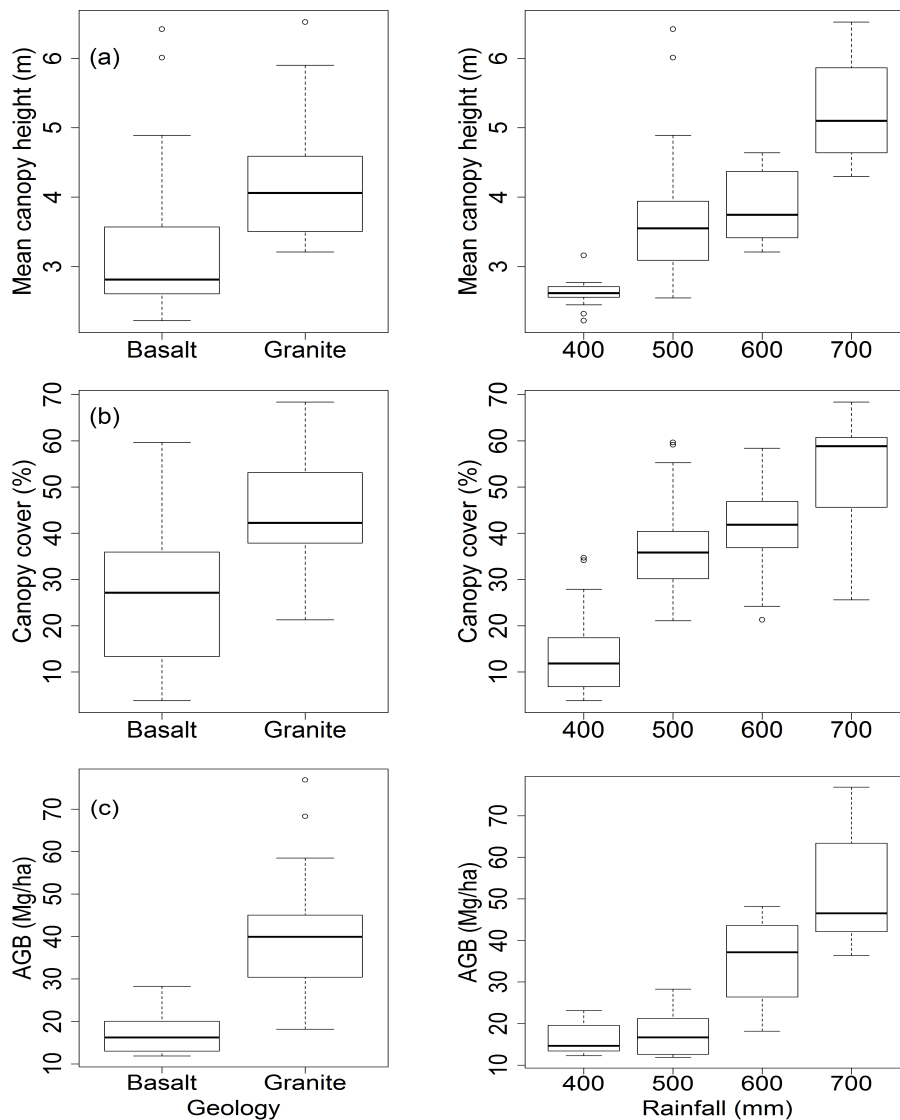


Figure 5.4: Boxplots of estimates of mean canopy height, cover and AGB in two geologies and along a rainfall gradient.

Impact of variation in height cut-off

As the height threshold for classifying ground and vegetation 3D points increased, variation in canopy cover became apparent, which showed differences in canopy cover associated with different vegetation structure (trees and shrubs) (Figure 5.5 a,b). The higher canopy cover estimates at 0.5 m relative to estimates at 1.5 m in the 20-60% cover range are seen

in the linear regression model. This indicates that in areas of high canopy cover, a 0.5 *m* height threshold detects greater amount of AGB. Distribution of canopy cover shows that the higher threshold estimates result in relatively lower cover, whereas, lower cut-off thresholds are more concentrated on the higher end with a range between 30-80% (Figure 5.5c).

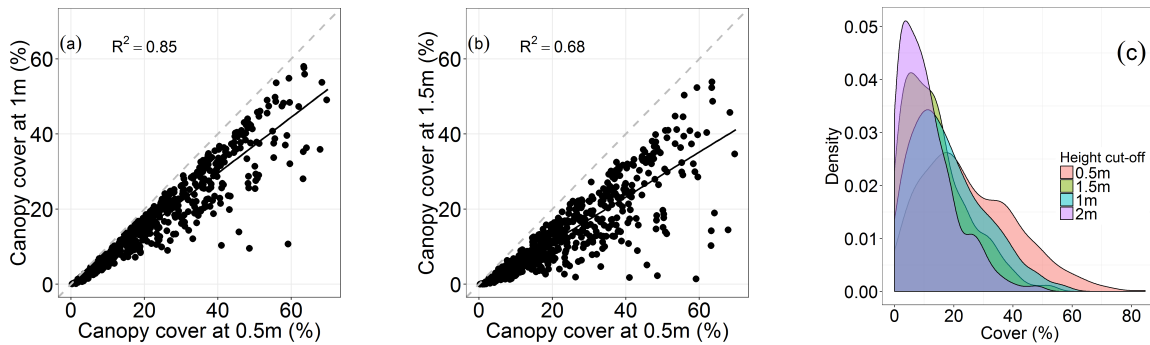


Figure 5.5: Estimates of canopy cover at 1m and 1.5m height threshold derived for the scanned sites. Lines represent linear model fit with dashed line as 1:1 (a,b). Distribution of canopy cover at different height thresholds (c).

5.3.2 Sensitivity of remote sensing data to vegetation metrics

Regressing canopy cover and AGB calculated from LR-TLS using different height cut-offs with the PALSAR-2 backscatter data, showed that the best relationships corresponded to height thresholds between 1.5-2 *m*, with maximum coefficient of determination of 0.72 (Figure 5.6a). The same analysis when repeated using the Sentinel-1 backscatter data also confirmed a high coefficient of determination at a height threshold of 1.5 *m*, explaining more than 50% of canopy cover variation (Figure 5.6b). As the height threshold increased, coefficient of determination continued to increase to approximately 72% at the 2 *m* height cut-off. At smaller height cut-offs, there is a possible addition of higher grass layer, which causes these higher values of biomass. These variations are averaged out with greater values of height cut-off. Based on this analysis for the later results, a height threshold of 2 *m* was defined for AGB and canopy cover estimations.

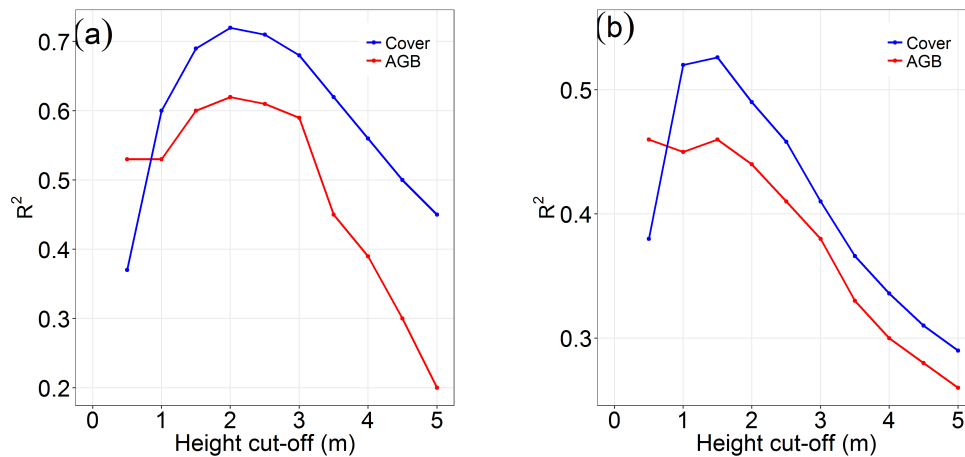


Figure 5.6: Distribution of R^2 between height thresholds used to determine woody cover and AGB in the scanned sites for ALOS-PALSAR 2 (a) and Sentinel-1 (b).

Backscatter coefficients of HH, HV, and VV, VH polarizations from ALOS-PALSAR 2 and Sentinel-1 respectively, were extracted from 100 m pixel resolution. We extracted backscatter coefficients from 427 plots from 54 different sites. The relationship between polarized backscatter and AGB and cover are shown in Figure 5.7 and 5.8. The regression coefficients (R^2) were obtained by fitting a linear regression model (Equation 5.3) for canopy cover and a second order log polynomial regression model (Equation 5.4) for AGB to the backscatter data at each polarization. For the L band co-polarized (HH) backscatter measurements, R^2 values were 0.46 and 0.47 respectively for canopy cover and AGB, and cross polarized (HV) backscatter measurement R^2 values were 0.71 and 0.70 respectively for canopy cover and AGB. The R^2 values for C band Sentinel-1 VV measurements were 0.41 and 0.49 respectively for canopy cover and AGB, while VH polarization resulted in R^2 of 0.52 and 0.50 for canopy cover and AGB. In both frequencies, the HV and VH sensitivity to AGB and canopy cover was much higher. Plot level backscatter from the L-band data shows higher sensitivity to AGB, while C-band backscatter data show large variation with better sensitivity for low biomass values. The correlation between L-band HH polarization channel and biomass is relatively lower than HV channel, with a loss of sensitivity occurring at lower biomass values (Figure 5.7b,d).

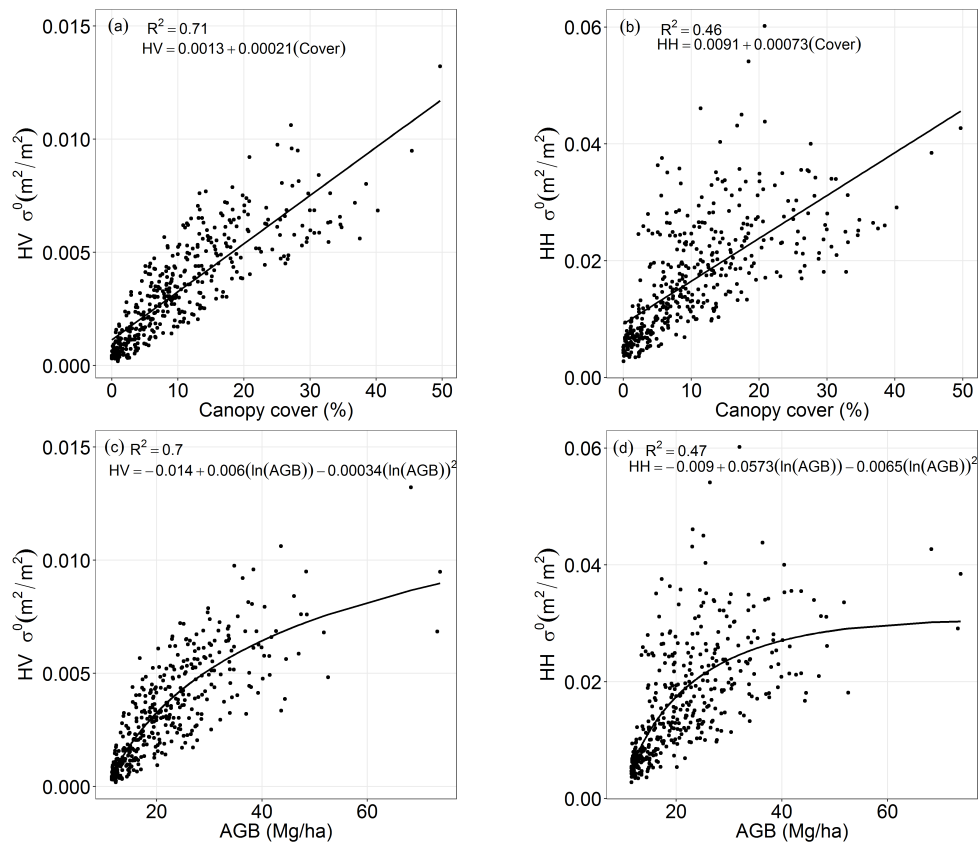


Figure 5.7: Relationship of L-band radar backscatter power (m^2m^{-2}) at two polarizations of HH and HV with the woody cover (%) and AGB (Mg/ha).

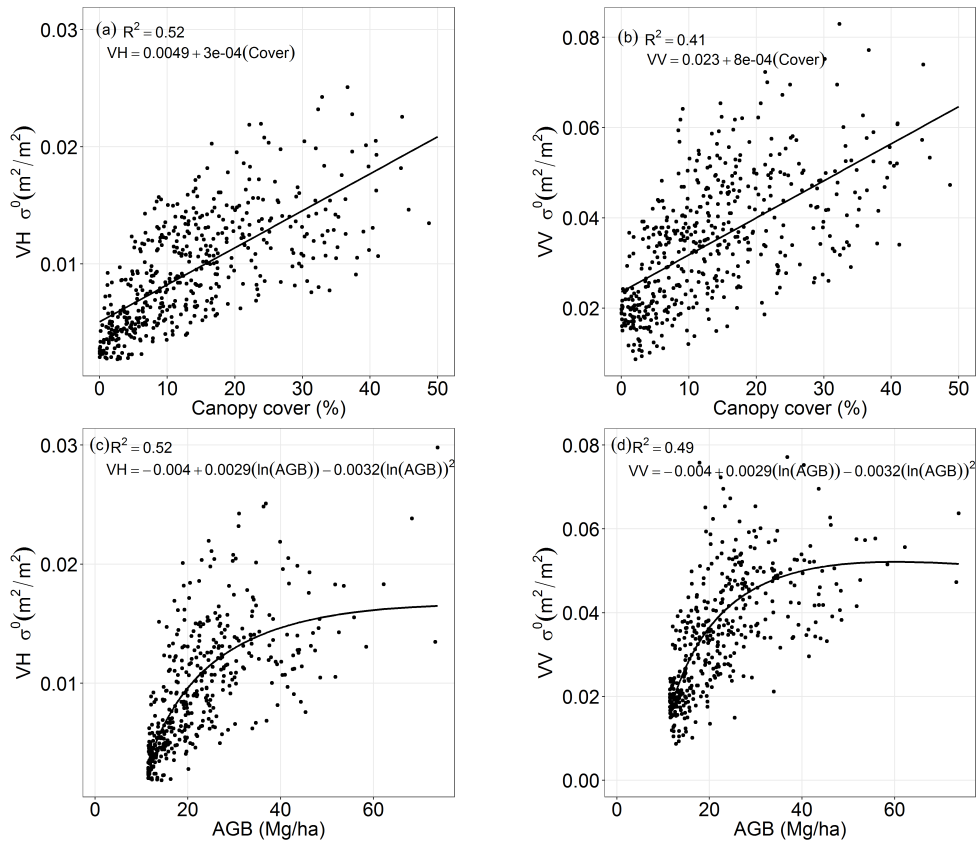


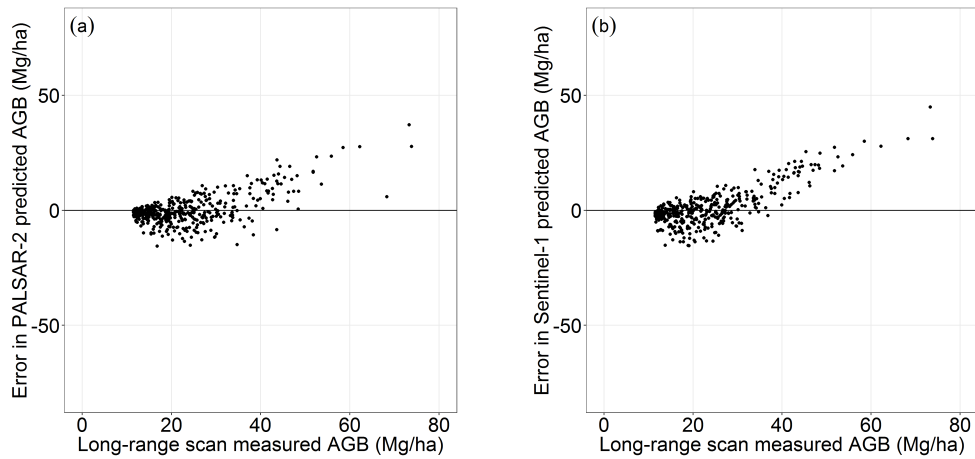
Figure 5.8: Relationship of C-band radar backscatter power (m^2m^2) at two polarizations of VH and VV with the woody cover (%) and AGB (Mg/ha).

5.3.3 Mapping

Equation 5.5 was applied to map the estimates of AGB and canopy cover across the whole KNP by using backscatter from PALSAR-2 and Sentinel-1 sensors. Table 5.1 shows the model estimates, fitting coefficients, and 10 fold cross validation statistics for the model. There is significant improvement in model fitting when ALOS-PALSAR-2 backscatter data is used rather than the Sentinel-1 backscatter. Additionally, Figure 5.9 shows the scatterplots of the long-range scan calculated AGB versus error in AGB, calculated using cross validation values from ALOS-PALSAR-2 and Sentinel-1 backscatter data. The error in ALOS-PALSAR-2 and Sentinel AGB predictions increase as biomass increases. The plot-by-plot difference between the backscatter predicted and long-range scan estimated biomass showed an increasing bias towards higher AGB values. By focusing at $\text{AGB} < 50 \text{ Mg}\text{ha}^{-1}$, the bias reduces substantially, and the difference becomes approximately normally distributed. The overall RMSE for these data is $6.65 \text{ Mg}\text{ha}^{-1}$, however this decreases to $2 \text{ Mg}\text{ha}^{-1}$ for values below $40 \text{ Mg}\text{ha}^{-1}$.

Table 5.1: R^2 , RMSE and MAE of mapped AGB from ALOS-PALSAR-2 and Sentinel-1

Metric	a_0	a_1	a_2	a_3	a_4	R^2	RMSE	MAE
ALOS AGB (Mg/ha)	2.44	267.78	-9238.67	-8.10	-38.21	0.72	6.65	4.30
Sentinel AGB (Mg/ha)	2.08	63.93	-953.57	19.59	-156.49	0.56	8.04	5.37

**Figure 5.9:** Errors in predicting AGB from the ALOS (a) and Sentinel-1 (b) backscatter plotted against long-range scan quantified woody properties.

5.3.4 Spatial distribution of AGB

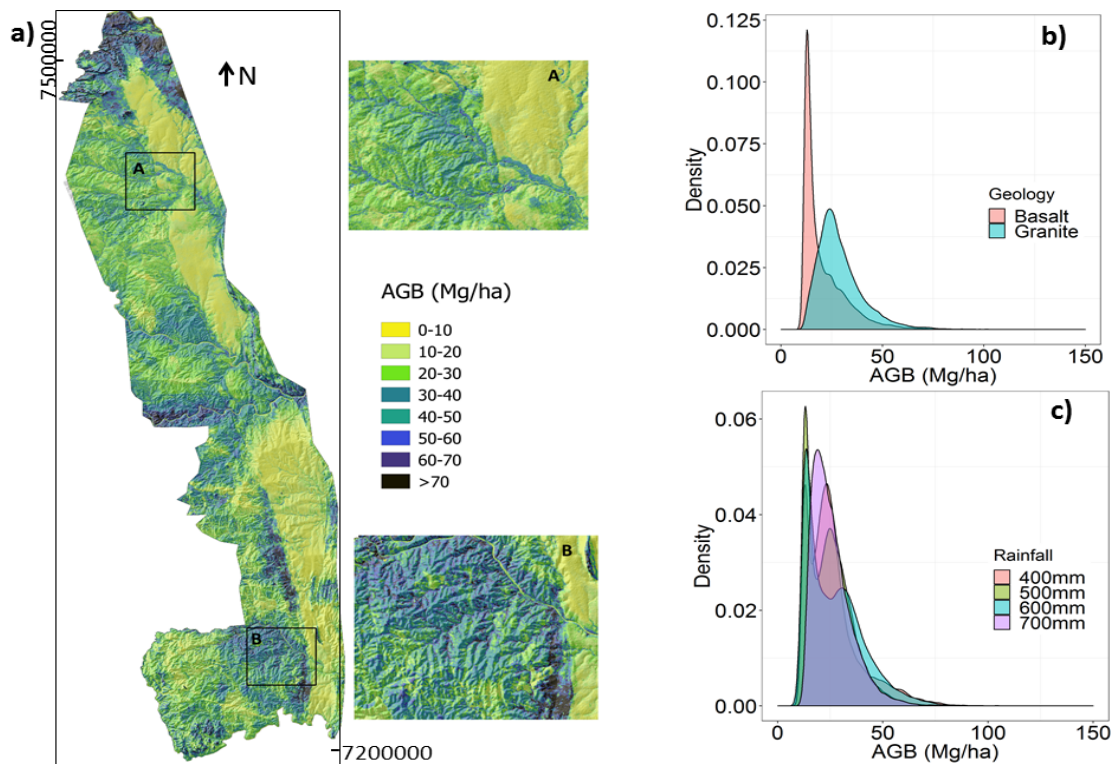


Figure 5.10: AGB map of KNP and associated analyses. (a) Spatial pattern of AGB in KNP. Example A shows the riparian vegetation stands in the northern part of the park. Example B displays the catenas with high AGB. (b) frequency distribution of AGB for two substrate type, and (c) frequency distribution of AGB for each rainfall zone.

Distribution of biomass predicted from the Equation 5.5 are shown in Figure 5.10 at 100 m x 100 m (1 ha) gridded map. The AGB in the study site exhibits a striking east-west gradient related to the geology, with AGB as low as 11.7 Mg ha^{-1} in the basalts to as high as 63.61 Mg ha^{-1} in the granites. There is a higher concentration of biomass at upper slopes of catenas, and around riparian areas. In the northern portion of the park, substantial biomass is restricted to the riparian woodland, with an AGB of $40\text{-}50 \text{ Mg ha}^{-1}$. Imposed on this topo-edhaptic pattern, effects of increasing rainfall are obvious with an AGB estimate $>50 \text{ Mg ha}^{-1}$ in the zones of the park with highest rainfall. The largest stretch of high AGB is across the northern border region of KNP. The closed woodlands are distributed over riparian areas, with an average AGB of $104.52 \text{ Mg ha}^{-1}$, and AGB values greater than 80 Mg ha^{-1} are observed over significant 1 ha pixels. Another distinct AGB pattern extends in the southern KNP at the boundary of granites and basalts. These woodlands occupy a high slope terrain over the solonetzic duplex soils, with a mean biomass of 57.51 Mg/ha .

5.4 Discussion

The goal of this study was to infer woody properties in a semi-arid savanna site of South Africa by investigating multi-frequency L-band ALOS-2 PALSAR-2 and C-band Sentinel-1, with empirical biomass models developed from long-range scanning using TLS. The study reports both the relative and absolute errors of AGB (ranging from 0-100 $Mgha^{-1}$) and woody cover, across the landscapes nested in rainfall and geological gradient, by using backscatter coefficients from C and L- band independently. Long-range scans provided direct measures of canopy height, cover and vertical distribution of vegetation at landscape scale, which were later used to estimate the aboveground biomass. The large scale synoptic view of SAR enabled us to scale the long-range scans derived woody properties from landscape to regional scale, in addition to exploring differences in vegetation structure across the full expanse of the site. Furthermore, varying the height cut-offs for TLS derived woody properties provided a means to evaluate the degree of sensitivity of SAR data to savanna vegetation structure. There are important implications of this sensitivity for understanding savanna vegetation structure.

5.4.1 Mapping savanna vegetation structure with long-range scans

Our LR-TLS dataset were promising for several reasons. First, woody properties such as canopy height, canopy cover and the vertical distribution of woody vegetation structure were quantified using single long-range scans for up to 150 ha at individual sites in the diverse vegetation conditions, terrain, species and management activities. Landscape scale sampling from the long-range scanning (LRS) facilitated not only capturing the size class distribution of the vegetation but also helped in co-registering the LRS with the spaceborne SAR measurements, and reducing sample variance. The footprint of LR-TLS can vary with the scanner altitude, beam divergence and scan angle. Previous studies report that single scanning approach is less accurate, as it measures only 70% of the trees in the sense forest (Liang et al., 2016). In our study site, the strong performance of single long-range scans in estimating canopy height and cover is due to the relatively short vegetation height, selecting sites with a clear line of sight, and scanning in late dry season which led to a considerable reduction in occlusion due to absence of grass layer. Also, wide spacing between the trees caused less attenuation in laser pulses with the increasing distance. Similar investigations in the Australian open woodlands confirm the potential of single scans for mapping tree height and canopy cover at a coefficient of determination of 0.90 (Muir et al., 2018). The laser attenuation at 1000 m was only 0.3 m , which is still capable of documenting large woody trees. Also, canopy cover models derived from the LR-TLS were less affected by a reduction in point density at distances far away from scanner ($>600 m$), as interpolation for canopy height models was performed at 1 m . Second, a simple *canopy height X canopy cover* metric was able to capture the variations in AGB across KNP. Last, not only LR-TLS data allowed to estimate the woody vegetation metrics (canopy height and cover) continuously over large areas, LR-TLS also provided the vertical vegetation profiles, that help to explain the geometrical

distribution of of vegetation across the landscapes, which are challenging to measure from ground.

However, we note that oblique scanning from elevated points, results in good coverage of woody trees but fewer pulses overall penetrate to the ground, which affects determination of the surface and therefore the ability to calculate vegetation height.

5.4.2 Backscatter sensitivity to biomass

Cross-polarized (HV and VH) backscatter responded strongly to woody properties, across the sites differing in their structure and physiognomy. The smaller variance is due to the low sensitivity of cross-polarized backscatter to moisture content, surface roughness and topography. However, within some sites, comparatively lower levels of backscatter were observed for higher AGB. This could be because of the lower densities of canopy, and shorter vegetation heights, collectively reducing the number of scattering elements. In savanna and other open ecosystems, substantial AGB is contained in sub-canopy shrubs of small canopy area and height, which may not be detectable using the SAR system. The influence of vegetation structure (tree density, vegetation size) on SAR backscatter has been widely reported. For instance, Lucas et al. (2010) attributed differences in SAR backscatter across forests and woodlands due to differences in stem density and vegetation size in the two ecosystems.

A better correlation between L-band HH and HV backscatter and long-range scan estimates was observed than C -band VH and VV polarizations for the retrieval of woody vegetation structure. The inclusion of C-band Sentinel-1 data for AGB and cover estimations did not improve the retrieval results. This also corroborates a study across the low-veld region of north-eastern South Africa, which concurred that longer wavelengths are more correlated with the vegetation structure attributes than the shorter wavelengths both as individual or combined (Naidoo et al., 2015). The high performance of L-band is because longer wavelengths can penetrate deep in the vegetation canopy, allowing the SAR signal to interact with trunk and branches, and thus producing stronger correlation with the LR-TLS derived woody vegetation metrics. Moreover SAR data was collected during the late dry season when errors associated with moisture are minimum, which improves the sensitivity of HV and VH backscatter to woody properties. Also, this study utilized large number of 1 *ha* well geolocated long-range scanned plots for calibration and validation of Radar data, which could be another reason for having high agreement between long-range derived vegetation metrics and Radar backscatter. Despite the leaf-off condition, shorter wavelengths have lower correlation with the LR-TLS metrics due to their limited ability to penetrate the canopy. High variance in the Sentinel-1 data could also be explained due to it's sensitivity to surface roughness due to high variability in grass cover. Some signal penetration in Sentinel-1 is also possible as the canopies in savannas are not homogeneous, rather canopies are not generally homogeneous and have gaps that promote the signal penetration.

A semi-empirical modelling approach was more suited for this study as the analysis is

done with only four predictor variables (L-band HH and HV, C-band VV and VH) using data from a single time-period. The model considered double bounce and surface scattering arising from one single resolution cell as the predictors. However, empirical models have some limitations, due to over-fitting and parameter interpretation. When applying Equation 5.5 to the PALSAR-2 and Sentinel-1 scenes, errors of 20-30% are expected, which will increase by 10%, if specific tree allometries are taken into account.

5.4.3 Spatial distribution of woody biomass

Rainfall and edaphic conditions in KNP control the spatial heterogeneity of AGB and woody cover. In a semi-arid ecosystem, the maximum potential of woody cover is often limited by the MAP (Sankaran et al., 2005). Interestingly, in KNP geology has much larger effect on the distribution and heterogeneity of AGB and woody cover, which is consistent with the findings from Vaughn et al. (2015). We observed sharp transitions in the AGB across the geological boundary, where there is negligible difference in MAP. At these geological boundaries AGB drops by two-fold in the basalt geology. The lower biomass in basalt terrains can be explained by high intensity fires that result from large fuel loads derived drying out of highly productive grasses that grow in this nutrient rich clay soil. The variations in land elevation and slope, related to catena formations, which affects the hydrological features and soil properties were also related to systematic variations in AGB. The woodlands mainly distributed along the rivers (seasonal or perennial) have a more predictable pattern related to water availability.

5.4.4 Uncertainties in the prediction of woody properties

While relating SAR backscatter to the LR-TLS derived woody properties, we observed some anomalies. For instance, at some sites low HV backscatter was seen for the high AGB sites. High AGB values could be due to considering mean canopy height and cover at plot scales. This error can be eliminated by incorporating the canopy height and crown area of individual trees by using object based methods, and estimating the biomass. Despite the significant large area mapped by the LR-TLS, some sites possessed shadowing due to attenuation of laser pulses by vegetation. We therefore recommend acquiring multiple long-range scans from different positions to minimize the occlusion. Additionally, open landscapes with no vegetation are not reliable for the calibration of SAR backscatter, as the backscatter values from surface due to double bounce effect mimic the backscatter values similar to those of vegetation. The accuracy of biomass estimation in savannas from SAR measurements could be further improved by the addition of optical vegetation indices, which provide additional suite of information to address the vegetation structure heterogeneity in savannas. This combined data approach has been implemented at coarser to medium scales in the Amazonia (Saatchi et al., 2007b). In general, a combined data approach can overcome the potential errors, and improve the accuracy.

5.5 Conclusion

The savanna vegetation structure inventory with LR-TLS data provided the first physiological variations of canopy height and woody cover at landscape scales in the KNP. Using the C and L-band SAR backscatter trained with the LR-TLS, we were able to map the regional scale savanna biomass distribution. Climate and edaphic variables are largely responsible for the heterogeneity in spatial distribution of biomass and vegetation structure across KNP. The development of regional carbon estimates from the synergy of LR-TLS and SAR data will significantly overcome the current major limitations of manual field inventory and opens the opportunity to use LR-TLS scans at landscape scales, providing a useful tool for direct calibration and validation of satellite derived biophysical attributes.

Chapter 6

Synthesis

6.1 Synthesis

The central theme of this dissertation was to characterize savanna vegetation structure with high resolution 3D data and Radar data products, as well as to showcase their utility in the context of assessing vegetation structure patterns under diverse environmental drivers. The thesis is therefore intended to make both technical and applied research contributions in the field of savanna vegetation ecology. Particular emphasis was put on mapping canopy cover, aboveground biomass and vertical vegetation profiles across disturbance and rainfall gradient in varying geologies. These environmental drivers were chosen because they are thematically connected in regulating savanna vegetation structure (see Chapter 1 section 1.2), and in the face of changing climate determining their individual as well as collective role in constraining vegetation structure is imperative. Also, vegetation inventories in savannas are sparse with coarse spatial resolution, which limits our ability in realizing the full potential of environmental drivers. In the following section, the achievements of this dissertation with respect to each study objectives are summarised, discussed, and employed to outline the potential avenues for future research.

6.1.1 Summary

Study objective 1 - Analyzing vegetation structure and spatial organization across fire-regimes

In Chapter 3, a quantitative effect of increasing fire frequencies on aboveground biomass and vertical vegetation profiles of semi-arid savanna was performed. Special attention was paid to understand how fires interact with rainfall and landscape to shape the vegetation structure dynamics. For this purpose, the study assessed the response of vegetation structure to 63 years of experimental fire manipulation in South Africa's Kruger National Park. These experiments applied three late dry season fire regimes (biennial, triennial and unburnt), nested across a topography and precipitation gradient. Vegetation structure of the fire manipulation experiment was mapped in 3D high spatial resolution with Terrestrial LiDAR, which were converted to canopy height, cover, aboveground biomass and vertical vegetation profiles. The study results highlighted that fire frequencies had most effect on woody vegetation structure and biomass in more wet savanna sites, but this effect was weak in dry savanna sites, where only the occurrence of fires constrained the vegetation structure. The highest rate of biomass removal occurred with the triennial fire regimes in the most productive sites, indicating a shift from woody carbon storage sink to source. This study concludes that effects of fire regimes are context dependent, and these interactions have substantial implications for carbon storage and emissions emerging from savanna ecosystems.

Study objective 2 - Characterizing savanna vegetation structural attributes at landscape scale - method development

In Chapter 4, a new savanna vegetation sampling approach by terrestrial LiDAR was implemented and evaluated. The aim was to overcome the plot-scale inventories, and incorporate wider landscape scale vegetation structure to capture the spatial heterogeneity embedded in savannas. To this end, terrestrial LiDAR scans at reduced pulse repetition rate (50 kHz) were acquired from vantage points at two sites in Southern KNP. The 3D data from long-range scans was converted to canopy height, cover and vertical distribution of 3D points. To determine the accuracy of LR-TLS quantified biophysical parameters, a set of multiple TLS scanned reference plots were used, which were laid in the footprint of long-range scans with increasing distance. The resulting long-range scans from the two sites underscore the plausibility of extending the traditional sampling range of TLS from plot scale (<1 ha) to 100's of ha in less time. Finally, the experiences gained from the assessment of LR-TLS led us to perform comprehensive scanning across different vegetation landscapes of KNP, and provide an alternative approach to vegetation inventory for efficient and precise assessment of savanna carbon resources.

Study objective 3- Assessing spatial patterns of woody structure in a savanna system with earth observation data

In Chapter 5, long-range scans acquired across different geologies and rainfall regimes were used to scale up the estimates of tree cover and AGB to regional scale. Focus was laid on determining the uncertainty that can originate from ambiguous thresholds for defining tree cover in savannas. In addition to the threshold determination, varied radar backscatter response to long-range scan derived tree cover and AGB were examined. For this purpose, dry season acquired C-band Sentinel-1 and ALOS-PALSAR-2 radar images were used. The results of the study demonstrate that Radar backscatter sensitivity to biophysical parameters is stronger when a vegetation height threshold of 1.5m is considered. Even though dry season radar images were utilized, C-band Sentinel-1 derived tree cover and AGB were outperformed by the L-band backscatter. The analysis of spatial distribution of biomass revealed strong variations across geologies and topography with thickets and shrubs contributing high AGB. The study also highlights an important point that high accuracy in mapping tree cover and AGB at regional scale can be achieved by minimizing the time gap between backscatter and training data. Since previous research was based on linking backscatter to training data acquired at fewer locations, the findings of this study provide land managers with a complete picture of spatial distribution of cover and AGB.

6.2 Reflection

Motivated by a selection of existing research needs, three scientific contributions were made in the field of savanna vegetation ecology. The core of the individual contributions are detailed quality vegetation structure data produced by the synergistic use of TLS

and Radar imageries for a better understanding of multiple facets of savanna ecosystem's structure and dynamics. This section reflects on the objectives of this study, proposed methods, strengths as well as their implications. A concise summary of discussions on the objectives taken in this study are provided in the Table 6.1.

Table 6.1: Summary of the discussions on each scientific contributions

Contributions	Strengths	Limitations	Requirements
Objective 1 (<i>Singh et al., 2018</i>)	<ol style="list-style-type: none"> 1. Holistic assessment of 63 years of management fires 2. Late dry-season fire frequency and vegetation relationships across precipitation gradient 3. First quantitative test for consumer control by fire regimes 	<ol style="list-style-type: none"> 1. No consideration of 3D inventory metrics like individual tree biomass 2. Herbivory abundance not taken into account 	<ol style="list-style-type: none"> 1. Multi-scan TLS data across 24 7 ha plots
Objective 2 (<i>Singh et al., in press</i>)	<ol style="list-style-type: none"> 1. First demonstration of long-range scanning for vegetation structure mapping 2. 150-200 ha of vegetation landscapes covered 3. Detailed inspection of error propagation 	<ol style="list-style-type: none"> 1. Limited sites 2. Dependence on scanner height above canopy 	<ol style="list-style-type: none"> 1. 2 Long-range scans 2. 13 multi-scan reference plots
Objective 3	<ol style="list-style-type: none"> 1. Incorporation of TLS reference data 2. Height threshold impact on aboveground biomass 3. Spatial variability of biophysical parameters 	<ol style="list-style-type: none"> 1. 100m resolution 2. No account of temporal variability 	<ol style="list-style-type: none"> 1. Long-range scans 2. Sentinel-1 and ALOS-PALSAR-2 Radar data

6.2.1 Analyzing vegetation structure and spatial organization across fire-regimes

Despite a general recognition of the important role of fire-regimes in maintaining the open state of savanna ecosystems, altered fire-regime effects on vegetation structure and biomass across topographic gradients are still not clear. Bond & Keeley (2005), suggested that extent of consumer control by fire results from interaction with the available moisture content for plants, but so far research has not provided empirical evidence for the regulation of these interactions. The fact that fire effects are dependent on the season and frequency of occurrence (Govender et al., 2006), has led to the view that vegetation structure recede rapidly with increasing fire frequency and late dry season burns will have severe consequence on vegetation structure (Murphy et al., 2014; Andersen et al., 2005). Previous studies on fire-vegetation relationships were reported to originate from a small spatial scale (Enslin et al., 2000; O'Regan, 2005) or for fewer landscapes only in the early dry season time period (Devine et al., 2015). Moreover, these methods often relied on manual measurements, or even data from airborne LiDAR was not sufficient enough to document the smaller vegetation. The present thesis has addressed these deficits by

analyzing the effects of 63 years of late dry season experimental burning with varied fire frequencies on woody properties along a rainfall (496-700 mm yr^{-1}) and topographic gradient (basalt and granite).

Across the rainfall gradient, biomass increased rapidly on the unburnt plots, with upto 30 t/ha in the wettest regions. Previous studies in South African savannas have documented the same trend, where fire absence led to six times higher woody biomass than in plots receiving less mean annual precipitation (Higgins et al., 2007). Analogous to high biomass in wet regions, fire caused a larger percentage biomass reduction in the more dense wooded wet landscapes than in drier savanna system, which reinforces Bond & Keeley (2005) consumer effect but with an added empirical evidence. My results challenge the current widely held belief that fire-regimes do not have an influence on vegetation in dry savanna. This study provides evidence that fire caused a substantial decline in biomass and woody cover in dry savanna, though fire frequency had negligible influence. Long-term exposure to biennial and triennial fires at dry savanna sites, reduced woody cover and height with the equal magnitude. While, instead of biennial fires, triennial fires were more effective in reducing the structure at wet sites by tree topkill. This result is significant since previous studies do not provide empirical evidence of effect of additional year on vegetation structure in wet and dry savanna. I argue that the greater influence of decreasing fire frequency on wet savanna is due to the reduced competition between trees and grasses during an additional year which leads to greater fuel accumulation in wet savanna.

The landscapes considered in this study differ in terms of soil type, which regulates hydrology, nutrients, vegetation type and herbivore densities (Venter et al., 2003), and this subsequently modifies the fire-vegetation relationships. Previous studies claimed that effects of fire are more prominent on basalts, but my study shows the opposite trend, with large absolute losses on granite sites with increased fire. However, I argue that this could be due to declines in fuel load across basalt substrates due to the ongoing drought that took place during the year of data acquisition. This result is an indicator of complex fire-vegetation relationships spatially as well as temporally.

Altered fire regimes may be involved in homogenizing the vegetation structure in savannas. I tested this hypothesis by assessing the segmented vegetation of three height classes from 3D data along a gradient of rainfall. In both dry and wet extremes of rainfall gradient, homogenization in the structure is evident at decreased fire frequency plots: dry savanna sites had more homogeneous structure in unburnt plots while in wet savanna region medium height class shrubs continuously increased with decreased fire frequency (Figure 6.1). This suggests that regulation of fire frequency may play a key role in regulating the structure of savannas in an attempt to achieve equilibrium between trees and shrubs under changing resource availability. Also, this result is of increasing importance for biodiversity conservation since a homogeneous structure can jeopardise the habitat suitability of faunal assemblages.

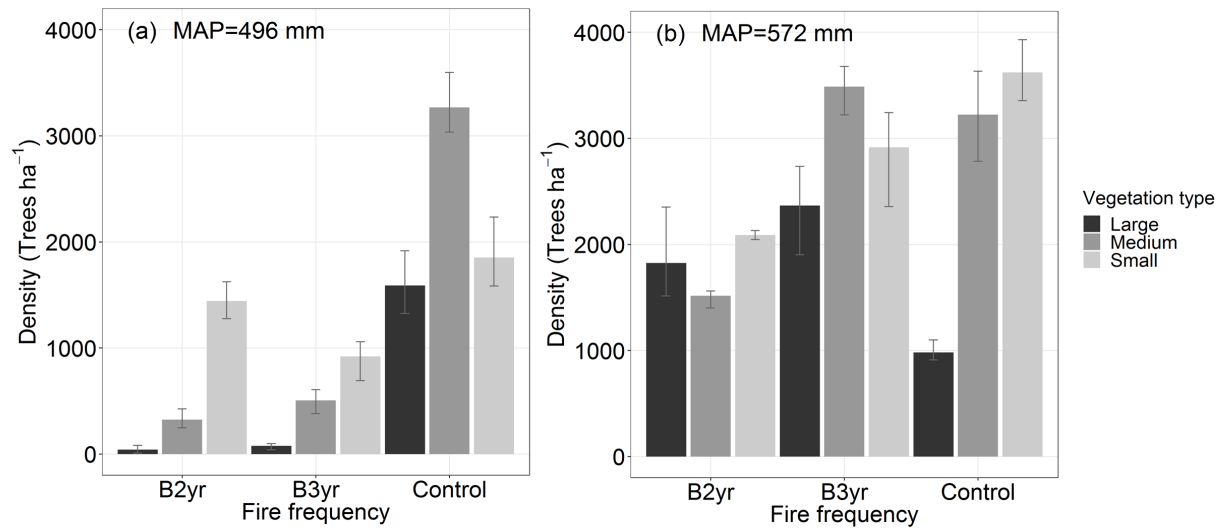


Figure 6.1: Bar plots for distribution of trees in 3 height classes with varying frequencies.

Taken together, this chapter of the thesis provides evidence that effects of fire regimes are context dependent (Figure 6.2), and similar fire regime or ignition pattern might not hold true for all the landscapes. For example, in dry savanna only the presence of fire constrained the structure, while wet savanna sites demanded frequent fires. Also, this study can give several management advices, e.g. use of spatio-temporal variability in fire regimes instead of fixed fire regimes, to enable more cohorts of adult tree to escape the fire-trap. This will ensure heterogeneity in the landscapes.

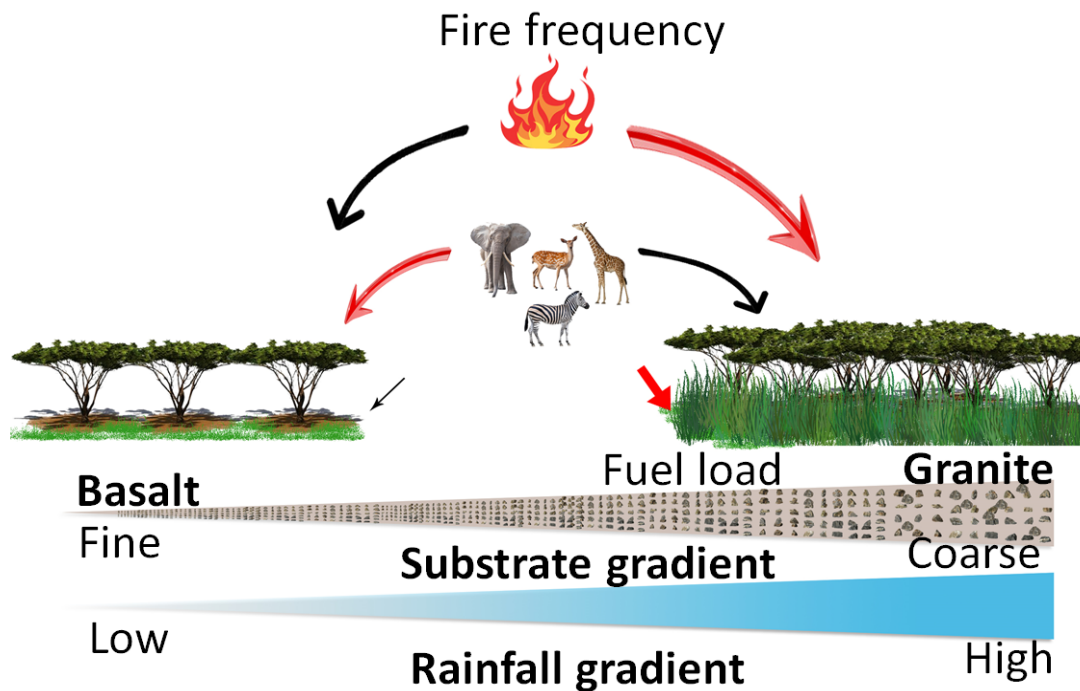


Figure 6.2: A graphical representation showing varying effects of fire regimes across basalt and granite substrate of KNP. Arrows indicate the strength of fire influence on vegetation, where red symbolises greater effect while black indicates a weak effect.

6.2.2 Characterizing savanna vegetation structural attributes at landscape scale - method development

A prevailing concern in savanna ecosystems is the lack of accurate landscape scale vegetation structure characterization which span climatic, edaphic and biotic gradients (Staver, 2018). Over the last 30 years, savanna vegetation structural descriptors have relied exclusively on manual plot-based studies ($<1\text{ ha}$), which are site specific and cover a small spatial subset of the landscape. Although plot-scale results are providing advances in savanna structure estimation, they *suffer from the classic conundrum of savanna structure i.e. to account for clumping and multi-stem vegetation structures* (see Chapter 1 section 1.2.2). Recent attempts in mapping vegetation structure from airborne LiDAR have led to increased spatial coverage as well as describing 3D structural descriptors compared to existing manual inventories (Asner et al., 2007). However, the challenge always lies in depiction of shrubs and other smaller vegetation that occur beneath the tree canopy and contribute substantial carbon storage. Clearly, tools with the ability to measure structural details and encompassing vegetation of all size classes will help to fine tune many descriptive characterizations of savannas. To address these shortcomings, I utilized long-range terrestrial laser scanning as a means to acquire savanna vegetation structure over wider scales.

In comparison to earlier studies, two major improvements were made by the long-range

scanning in savanna vegetation structure estimation (Chapter 4). The first one refers to the characterization of vegetation structure for up to 100's of *ha* with single long-range scan, including areas that are inaccessible for in-situ measurements. The 3D data captured varied height class vegetation which ranged from small shrubs (1- 3 *m*) to big trees (8-10 *m*), suggesting that data encompasses spatial variability. In the course of investigation of the feasibility of long-range scans, four biophysical parameters - canopy height, cover, aboveground biomass and vegetation vertical profiles were characterized and compared against reference plot measurements. The biophysical parameters matched well with the reference plots up to 500 *m* distance (Figure 6.3). In both sites, canopy height displayed a low RMSE up to 600 *m* distances from the scanner, indicating that increasing laser beam divergence has little consequence on canopy height determination in savanna ecosystems. By contrast, canopy cover was apparently limited by the point density, which degraded with increasing distance from the scanner. Although, uniform point density is a pre-requisite for various vegetation metrics (Wilkes et al., 2017), this study suggest of increasing *z* value with increased pulse divergence for precise canopy cover estimations. The second type of improvement is related to the minimal effort in deployment and time required to acquire the landscape scale 3D data. In particular, the long-range scan approach minimized the time required for registering the scans together to form a coherent 3D data. We also demonstrate that point density dilutes exponentially with the increasing distance from the scanner. However, the point density were not completely depleted, and long-range scans were able to depict the branching structure of large trees up to 400 *m* distance (Chapter 4, Figure 4.8). These results are a strong motivation for improvements in measurements of savanna vegetation structure, and moving beyond simple measures of height and diameter offered with manual inventory methods.

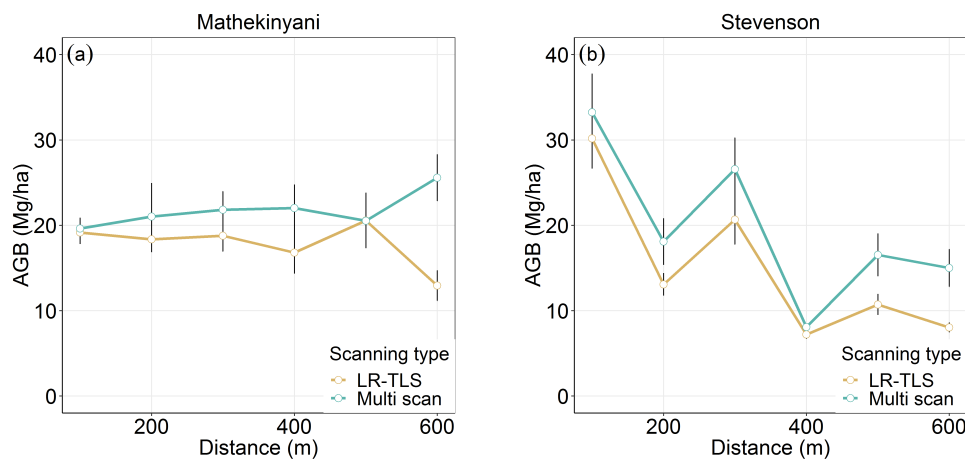


Figure 6.3: Estimation of aboveground biomass from the long-range and multi-scan setup for (a) Mathekenyani and (b) Stevenson.

In spite of the advantages of long-range scanning to manual inventory, it is important to note that the success of the proposed long-range scanning mainly relied on the scanner height above the canopy, slope, vegetation structure and season of scanning. Thus, differ-

ent vegetation and topographic settings may result in differing performance of long-range scans. For example, an increase in terrain slope may cause loss of ground points due to shadowing, which will ultimately result in overestimation of canopy height. Although, at some higher slope ($>1^\circ$) plots in our setup, a high ground point density of 70 pts/m² was recorded, which is due to mixing of vegetation returns with ground returns. Additionally, in the context of savanna ecosystems, season of scanning is very crucial, as shadowing will greatly differ between dry and wet season. Low understorey in dry season will permit deep penetration of laser pulses, which will help to get more ground points and subsequently will aid in accurate estimation of canopy height. However, wet season mapping by long-range scans should aim at taking multiple long-range scans from elevated points, preferably with different line of sight to minimize the shadows.

My approach of long-range scanning results are based on a limited sample of two sites in a Southern Africa savanna. Nevertheless, the validation of our approach provides an insight into the potential of long-range terrestrial laser scanning to account for vegetation structure, providing enough detailed architectural information to scale from landscape to regional spatial scale. This approach can be used further to estimate the vegetation structure in other arid and semi-arid regions, which might improve the current understanding of savanna structure.

In recent years, spaceborne data collection capabilities have largely increased, e.g. open access Sentinel data streams, where measurement frequency and spatial resolution are high enough to capture the vegetation dynamics of savanna. While, this growing volume of spaceborne data represents a unique opportunity for savanna vegetation structure science, it also poses a major challenge of fully exploiting these data. These earth observation missions are dependent on accurate and representative vegetation structure data for the training and validation of their algorithms. However, accurate ground vegetation inventory data for savannas are limited, which is a major cause for uncertainty in biomass and canopy cover extrapolations at savanna sites. In my study of long-range scans, AGB estimates had RMSE of 0.5 $Mgha^{-1}$ and 8 $Mgha^{-1}$ respectively at nearest and farthest plots (Figure 6.3). This evidence proves that long-range scan 3D data can play a critical role in calibration and validation of spaceborne datasets.

6.2.3 Assessing spatial patterns of woody structure in a savanna system with earth observation data

Woody biomass and cover are important descriptors of savanna structure that capture processes driven by geology, rainfall and topography. The last part of my thesis uses long-range terrestrial laser scans for scaling up the estimates of biomass and cover to regional scale using Radar data. Prior to this work, bulk of previous work exclusively focused on the manual inventory or airborne LiDAR data as training and validation of Radar data. Moreover, previous research findings were based on the examination of single landscape, thus failing to determine the spatial variability at regional scale. The present thesis picked up these flaws and addressed the famous remote sensing question for savanna vegetation

i.e. what does the Radar data sense?

My study on scaling up vegetation inventories from landscape to regional scale provides new insights into understanding and predicting Radar backscatter interaction with savanna vegetation. For example, similar height thresholds are applied on manual inventory or LiDAR data for training and validating the different wavelength Radar sensor. However, I argue that this is not true for all the landscapes in savanna, where a lower vegetation threshold showed higher correlation with smaller wavelength Radar data, while the opposite trend was observed for the longer wavelength Radar data. However, in a homogeneous ecosystem, e.g. forest, varying the height threshold will not have a significant impact on biomass estimates. This result points to one of key reason for carbon sequestration uncertainty in savanna ecosystems. Furthermore, the study showcases the significance of minimizing the time gap between training and Radar data to quantify the biomass stored in savannas. In doing so, point of time biomass will be quantified instead of a more general representation of vegetation with larger uncertainty. This finding is in accordance with the temporal variability in savannas due to droughts, herbivory or fire.

The procedures used in this work are of significant interest for implementing a park wide monitoring program. In particular, heterogeneity in biomass has emerged as a management goal in KNP, in association with maintenance of biodiversity (Rogers et al., 2003). The biomass and woody cover maps generated in Chapter 5 can provide information at a watershed or landscape scale, at which park is maintained.

6.3 Closing thoughts

By accounting for existing research needs in the field of savanna vegetation structure dynamics, a suite of high resolution remote sensing methods were explored in the present thesis. These methods are used in unravelling the vegetation structure patterns across altered fire regimes, rainfall and topographic gradients. The acquired terrestrial laser scanner 3D dataset proved to be suitable for accurate characterization of different savanna vegetation biophysical parameters, including canopy height, cover, aboveground biomass and vertical vegetation profiles. Moreover, the ability to extend these parameters from plot to landscape scale were documented from long-range terrestrial scans. From a geographical perspective, much of the work is concentrated on managed savanna lands located in South Africa. However, the described methods and data are expected to work well for any other savanna landscapes, as long as the used 3D data are of certain standard. Fortunately, these requirements are growing, with increased deployment of terrestrial laser scanner and Radar data in the savanna regions of the world. On the application side, the derived products demonstrate that rainfall, soil types and fire regimes influence vegetation structure differently. The dataset reinforce Bond & Keeley (2005) consumer control by fire and that influence of fire regimes increases along the rainfall gradient. Overall the results highlight that increased fire frequencies are necessary to maintain open savanna

system in wet regions, but this is not the case in dry savanna. In the final investigation of this work (Chapter 5), the acquired dataset were effectively employed to produce regional scale woody biomass map. These maps were then used to determine the spatial relationship between rainfall, geology and biomass. This study was exemplary for showing that landscape and hillslope scale 3D data are accurate and can be integrated with spaceborne imageries for large scale vegetation mapping.

6.4 Looking to the future

The study objectives taken in this dissertation opens new issues and leaves unsolved problems, therefore this section proposes concepts for future research. The future opportunities directly build upon the dataset acquired for this dissertation i.e. 3D data from TLS and spaceborne Radar data. New tasks aim at optimizing vegetation mapping protocols and exploiting more detailed structural vegetation properties, which will further contribute to our understanding of savanna ecosystems.

6.4.1 Individual tree scale architecture

Vegetation allometry and architecture are of great ecological significance, as they scale up to shape the structure and dynamics of any ecosystem. In savanna ecosystems, trade-off between disturbance regimes such as fire and herbivory, and the resource availability promotes the exquisite architecture of woody vegetation and shrubs (Figure 6.4). Both tree height and canopy cover have been shown to be good predictors of vegetation allometry and architecture. In Chapter-3, I evidenced the influence of disturbances and resources (mean annual precipitation and substrate) on the horizontal and vertical stature of vegetation from plot-scale analysis of high resolution 3D data. However, averaged plot-scale analysis conceals the legacy effect of disturbances and environmental factors operating on woody and shrub guilds from seedling to maturity.

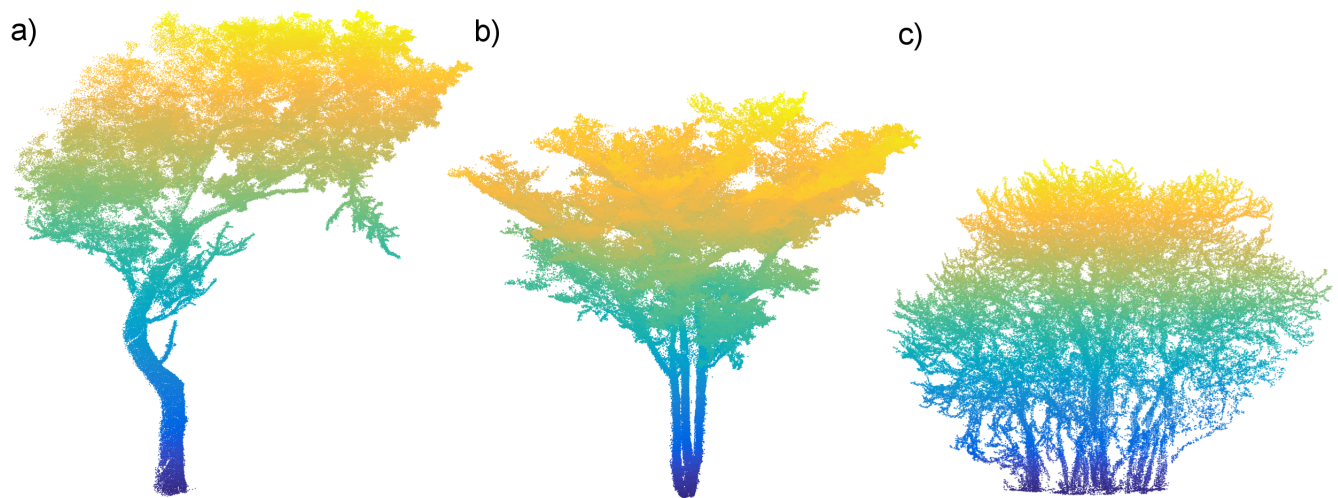


Figure 6.4: Individual tree point clouds (a) Marula, (b) and (c) Mopane in Experimental burn plots of Kruger National Park, South Africa, coloured by height from low (blue) to high (yellow). The contrasting three-dimensional structures across EBPs are associated with the fire frequency and intensity.

Patterns of tree allometries and architecture in savannas partly reflect growth vs survival strategies arising from the repeated disturbance effects. For instance, during repeated fire events, vegetation architecture is geared towards rapid height growth to escape the fires, and minimize topkill. In addition to vertical growth, increasing herbivory pressure on vegetation promotes structural defenses by increased branching and wide canopies. These architectural changes are reflected in stem diameter-height relationships, branching angles and volume. Measurement of branching angle, volume and canopy spread necessitates detailed sampling efforts and repeated measurements. This is an area where TLS has the potential to make new contributions and strategy relationships, e.g. canopy height-stem volume or stem volume-branching order.

Figure 6.5 shows how complex tree architecture parameters are extracted from point clouds using Quantitative Structure Models (QSM) (Raumonen et al., 2013). QSM approach involves fitting combinations of multiple cylinders varying in radius and height. Total volume, stem and branch volume, branching angles, height and diameter at breast are some of the complex attributes that can be estimated from the QSM models. I foresee vegetation QSMs as next step in improving the savanna tree allometries and subsequently inferring the growth rates, carbon losses after the disturbance events in savannas. While most reconstruction algorithms have been trained for the temperate trees, several advancements need to follow to accurately create the structure models for multi-stem vegetation in savannas.

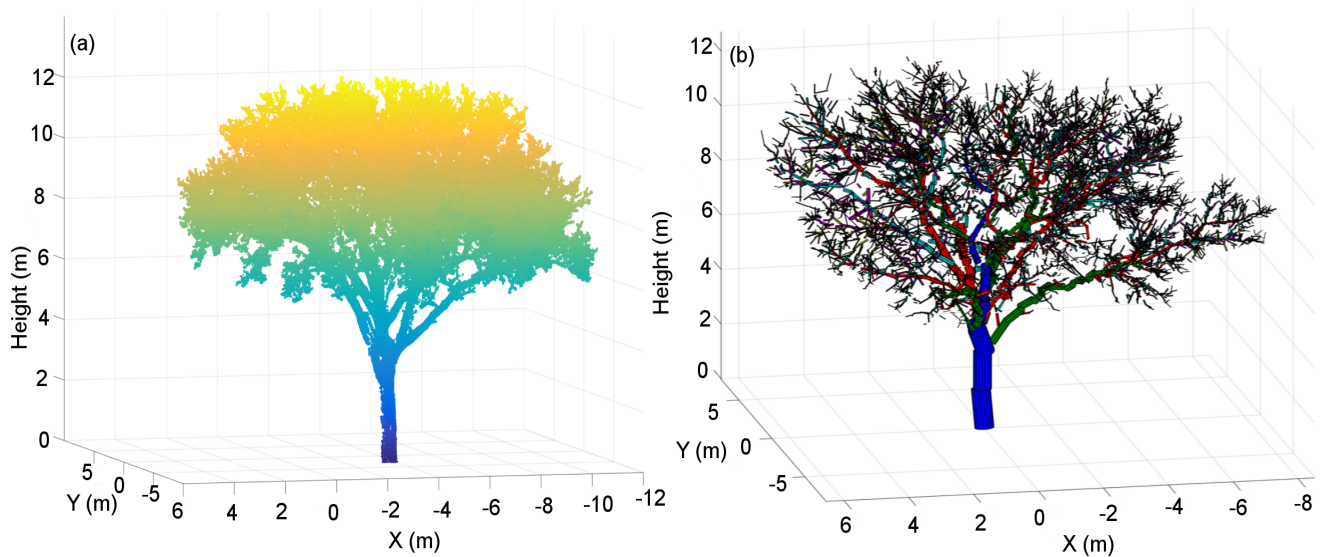


Figure 6.5: a) TLS point cloud of a Marula (*Sclerocarya birrea*) coloured by height low (blue) to high (yellow). (b) QSM model derived from using (Raumonen et al., 2013) algorithm. The total volume, branch volume and DBH of the tree were 5210 cm³, 3841 cm³ and 53 cm respectively.

6.4.2 Comparison of long-range scans performance over different savanna landscapes- benchmark study

Despite the suitability of long-range scanning in describing vegetation structure with unprecedented detail, the method described in Chapter 4 revealed certain limitations. For instance, the accuracy of long-range scanning across varying topographic gradients i.e slope, elevation, and vegetation types have not been characterized properly. The focus of outlook-2, therefore lies in overcoming and addressing these limitations and improving the scanning mechanism. One way to ensure the efficiency of long-range scanning is to classify acquired 106 long-range scans across KNP based on vegetation type (low to closed canopy cover) and topography. A point density measure along increasing distance can be used later to determine the efficiency of long-range scanning across all landscapes (Figure 6.6). Also, from the experiences gained in this thesis, I assume that scanning savanna ecosystems is very different than tropical and temperate ecosystems, due to more open vegetation structure. This opens up an opportunity to devise the first scanning protocols for mapping savanna ecosystems, which can encompass data acquisition essentials such as number of scanning positions requirement, pulse repetition rate and scan time. A standard scanning protocol will allow data interoperability and comparison of long-range vegetation metrics across other savanna sites.

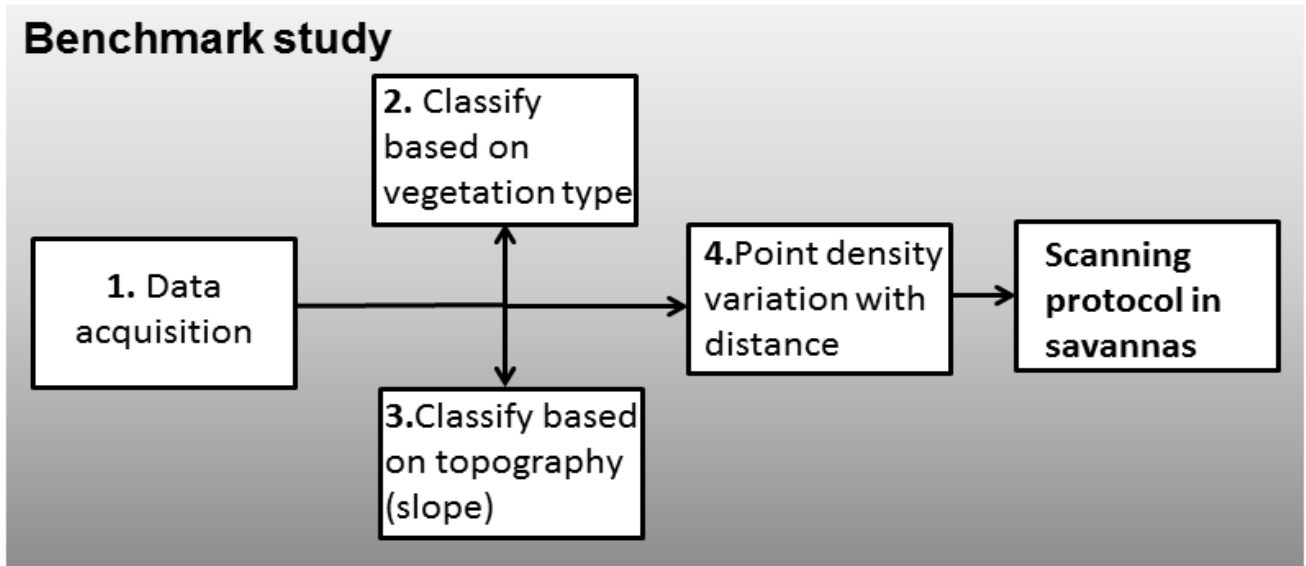


Figure 6.6: Work task of the concept for LR-TLS benchmark study.

With several upcoming satellite missions in the coming decade, the number of vegetation biophysical products will greatly increase. Despite the recognition of biophysical mapping in policy making and management applications in savanna ecosystems, there is a need to provide accurate product validation (Duncanson et al., 2019). The high resolution multi-scan and long-range terrestrial laser scan data collected for this thesis work can be tools for satellite derived products validation.

6.4.3 Temporal change analysis

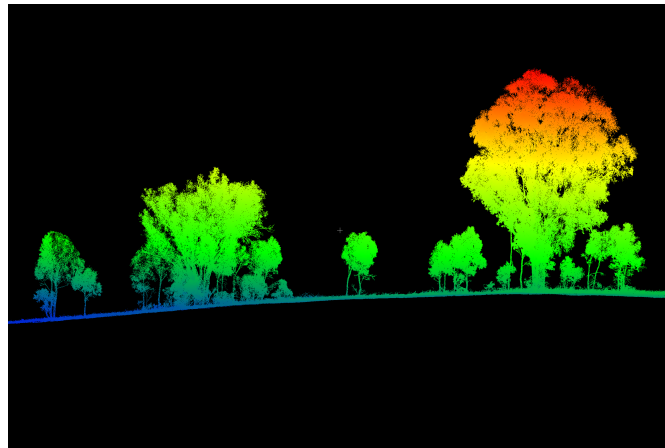
The recent IPCC report on Climate change and Land highlighted altered rainfall regimes across arid and semi-arid areas have been highlighted as major predictors of climate change (IPCC, 2019). Extremely high rainfall events may be one outcome of this change, but concerns remain around the occurrence of droughts, as water availability is a key determinant of savanna structure and function (Sankaran et al., 2005). For example, Kruger National Park, on which this dissertation work is based, experienced a major 2 year (2014-2016) drought. These drought events open up savannas by rendering increased tree mortality and imposing implications on terrestrial carbon sink. Drought related savanna vegetation structure alterations have been reported in several previous studies (Fensham & Holman, 1999; Fensham & Fairfax, 2007; Swemmer et al., 2018). While these studies are from different regions of the world, but are consistent with the fact that drought effects are spatially variable across the landscapes and are related to soil texture and properties. Understanding how these different landscapes differ in vegetation structure distribution before and after the drought events represents a major task for savanna ecologists.

The enormous 3D data collected during this dissertation in 2016 will be a great asset in

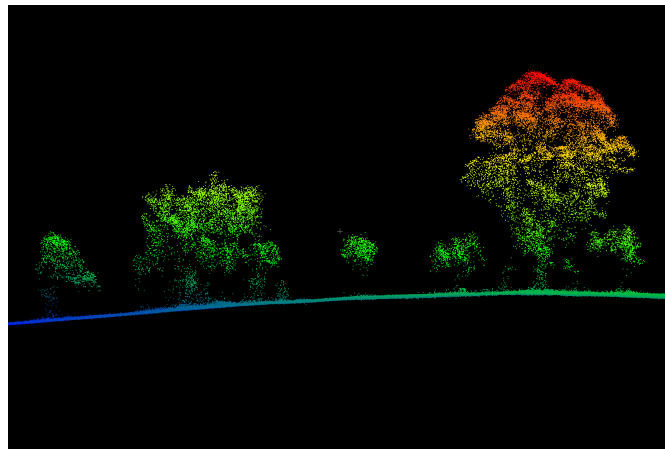
understanding the effects of drought, as the data spans a topographic as well as rainfall gradient. Canopy cover and biomass from the 3D data, as illustrated in Chapter 4, can be used to back-calibrate freely available ALOS-PALSAR Radar mosaics for the year 2010, to generate regional canopy cover and biomass map. Here, back-calibration refers to estimating canopy cover and biomass for few suspected unchanged regions in the year 2016. Later, a change detection between landscapes can be performed by matching 2010 map with the 2016 ALOS-PALSAR-2 derived vegetation map presented in this thesis.

6.4.4 Beyond terrestrial LiDAR

As stated in Chapters 3,4 and 5, the TLS point clouds analyzed in this thesis were acquired from Riegl VZ-2000 terrestrial LiDAR. The data from Riegl VZ-2000 was efficient enough to unravel the methods development and their application to savanna ecological questions. One of the major limitation encountered in the long-range scanning was gradual loss of ground points with increasing distance. I foresee that this limitation of long-range scans can be overcome by merging long-range scans data with UAV (Unmanned aerial vehicle) 3D data. A UAV mounted with LiDAR sensor can increase the spatial coverage of 3D data to a great extent. Also, UAV scans at low altitude than airborne LiDAR thereby providing sufficient information on understory and vegetation trunks. This is important for the structural description of savannas. Future research should use the fusion of point clouds from UAV LiDAR with the long-range scanning, to better characterize the ground.



(a)



(b)

Figure 6.7: (a) TLS and (b) Unmanned aerial vehicle acquired point cloud across Northern Australian savanna sites. It is evident from UAV point clouds that stems of the vegetation are not properly characterized. The data quality from UAV is greatly influenced by the flight paths, overlap and laser sensor. (Data courtesy: Shaun Levick)

References

- Abreu, R. C., Hoffmann, W. A., Vasconcelos, H. L., Pilon, N. A., Rossatto, D. R., & Durigan, G. (2017). The biodiversity cost of carbon sequestration in tropical savanna. *Science Advances*, *3*, e1701284.
- Alizai, H. U., & Hulbert, L. C. (1970). Effects of soil texture on evaporative loss and available water in semi-arid climates. *Soil Science*, *110*, 328–332.
- Andela, N., Morton, D., Giglio, L., Chen, Y., Van Der Werf, G., Kasibhatla, P., DeFries, R., Collatz, G., Hantson, S., Kloster, S. et al. (2017). A human-driven decline in global burned area. *Science*, *356*, 1356–1362.
- Andersen, A. N., Cook, G. D., Corbett, L. K., Douglas, M. M., Eager, R. W., Russell-Smith, J., Setterfield, S. A., Williams, R. J., & Woinarski, J. C. (2005). Fire frequency and biodiversity conservation in australian tropical savannas: implications from the kapalga fire experiment. *Austral Ecology*, *30*, 155–167.
- Anderson, K. E., Glenn, N. F., Spaete, L. P., Shinneman, D. J., Pilliod, D. S., Arkle, R. S., McIlroy, S. K., & Derryberry, D. R. (2018). Estimating vegetation biomass and cover across large plots in shrub and grass dominated drylands using terrestrial lidar and machine learning. *Ecological Indicators*, *84*, 793–802.
- Archibald, S., & Bond, W. J. (2003). Growing tall vs growing wide: tree architecture and allometry of acacia karroo in forest, savanna, and arid environments. *Oikos*, *102*, 3–14.
- Archibald, S., Lehmann, C. E., Gómez-Dans, J. L., & Bradstock, R. A. (2013). Defining pyromes and global syndromes of fire regimes. *Proceedings of the National Academy of Sciences*, *110*, 6442–6447.
- Archibald, S., Nickless, A., Govender, N., Scholes, R. J., & Lehsten, V. (2010). Climate and the inter-annual variability of fire in southern africa: a meta-analysis using long-term field data and satellite-derived burnt area data. *Global Ecology and Biogeography*, *19*, 794–809.
- Archibald, S., & Scholes, R. (2007). Leaf green-up in a semi-arid african savanna—separating tree and grass responses to environmental cues. *Journal of Vegetation Science*, *18*, 583–594.
- Asner, G. P., Elmore, A. J., Olander, L. P., Martin, R. E., & Harris, A. T. (2004). Grazing systems,ecosystem responses, and global change. *Annual Review of Environment and*

- Resources*, 29, 261–299.
- Asner, G. P., Knapp, D. E., Kennedy-Bowdoin, T., Jones, M. O., Martin, R. E., Boardman, J. W., & Field, C. B. (2007). Carnegie airborne observatory: in-flight fusion of hyperspectral imaging and waveform light detection and ranging for three-dimensional studies of ecosystems. *Journal of Applied Remote Sensing*, 1, 013536.
- Asner, G. P., & Levick, S. R. (2012). Landscape-scale effects of herbivores on treefall in african savannas. *Ecology Letters*, 15, 1211–1217.
- Asner, G. P., Levick, S. R., Kennedy-Bowdoin, T., Knapp, D. E., Emerson, R., Jacobson, J., Colgan, M. S., & Martin, R. E. (2009). Large-scale impacts of herbivores on the structural diversity of african savannas. *Proceedings of the National Academy of Sciences*, 106, 4947–4952.
- Asner, G. P., Vaughn, N., Smit, I. P., & Levick, S. (2015). Ecosystem-scale effects of megafauna in african savannas. *Ecography*, 39, 240–252.
- Astrup, R., Ducey, M. J., Granhus, A., Ritter, T., & von Lüpke, N. (2014). Approaches for estimating stand-level volume using terrestrial laser scanning in a single-scan mode. *Canadian Journal of Forest Research*, 44, 666–676.
- Atkins, J. W., Bohrer, G., Fahey, R. T., Hardiman, B. S., Morin, T. H., Stovall, A. E., Zimmerman, N., & Gough, C. M. (2018). Quantifying vegetation and canopy structural complexity from terrestrial li dar data using the forest r package. *Methods in Ecology and Evolution*, 9, 2057–2066.
- Beland, M., Parker, G., Sparrow, B., Harding, D., Chasmer, L., Phinn, S., Antonarakis, A., & Strahler, A. (2019). On promoting the use of lidar systems in forest ecosystem research. *Forest Ecology and Management*, 450, 117484.
- Biggs, R., Biggs, H. C., Dunne, T. T., Govender, N., & Potgieter, A. L. F. (2003). Experimental burn plot trial in the Kruger National Park: history, experimental design and suggestions for data analysis. *Koedoe*, 46, 1–15.
- Boggs, G. (2010). Assessment of spot 5 and quickbird remotely sensed imagery for mapping tree cover in savannas. *International Journal of Applied Earth Observation and Geoinformation*, 12, 217–224.
- Bond, W., & Keeley, J. (2005). Fire as a global ‘herbivore’: the ecology and evolution of flammable ecosystems. *Trends in Ecology & Evolution*, 20, 387–394.
- Bond, W., Midgley, G., & Woodward, F. (2003). The importance of low atmospheric CO₂ and fire in promoting the spread of grasslands and savannas. *Global Change Biology*, 9, 973–982.
- Bond, W. J. (2008). What limits trees in c4 grasslands and savannas? *Annual Review of Ecology, Evolution, and Systematics*, 39, 641–659.
- Bond, W. J., & Midgley, G. F. (2012). Carbon dioxide and the uneasy interactions of trees and savannah grasses. *Philosophical Transactions of the Royal Society B: Biological*

- Sciences*, 367, 601.
- Bond, W. J., & Parr, C. L. (2010). Beyond the forest edge: ecology, diversity and conservation of the grassy biomes. *Biological Conservation*, 143, 2395–2404.
- Bond, W. J., Woodward, F. I., & Midgley, G. F. (2005). The global distribution of ecosystems in a world without fire. *New Phytologist*, 165, 525–537.
- Bradshaw, C. J., Bowman, D. M., Bond, N. R., Murphy, B. P., Moore, A. D., Fordham, D. A., Thackway, R., Lawes, M. J., McCallum, H., Gregory, S. D. et al. (2013). Brave new green world—consequences of a carbon economy for the conservation of Australian biodiversity. *Biological Conservation*, 161, 71–90.
- Brain, C. K., & Sillent, A. (1988). Evidence from the Swartkrans cave for the earliest use of fire. *Nature*, 336, 464–466.
- Bucini, G., & Hanan, N. P. (2007). A continental-scale analysis of tree cover in African savannas. *Global Ecology and Biogeography*, 16, 593–605.
- Bucini, G., Hanan, N. P., Boone, R. B., Smit, I. P., Saatchi, S. S., Lefsky, M. A., & Asner, G. P. (2010). Woody fractional cover in Kruger National Park, South Africa: Remote sensing-based maps and ecological insights. *Ecosystem Function in Savannas*, (pp. 259–278).
- Buitenwerf, R., Bond, W., Stevens, N., & Trollope, W. (2012). Increased tree densities in South African savannas: >50 years of data suggests CO₂ as a driver. *Global Change Biology*, 18, 675–684.
- Burnham, K. P., & Anderson, D. R. (2002). A practical information-theoretic approach. In *Model selection and multimodel inference*, 2nd ed. Springer, New York.
- Burt, A., Disney, M., & Calders, K. (2018). Extracting individual trees from lidar point clouds using treeseg. *Methods in Ecology and Evolution*, 10, 438–445.
- Calders, K., Armston, J., Newnham, G., Herold, M., & Goodwin, N. (2014). Implications of sensor configuration and topography on vertical plant profiles derived from terrestrial lidar. *Agricultural and Forest Meteorology*, 194, 104–117.
- Calders, K., Newnham, G., Burt, A., Murphy, S., Raunonen, P., Herold, M., Culvenor, D., Avitabile, V., Disney, M., Armston, J., & Kaasalainen, M. (2015). Nondestructive estimates of above-ground biomass using terrestrial laser scanning. *Methods in Ecology and Evolution*, 6, 198–208.
- Calders, K., Origo, N., Burt, A., Disney, M., Nightingale, J., Raunonen, P., Åkerblom, M., Malhi, Y., & Lewis, P. (2018). Realistic forest stand reconstruction from terrestrial lidar for radiative transfer modelling. *Remote Sensing*, 10, 933.
- Carreiras, J. M., Vasconcelos, M. J., & Lucas, R. M. (2012). Understanding the relationship between aboveground biomass and ALOS PALSAR data in the forests of Guinea-Bissau (West Africa). *Remote Sensing of Environment*, 121, 426–442.
- Ciais, P., Bombelli, A., Williams, M., Piao, S., Chave, J., Ryan, C., Henry, M., Brender,

- P., & Valentini, R. (2011). The carbon balance of Africa: synthesis of recent research studies. *Philosophical Transactions of the Royal Society A: Mathematical, Physical and Engineering Sciences*, *369*, 2038–2057.
- Clarke, P. J., Knox, K. J., Wills, K. E., & Campbell, M. (2005). Landscape patterns of woody plant response to crown fire: disturbance and productivity influence sprouting ability. *Journal of Ecology*, *93*, 544–555.
- Colgan, M., Asner, G., Levick, S. R., Martin, R., & Chadwick, O. (2012). Topo-edaphic controls over woody plant biomass in south african savannas. *Biogeosciences*, *9*, 1809–1821.
- Colgan, M. S., Asner, G. P., & Swemmer, T. (2013). Harvesting tree biomass at the stand level to assess the accuracy of field and airborne biomass estimation in savannas. *Ecological Applications*, *23*, 1170–1184.
- Cook, G. D., Liedloff, A. C., Eager, R. W., Chen, X., Williams, R., O'Grady, A. P., & Hutley, L. B. (2005). The estimation of carbon budgets of frequently burnt tree stands in savannas of northern Australia, using allometric analysis and isotopic discrimination. *Australian Journal of Botany*, *53*, 621–630.
- Côté, J.-F., Fournier, R. A., Frazer, G. W., & Niemann, K. O. (2012). A fine-scale architectural model of trees to enhance lidar-derived measurements of forest canopy structure. *Agricultural and Forest Meteorology*, *166*, 72–85.
- Coughenour, M. B., & Ellis, J. E. (1993). Landscape and climatic control of woody vegetation in a dry tropical ecosystem: Turkana District, Kenya. *Journal of Biogeography*, *20*, 383.
- Cumming, D. H., Fenton, M. B., Rautenbach, I. L., Taylor, R. D., Cumming, G. S., Cumming, M. S., Dunlop, J. M., Ford, A. G., Hovorka, M. D., Johnston, D. S. et al. (1997). Elephants, woodlands and biodiversity in southern africa. *South African Journal of Science*, *93*, 231–236.
- Cuni-Sanchez, A., White, L. J., Calders, K., Jeffery, K. J., Abernethy, K., Burt, A., Disney, M., Gilpin, M., Gomez-Dans, J. L., & Lewis, S. L. (2016). African savanna-forest boundary dynamics: A 20-year study. *PloS one*, *11*, e0156934.
- Dassot, M., Colin, A., Santenoise, P., Fournier, M., & Constant, T. (2012). Terrestrial laser scanning for measuring the solid wood volume, including branches, of adult standing trees in the forest environment. *Computers and Electronics in Agriculture*, *89*, 86–93.
- Dassot, M., Constant, T., & Fournier, M. (2011). The use of terrestrial lidar technology in forest science: application fields, benefits and challenges. *Annals of Forest Science*, *68*, 959–974.
- Davies, A. B., Gaylard, A., & Asner, G. P. (2018). Megafaunal effects on vegetation structure throughout a densely wooded african landscape. *Ecological Applications*, *28*, 398–408.

- Devine, A. P., Stott, I., McDonald, R. A., & Maclean, I. M. D. (2015). Woody cover in wet and dry African savannas after six decades of experimental fires. *Journal of Ecology*, *103*, 473–478.
- Disney, M. I., Boni Vicari, M., Burt, A., Calders, K., Lewis, S. L., Raunonen, P., & Wilkes, P. (2018). Weighing trees with lasers: advances, challenges and opportunities. *Interface Focus*, *8*, 20170048.
- Dittmann, S., Thiessen, E., & Hartung, E. (2017). Applicability of different non-invasive methods for tree mass estimation: A review. *Forest Ecology and Management*, *398*, 208–215.
- Dobson, M. C., Ulaby, F. T., LeToan, T., Beaudoin, A., Kasischke, E. S., & Christensen, N. (1992). Dependence of radar backscatter on coniferous forest biomass. *IEEE Transactions on Geoscience and Remote Sensing*, *30*, 412–415.
- Donaldson, J. E., Archibald, S., Govender, N., Pollard, D., Luhdo, Z., & Parr, C. L. (2018). Ecological engineering through fire-herbivory feedbacks drives the formation of savanna grazing lawns. *Journal of Applied Ecology*, *55*, 225–235.
- Du Toit, P. (1972). Acacia karroo intrusion: the effect of burning and sparing. *Proceedings of the Annual Congresses of the Grassland Society of Southern Africa*, *7*, 23–27.
- Dubayah, R. O., & Drake, J. B. (2000). Lidar remote sensing for forestry. *Journal of Forestry*, *98*, 44–46.
- Ducey, M. J., Astrup, R., Seifert, S., Pretzsch, H., Larson, B. C., & Coates, K. D. (2013). Comparison of forest attributes derived from two terrestrial lidar systems. *Photogrammetric Engineering & Remote Sensing*, *79*, 245–257.
- Duncanson, L., Armston, J., Disney, M., Avitabile, V., Barbier, N., Calders, K., Carter, S., Chave, J., Herold, M., Crowther, T., & Falkowski, M. (2019). The importance of consistent global forest aboveground biomass product validation. *Surveys in geophysics*, *40*, 979–999.
- Dwyer, E., Pinnock, S., Grégoire, J.-M., & Pereira, J. (2000). Global spatial and temporal distribution of vegetation fire as determined from satellite observations. *International Journal of Remote Sensing*, *21*, 1289–1302.
- Eckhardt, H., Van Wilgen, B., & Biggs, H. (2000). Trends in woody vegetation cover in the Kruger National Park, South Africa, between 1940 and 1998. *African Journal of Ecology*, *38*, 108–115.
- Edwards, A., Kennett, R., Price, O., Russell-Smith, J., Spiers, G., & Woinarski, J. (2003). Monitoring the impacts of fire regimes on vegetation in northern Australia: an example from Kakadu National Park. *International Journal of Wildland Fire*, *12*, 427–440.
- Ehbrecht, M., Schall, P., Ammer, C., & Seidel, D. (2017). Quantifying stand structural complexity and its relationship with forest management, tree species diversity and microclimate. *Agricultural and Forest Meteorology*, *242*, 1–9.

- Enslin, B., Potgieter, A. L. F., Biggs, H. C., & Biggs, R. (2000). Long term effects of fire frequency and season on the woody vegetation dynamics of the *Sclerocarya birra*/*Accacia nigrescens* savanna of the Kruger National Park. *Koedoe*, *43*, 27–37.
- February, E. C., Higgins, S. I., Bond, W. J., & Swemmer, L. (2013). Influence of competition and rainfall manipulation on the growth responses of savanna trees and grasses. *Ecology*, *94*, 1155–1164.
- Fensham, R., & Fairfax, R. (2007). Drought-related tree death of savanna eucalypts: species susceptibility, soil conditions and root architecture. *Journal of Vegetation Science*, *18*, 71–80.
- Fensham, R., & Holman, J. (1999). Temporal and spatial patterns in drought-related tree dieback in Australian savanna. *Journal of Applied Ecology*, (pp. 1035–1050).
- Fensham, R. J., Butler, D. W., & Foley, J. (2015). How does clay constrain woody biomass in drylands? *Global Ecology and Biogeography*, *24*, 950–958.
- Fernandez-Illescas, C. P., Porporato, A., Laio, F., & Rodriguez-Iturbe, I. (2001). The ecohydrological role of soil texture in a water-limited ecosystem. *Water Resources Research*, *37*, 2863–2872.
- Frazer, G., Magnussen, S., Wulder, M., & Niemann, K. (2011). Simulated impact of sample plot size and co-registration error on the accuracy and uncertainty of lidar-derived estimates of forest stand biomass. *Remote Sensing of Environment*, *115*, 636–649.
- Frost, P., Menaut, J., Walter, B., Medina, E., Solbrig, O., & Swift, M. (1986). Response of savannas to stress and disturbance: a proposal for a collaborative programme of research report of IUBS working group on decade of the tropics programme. *Biology International*, (p. 82).
- Galvin, K. A., & Reid, R. S. (2010). People in savanna ecosystems: land use, change, and sustainability. In *Ecosystem Function in Savannas* (pp. 521–536). CRC Press.
- Gaughan, A. E., Holdo, R. M., & Anderson, T. M. (2013). Using short-term modis time-series to quantify tree cover in a highly heterogeneous African savanna. *International Journal of Remote Sensing*, *34*, 6865–6882.
- Gertenbach, W. D. (1983). Landscapes of the Kruger National Park. *Koedoe*, *26*, 9–121.
- Gessner, U., Machwitz, M., Conrad, C., & Dech, S. (2013). Estimating the fractional cover of growth forms and bare surface in savannas. a multi-resolution approach based on regression tree ensembles. *Remote Sensing of Environment*, *129*, 90–102.
- Gill, A. M. (1975). Fire and the Australian flora: a review. *Australian Forestry*, *38*, 4–25.
- Gillson, L. (2004). Evidence of hierarchical patch dynamics in an East African savanna? *Landscape Ecology*, *19*, 883–894.
- Goldbergs, G., Levick, S. R., Lawes, M., & Edwards, A. (2018). Hierarchical integration of individual tree and area-based approaches for savanna biomass uncertainty estimation

- from airborne lidar. *Remote Sensing of Environment*, 205, 141–150.
- Goldewijk, K. K. (2001). Estimating global land use change over the past 300 years: the hyde database. *Global Biogeochemical Cycles*, 15, 417–433.
- Govender, N., Trollope, W. S. W., & Van Wilgen, B. W. (2006). The effect of fire season, fire frequency, rainfall and management on fire intensity in savanna vegetation in South Africa: Fire intensity in savanna. *Journal of Applied Ecology*, 43, 748–758.
- Grace, J., Jose, J. S., Meir, P., Miranda, H. S., & Montes, R. A. (2006). Productivity and carbon fluxes of tropical savannas. *Journal of Biogeography*, 33, 387–400.
- Grady, J. M., & Hoffmann, W. A. (2012). Caught in a fire trap: recurring fire creates stable size equilibria in woody resprouters. *Ecology*, 93, 2052–2060.
- Gwenzi, D., & Lefsky, M. A. (2014). Modeling canopy height in a savanna ecosystem using spaceborne lidar waveforms. *Remote Sensing of Environment*, 154, 338–344.
- Hackenberg, J., Wassenberg, M., Spiecker, H., & Sun, D. (2015). Non destructive method for biomass prediction combining tls derived tree volume and wood density. *Forests*, 6, 1274–1300.
- Hanan, N., Sea, W., Dangelmayr, G., & Govender, N. (2008). Do Fires in Savannas Consume Woody Biomass? A Comment on Approaches to Modeling Savanna Dynamics. *The American Naturalist*, 171, 851–856.
- Hansen, M. C., Potapov, P. V., Moore, R., Hancher, M., Turubanova, S., Tyukavina, A., Thau, D., Stehman, S., Goetz, S., Loveland, T. R. et al. (2013). High-resolution global maps of 21st-century forest cover change. *Science*, 342, 850–853.
- Hardiman, B., LaRue, E., Atkins, J., Fahey, R., Wagner, F., & Gough, C. (2018). Spatial variation in canopy structure across forest landscapes. *Forests*, 9, 474.
- Hastie, T., Tibshirani, R., & Friedman, J. (2009). *The elements of statistical learning: data mining, inference, and prediction*. Springer Science & Business Media.
- Helm, C., Wilson, G., Midgley, J., Kruger, L., & Witkowski, E. (2011). Investigating the vulnerability of an african savanna tree (*Sclerocarya birrea ssp. caffra*) to fire and herbivory. *Austral Ecology*, 36, 964–973.
- Helm, C. V., & Witkowski, E. (2012). Characterising wide spatial variation in population size structure of a keystone african savanna tree. *Forest Ecology and Management*, 263, 175–188.
- Herrick, J. E., Van Zee, J. W., Havstad, K. M., Burkett, L. M., Whitford, W. G. et al. (2005). *Monitoring manual for grassland, shrubland and savanna ecosystems. Volume I: Quick Start. Volume II: Design, supplementary methods and interpretation..* USDA-ARS Jornada Experimental Range.
- Higginbottom, T. P., Symeonakis, E., Meyer, H., & van der Linden, S. (2018). Mapping fractional woody cover in semi-arid savannahs using multi-seasonal composites from landsat data. *ISPRS Journal of Photogrammetry and Remote Sensing*, 139, 88–102.

- Higgins, S. I., Bond, W. J., Combrink, H., Craine, J. M., February, E. C., Govender, N., Lannas, K., Moncreiff, G., & Trollope, W. S. (2012). Which traits determine shifts in the abundance of tree species in a fire-prone savanna? *Journal of Ecology*, *100*, 1400–1410.
- Higgins, S. I., Bond, W. J., February, E. C., Bronn, A., Euston-Brown, D. I., Enslin, B., Govender, N., Rademan, L., O'Regan, S., Potgieter, A. L. et al. (2007). Effects of four decades of fire manipulation on woody vegetation structure in savanna. *Ecology*, *88*, 1119–1125.
- Higgins, S. I., Bond, W. J., & Trollope, W. S. (2000). Fire, resprouting and variability: a recipe for grass–tree coexistence in savanna. *Journal of Ecology*, *88*, 213–229.
- Higgins, S. I., Shackleton, C. M., & Robinson, E. R. (1999). Changes in woody community structure and composition under contrasting landuse systems in a semi-arid savanna, south africa. *Journal of Biogeography*, *26*, 619–627.
- Hilker, T., van Leeuwen, M., Coops, N. C., Wulder, M. A., Newnham, G. J., Jupp, D. L., & Culvenor, D. S. (2010). Comparing canopy metrics derived from terrestrial and airborne laser scanning in a douglas-fir dominated forest stand. *Trees*, *24*, 819–832.
- Hill, M. J., & Hanan, N. P. (2010). *Ecosystem function in savannas: Measurement and modeling at landscape to global scales*. CRC Press.
- Hoffmann, W. A., & Solbrig, O. T. (2003). The role of topkill in the differential response of savanna woody species to fire. *Forest Ecology and Management*, *180*, 273–286.
- Holdo, R. M. (2013). Revisiting the two-layer hypothesis: coexistence of alternative functional rooting strategies in savannas. *PLoS One*, *8*, e69625.
- Hopkinson, C., Chasmer, L., Young-Pow, C., & Treitz, P. (2004). Assessing forest metrics with a ground-based scanning lidar. *Canadian Journal of Forest Research*, *34*, 573–583.
- Isenburg, M. (2014). Lastools—efficient lidar processing software (version 140929); rapid-lasso gmbh: Gilching.
- Jacobs, O., & Biggs, R. (2001). The effect of different fire treatments on the population structure and density of the marula, *sclerocarya birrea* (a. rich.) subsp. *caffra* (sond.) *kokwaro* (kokwaro & gillet 1980) in the Kruger National Park. *African Journal of Range and Forage Science*, *18*, 13–23.
- Jeltsch, F., Milton, S., Dean, W., Van Rooyen, N., & Moloney, K. (1998). Modelling the impact of small-scale heterogeneities on tree—grass coexistence in semi-arid savannas. *Journal of Ecology*, *86*, 780–793.
- Kgope, B. S., Bond, W. J., & Midgley, G. F. (2010). Growth responses of African savanna trees implicate atmospheric CO₂ as a driver of past and current changes in savanna tree cover. *Austral Ecology*, *35*, 451–463.
- Khosravipour, A., Skidmore, A. K., Isenburg, M., Wang, T., & Hussin, Y. A. (2014). Generating pit-free canopy height models from airborne lidar. *Photogrammetric Engineering*

- ISPRS Journal of Photogrammetry and Remote Sensing*, 80, 863–872.
- Kraaij, T., & Ward, D. (2006). Effects of rain, nitrogen, fire and grazing on tree recruitment and early survival in bush-encroached savanna, South Africa. *Plant Ecology*, 186, 235–246.
- Lawes, M., Murphy, B., Midgley, J., & Russell-Smith, J. (2011). Are the eucalypt and non-eucalypt components of Australian tropical savannas independent? *Oecologia*, 166, 229–239.
- Le Toan, T., Beaudoin, A., Riou, J., & Guyon, D. (1992). Relating forest biomass to SAR data. *IEEE Transactions on Geoscience and Remote Sensing*, 30, 403–411.
- Lefsky, M. A., Cohen, W. B., Parker, G. G., & Harding, D. J. (2002). Lidar remote sensing for ecosystem studies: Lidar, an emerging remote sensing technology that directly measures the three-dimensional distribution of plant canopies, can accurately estimate vegetation structural attributes and should be of particular interest to forest, landscape, and global ecologists. *AIBS Bulletin*, 52, 19–30.
- Lehmann, C. E., Anderson, T. M., Sankaran, M., Higgins, S. I., Archibald, S., Hoffmann, W. A., Hanan, N. P., Williams, R. J., Fensham, R. J., Felfli, J. et al. (2014). Savanna vegetation-fire-climate relationships differ among continents. *Science*, 343, 548–552.
- Lehmann, C. E., Archibald, S. A., Hoffmann, W. A., & Bond, W. J. (2011). Deciphering the distribution of the savanna biome. *New Phytologist*, 191, 197–209.
- Levick, S., & Rogers, K. (2008). Structural biodiversity monitoring in savanna ecosystems: Integrating lidar and high resolution imagery through object-based image analysis. In *Object-Based Image Analysis* (pp. 477–491). Springer.
- Levick, S. R., & Asner, G. P. (2013). The rate and spatial pattern of treefall in a savanna landscape. *Biological Conservation*, 157, 121–127.
- Levick, S. R., Asner, G. P., & Smit, I. P. (2012). Spatial patterns in the effects of fire on savanna vegetation three-dimensional structure. *Ecological Applications*, 22, 2110–2121.
- Levick, S. R., Baldeck, C. A., & Asner, G. P. (2015). Demographic legacies of fire history in an African savanna. *Functional Ecology*, 29, 131–139.
- Levick, S. R., Hessenmöller, D., & Schulze, E.-D. (2016). Scaling wood volume estimates from inventory plots to landscapes with airborne lidar in temperate deciduous forest. *Carbon Balance and Management*, 11, 7.
- Levick, S. R., & Rogers, K. H. (2011). Context-dependent vegetation dynamics in an African savanna. *Landscape Ecology*, 26, 515–528.
- Liang, X., Kankare, V., Hyypä, J., Wang, Y., Kukko, A., Haggrén, H., Yu, X., Kaartinen, H., Jaakkola, A., Guan, F. et al. (2016). Terrestrial laser scanning in forest inventories. *ISPRS Journal of Photogrammetry and Remote Sensing*, 115, 63–77.
- Lindenmayer, D. B., Laurance, W. F., & Franklin, J. F. (2012). Global decline in large

- old trees. *Science*, *338*, 1305–1306.
- Lipsett-Moore, G. J., Wolff, N. H., & Game, E. T. (2018). Emissions mitigation opportunities for savanna countries from early dry season fire management. *Nature Communications*, *9*, 2247.
- Lovell, J., Jupp, D., Newnham, G., & Culvenor, D. (2011). Measuring tree stem diameters using intensity profiles from ground-based scanning lidar from a fixed viewpoint. *ISPRS Journal of Photogrammetry and Remote Sensing*, *66*, 46–55.
- Lu, H., Raupach, M. R., McVicar, T. R., & Barrett, D. J. (2003). Decomposition of vegetation cover into woody and herbaceous components using AVHRR NDVI time series. *Remote Sensing of Environment*, *86*, 1–18.
- Lucas, R., Armston, J., Fairfax, R., Fensham, R., Accad, A., Carreiras, J., Kelley, J., Bunting, P., Clewley, D., Bray, S. et al. (2010). An evaluation of the ALOS PALSAR L-band backscatter—above ground biomass relationship queensland, australia: Impacts of surface moisture condition and vegetation structure. *IEEE Journal of Selected Topics in Applied Earth Observations and Remote Sensing*, *3*, 576–593.
- Lucas, R. M., & Armston, J. (2007). ALOS PALSAR for characterizing wooded savannas in northern Australia. In *Geoscience and Remote Sensing Symposium, 2007. IGARSS 2007. IEEE International* (pp. 3610–3613). IEEE.
- Lucas, R. M., Moghaddam, M., & Cronin, N. (2004). Microwave scattering from mixed-species forests, queensland, australia. *IEEE Transactions on Geoscience and Remote Sensing*, *42*, 2142–2159.
- Ludwig, F., De Kroon, H., Berendse, F., & Prins, H. H. (2004). The influence of savanna trees on nutrient, water and light availability and the understorey vegetation. *Plant Ecology*, *170*, 93–105.
- Maas, H.-G., Bienert, A., Scheller, S., & Keane, E. (2008). Automatic forest inventory parameter determination from terrestrial laser scanner data. *International Journal of Remote Sensing*, *29*, 1579–1593.
- MacFadyen, S., Zambatis, N., Van Teeffelen, A. J., & Hui, C. (2018). Long-term rainfall regression surfaces for the kruger national park, south africa: a spatio-temporal review of patterns from 1981 to 2015. *International Journal of Climatology*, *38*, 2506–2519.
- Mascaro, J., Detto, M., Asner, G. P., & Muller-Landau, H. C. (2011). Evaluating uncertainty in mapping forest carbon with airborne lidar. *Remote Sensing of Environment*, *115*, 3770–3774.
- Mathieu, R., Naidoo, L., Cho, M. A., Leblon, B., Main, R., Wessels, K., Asner, G. P., Buckley, J., Van Aardt, J., Erasmus, B. F. et al. (2013). Toward structural assessment of semi-arid african savannahs and woodlands: The potential of multitemporal polarimetric radarsat-2 fine beam images. *Remote Sensing of Environment*, *138*, 215–231.
- Mermoz, S., Le Toan, T., Villard, L., Réjou-Méchain, M., & Seifert-Granzin, J. (2014).

- Biomass assessment in the Cameroon savanna using ALOS PALSAR data. *Remote Sensing of Environment*, 155, 109–119.
- Meyer, K. M., Wiegand, K., Ward, D., & Moustakas, A. (2007). The rhythm of savanna patch dynamics. *Journal of Ecology*, 95, 1306–1315.
- Mitchard, E. T., Saatchi, S. S., Lewis, S., Feldpausch, T., Woodhouse, I. H., Sonké, B., Rowland, C., & Meir, P. (2011). Measuring biomass changes due to woody encroachment and deforestation/degradation in a forest–savanna boundary region of central Africa using multi-temporal l-band radar backscatter. *Remote Sensing of Environment*, 115, 2861–2873.
- Mitchard, E. T., Saatchi, S. S., Woodhouse, I. H., Nangendo, G., Ribeiro, N., Williams, M., Ryan, C. M., Lewis, S. L., Feldpausch, T., & Meir, P. (2009). Using satellite radar backscatter to predict above-ground woody biomass: A consistent relationship across four different African landscapes. *Geophysical Research Letters*, 36.
- Moffiet, T., Mengersen, K., Witte, C., King, R., & Denham, R. (2005). Airborne laser scanning: Exploratory data analysis indicates potential variables for classification of individual trees or forest stands according to species. *ISPRS Journal of Photogrammetry and Remote Sensing*, 59, 289–309.
- Moncrieff, G. R., Chamaillé-Jammes, S., Higgins, S. I., O'Hara, R. B., & Bond, W. J. (2011). Tree allometries reflect a lifetime of herbivory in an African savanna. *Ecology*, 92, 2310–2315.
- Moreira, A. G. (2000). Effects of fire protection on savanna structure in Central Brazil. *Journal of Biogeography*, 27, 1021–1029.
- Moskal, L. M., & Zheng, G. (2011). Retrieving forest inventory variables with terrestrial laser scanning (TLS) in urban heterogeneous forest. *Remote Sensing*, 4, 1–20.
- Muir, J., Phinn, S., Eyre, T., & Scarth, P. (2018). Measuring plot scale woodland structure using terrestrial laser scanning. *Remote Sensing in Ecology and Conservation*, 4, 320–338.
- Murphy, B. P., Andersen, A. N., & Parr, C. L. (2016). The underestimated biodiversity of tropical grassy biomes. *Philosophical Transactions of the Royal Society B: Biological Sciences*, 371, 20150319.
- Murphy, B. P., Lehmann, C. E., Russell-Smith, J., & Lawes, M. J. (2014). Fire regimes and woody biomass dynamics in Australian savannas. *Journal of Biogeography*, 41, 133–144.
- Murphy, B. P., Liedloff, A. C., & Cook, G. D. (2015). Does fire limit tree biomass in Australian savannas? *International Journal of Wildland Fire*, 24, 1–13.
- Naidoo, L., Mathieu, R., Main, R., Kleynhans, W., Wessels, K., Asner, G., & Leblon, B. (2015). Savannah woody structure modelling and mapping using multi-frequency (X-, C- and L-band) synthetic aperture radar data. *ISPRS Journal of Photogrammetry and*

- Remote Sensing*, 105, 234–250.
- Newnham, G. J., Armston, J. D., Calders, K., Disney, M. I., Lovell, J. L., Schaaf, C. B., Strahler, A. H., & Danson, F. M. (2015). Terrestrial laser scanning for plot-scale forest measurement. *Current Forestry Reports*, 1, 239–251.
- Noy-Meir, I. (1973). Desert ecosystems: environment and producers. *Annual Review of Ecology and Systematics*, 4, 25–51.
- O'Connor, T. G., Puttick, J. R., & Hoffman, M. T. (2014). Bush encroachment in southern Africa: changes and causes. *African Journal of Range & Forage Science*, 31, 67–88.
- Olofsson, K., Holmgren, J., & Olsson, H. (2014). Tree stem and height measurements using terrestrial laser scanning and the ransac algorithm. *Remote Sensing*, 6, 4323–4344.
- Olofsson, K., & Olsson, H. (2018). Estimating tree stem density and diameter distribution in single-scan terrestrial laser measurements of field plots: a simulation study. *Scandinavian Journal of Forest Research*, 33, 365–377.
- Olsoy, P. J., Glenn, N. F., Clark, P. E., & Derryberry, D. R. (2014). Aboveground total and green biomass of dryland shrub derived from terrestrial laser scanning. *ISPRS Journal of Photogrammetry and Remote Sensing*, 88, 166–173.
- Olsoy, P. J., Mitchell, J. J., Levia, D. F., Clark, P. E., & Glenn, N. F. (2016). Estimation of big sagebrush leaf area index with terrestrial laser scanning. *Ecological Indicators*, 61, 815–821.
- Olsson, E. G. A., & Ouattara, S. (2013). Opportunities and challenges to capturing the multiple potential benefits of REDD+ in a traditional transnational savanna-woodland region in West Africa. *Ambio*, 42, 309–319.
- O'Regan, S. (2005). *Responses of the woody vegetation in the Pretoriuskop sourveld savannas of the Kruger National Park to fires burnt at different frequencies*. University of the Witwatersrand, Johannesburg (MSc Thesis).
- Parr, C. L., & Andersen, A. N. (2006). Patch mosaic burning for biodiversity conservation: a critique of the pyrodiversity paradigm. *Conservation Biology*, 20, 1610–1619.
- Parr, C. L., Lehmann, C. E., Bond, W. J., Hoffmann, W. A., & Andersen, A. N. (2014). Tropical grassy biomes: misunderstood, neglected, and under threat. *Trends in Ecology & Evolution*, 29, 205–213.
- Paynter, I., Genest, D., Saenz, E., Peri, F., Boucher, P., Li, Z., Strahler, A., & Schaaf, C. (2018). Classifying ecosystems with metaproperties from terrestrial laser scanner data. *Methods in Ecology and Evolution*, 9, 210–222.
- Pellegrini, A. F., Hedin, L. O., Staver, A. C., & Govender, N. (2015). Fire alters ecosystem carbon and nutrients but not plant nutrient stoichiometry or composition in tropical savanna. *Ecology*, 96, 1275–1285.
- Pellegrini, A. F., Pringle, R. M., Govender, N., Hedin, L. et al. (2017). Woody plant

- biomass and carbon exchange depend on elephant-fire interactions across a productivity gradient in african savanna. *Journal of Ecology*, *105*, 111–121.
- Pickett, S. T., Cadenasso, M. L., & Benning, T. L. (2003). Biotic and abiotic variability as key determinants of savanna heterogeneity at multiple spatiotemporal scales. *The Kruger Experience: Ecology and Management of Savanna Heterogeneity*, (pp. 22–40).
- Pinheiro, J., Bates, D., DebRoy, S., & Sarkar, D. (2014). R core team (2014) nlme: linear and nonlinear mixed effects models. r package version 3.1-117. Available at <http://CRAN.R-project.org/package=nlme>, .
- Platt, W. J., Beckage, B., Doren, R. F., & Slater, H. H. (2002). Interactions of large-scale disturbances: prior fire regimes and hurricane mortality of savanna pines. *Ecology*, *83*, 1566–1572.
- Pueschel, P. (2013). The influence of scanner parameters on the extraction of tree metrics from faro photon 120 terrestrial laser scans. *ISPRS Journal of Photogrammetry and Remote Sensing*, *78*, 58–68.
- Pugnaire, F. I., Haase, P., & Puigdefabregas, J. (1996). Facilitation between higher plant species in a semiarid environment. *Ecology*, *77*, 1420–1426.
- Ratnam, J., Bond, W. J., Fensham, R. J., Hoffmann, W. A., Archibald, S., Lehmann, C. E., Anderson, M. T., Higgins, S. I., & Sankaran, M. (2011). When is a ‘forest’ a savanna, and why does it matter? *Global Ecology and Biogeography*, *20*, 653–660.
- Ratnam, J., Tomlinson, K. W., Rasquinha, D. N., & Sankaran, M. (2016). Savannahs of asia: antiquity, biogeography, and an uncertain future. *Philosophical Transactions of the Royal Society B: Biological Sciences*, *371*, 20150305.
- Raunonen, P., Kaasalainen, M., Åkerblom, M., Kaasalainen, S., Kaartinen, H., Vastaranta, M., Holopainen, M., Disney, M., & Lewis, P. (2013). Fast automatic precision tree models from terrestrial laser scanner data. *Remote Sensing*, *5*, 491–520.
- Roderick, M. L., Noble, I. R., & Cridland, S. W. (1999). Estimating woody and herbaceous vegetation cover from time series satellite observations: GCTE/LUCC RESEARCH LETTER. *Global Ecology and Biogeography*, *8*, 501–508.
- Rodríguez-Iturbe, I., & Porporato, A. (2007). *Ecohydrology of water-controlled ecosystems: soil moisture and plant dynamics*. Cambridge University Press.
- Rogers, K. H. et al. (2003). Adopting a heterogeneity paradigm: implications for management of protected savannas. *The Kruger Experience. Ecology and Management of Savanna Heterogeneity*. Island Press. Washington, (pp. 41–58).
- Roques, K., O’connor, T., & Watkinson, A. (2001). Dynamics of shrub encroachment in an african savanna: relative influences of fire, herbivory, rainfall and density dependence. *Journal of Applied Ecology*, *38*, 268–280.
- Russell-Smith, J., Cook, G. D., Cooke, P. M., Edwards, A. C., Lendrum, M., Meyer, C., & Whitehead, P. J. (2013). Managing fire regimes in north Australian savannas:

- applying aboriginal approaches to contemporary global problems. *Frontiers in Ecology and the Environment*, 11, 55–63.
- Ryan, C. M., Hill, T., Woollen, E., Ghee, C., Mitchard, E., Cassells, G., Grace, J., Woodhouse, I. H., & Williams, M. (2012). Quantifying small-scale deforestation and forest degradation in African woodlands using radar imagery. *Global Change Biology*, 18, 243–257.
- Saarinen, N., Kankare, V., Vastaranta, M., Luoma, V., Pyörälä, J., Tanhuanpää, T., Liang, X., Kaartinen, H., Kukko, A., Jaakkola, A. et al. (2017). Feasibility of terrestrial laser scanning for collecting stem volume information from single trees. *ISPRS Journal of Photogrammetry and Remote Sensing*, 123, 140–158.
- Saatchi, S., Halligan, K., Despain, D. G., & Crabtree, R. L. (2007a). Estimation of forest fuel load from radar remote sensing. *IEEE Transactions on Geoscience and Remote Sensing*, 45, 1726–1740.
- Saatchi, S. S., HOUGHTON, R. A., Dos Santos Alvala, R., Soares, J. V., & Yu, Y. (2007b). Distribution of aboveground live biomass in the amazon basin. *Global Change Biology*, 13, 816–837.
- Saatchi, S. S., & Moghaddam, M. (2000). Estimation of crown and stem water content and biomass of boreal forest using polarimetric sar imagery. *IEEE Transactions on Geoscience and Remote Sensing*, 38, 697–709.
- Sankaran, M., Hanan, N. P., Scholes, R. J., Ratnam, J., Augustine, D. J., Cade, B. S., Gignoux, J., Higgins, S. I., Le Roux, X., Ludwig, F. et al. (2005). Determinants of woody cover in African savannas. *Nature*, 438, 846–849.
- Sankaran, M., Ratnam, J., & Hanan, N. (2008). Woody cover in African savannas: the role of resources, fire and herbivory. *Global Ecology and Biogeography*, 17, 236–245.
- Santoro, M., Eriksson, L., Askne, J., & Schmullius, C. (2006). Assessment of stand-wise stem volume retrieval in boreal forest from JERS-1 L-band SAR backscatter. *International Journal of Remote Sensing*, 27, 3425–3454.
- Santos, J., Lacruz, M. P., Araujo, L., & Keil, M. (2002). Savanna and tropical rainforest biomass estimation and spatialization using JERS-1 data. *International Journal of Remote Sensing*, 23, 1217–1229.
- Savadogo, P., Sawadogo, L., & Tiveau, D. (2007). Effects of grazing intensity and prescribed fire on soil physical and hydrological properties and pasture yield in the savanna woodlands of Burkina Faso. *Agriculture, Ecosystems & Environment*, 118, 80–92.
- Schenk, H. J., & Jackson, R. B. (2002). Rooting depths, lateral root spreads and below-ground/above-ground allometries of plants in water-limited ecosystems. *Journal of Ecology*, 90, 480–494.
- Schimel, D., Schneider, F. D., Carbon, J., & Participants, E. (2019). Flux towers in the sky: global ecology from space. *New Phytologist*, 224, 570–584.

- Scholes, R., & Archer, S. (1997). Tree-grass interactions in savannas. *Annual review of Ecology and Systematics*, 28, 517–544.
- Scholes, R. J., Kendall, J., & Justice, C. (1996). The quantity of biomass burned in southern Africa. *Journal of Geophysical Research*, 101, 667–676.
- Scott, A. C. (2000). The pre-queternary history of fire. *Palaeogeography, Palaeoclimatology, Palaeoecology*, 164, 281–329.
- Seidel, D., & Ammer, C. (2014). Efficient measurements of basal area in short rotation forests based on terrestrial laser scanning under special consideration of shadowing. *iForest-Biogeosciences and Forestry*, 7, 227.
- Shimada, M., Itoh, T., Motooka, T., Watanabe, M., & Thapa, R. (2016). Generation of the first PALSAR-2 global mosaic 2014/2015 and change detection between 2007 and 2015 using the PALSAR and PALSAR-2. In *2016 IEEE International Geoscience and Remote Sensing Symposium (IGARSS)* (pp. 3871–3872). IEEE.
- Siebert, F., & Eckhardt, H. C. (2008). The vegetation and floristics of the Nkhuflu exclosures, Kruger National Park. *Koedoe*, 50, 126–144.
- Singh, J., Levick, S. R., Guderle, M., & Schmullius, C. (2020). Moving from plot-based to hillslope-scale assessments of savanna vegetation structure with long-range terrestrial laser scanning (lr-tls). *International Journal of Applied Earth Observation and Geoinformation*, 90, 102070.
- Singh, J., Levick, S. R., Guderle, M., Schmullius, C., & Trumbore, S. E. (2018). Variability in fire-induced change to vegetation physiognomy and biomass in semi-arid savanna. *Ecosphere*, 9, e02514.
- Smit, I. P., Asner, G. P., Govender, N., Kennedy-Bowdoin, T., Knapp, D. E., & Jacobson, J. (2010). Effects of fire on woody vegetation structure in african savanna. *Ecological Applications*, 20, 1865–1875.
- Smit, I. P., Smit, C. F., Govender, N., Linde, M. v. d., & MacFadyen, S. (2013). Rainfall, geology and landscape position generate large-scale spatiotemporal fire pattern heterogeneity in an african savanna. *Ecography*, 36, 447–459.
- Smit, I. P. J., Asner, G. P., Govender, N., Vaughn, N. R., & van Wilgen, B. W. (2016). An examination of the potential efficacy of high-intensity fires for reversing woody encroachment in savannas. *Journal of Applied Ecology*, 53, 1623–1633.
- Srinivasan, S., Popescu, S. C., Eriksson, M., Sheridan, R. D., & Ku, N.-W. (2015). Terrestrial laser scanning as an effective tool to retrieve tree level height, crown width, and stem diameter. *Remote Sensing*, 7, 1877–1896.
- Staben, G., Lucieer, A., & Scarth, P. (2018). Modelling lidar derived tree canopy height from landsat TM, ETM+ and OLI satellite imagery—A machine learning approach. *International Journal of Applied Earth Observation and Geoinformation*, 73, 666–681.
- Staver, A. C. (2018). Prediction and scale in savanna ecosystems. *New Phytologist*, 219,

- 52–57.
- Staver, A. C., Archibald, S., & Levin, S. (2011). Tree cover in sub-Saharan Africa: rainfall and fire constrain forest and savanna as alternative stable states. *Ecology*, *92*, 1063–1072.
- Staver, A. C., & Levin, S. A. (2012). Integrating theoretical climate and fire effects on savanna and forest systems. *The American Naturalist*, *180*, 211–224.
- Stevens, N., Lehmann, C. E., Murphy, B. P., & Durigan, G. (2017). Savanna woody encroachment is widespread across three continents. *Global Change Biology*, *23*, 235–244.
- Stovall, A. E., Anderson-Teixeira, K. J., & Shugart, H. H. (2018). Assessing terrestrial laser scanning for developing non-destructive biomass allometry. *Forest Ecology and Management*, *427*, 217–229.
- Strahler, A. H., Jupp, D. L., Woodcock, C. E., Schaaf, C. B., Yao, T., Zhao, F., Yang, X., Lovell, J., Culvenor, D., Newnham, G. et al. (2008). Retrieval of forest structural parameters using a ground-based lidar instrument (echidna®). *Canadian Journal of Remote Sensing*, *34*, S426–S440.
- Swemmer, A. M., Bond, W. J., Donaldson, J., Hempson, G. P., Malherbe, J., & Smit, I. P. (2018). The ecology of drought—a workshop report. *South African Journal of Science*, *114*, 1–3.
- Gonzalez de Tanago, J., Lau, A., Bartholomeus, H., Herold, M., Avitabile, V., Raunonen, P., Martius, C., Goodman, R. C., Disney, M., Manuri, S. et al. (2018). Estimation of above-ground biomass of large tropical trees with terrestrial lidar. *Methods in Ecology and Evolution*, *9*, 223–234.
- Team-RCore (2016). R: A language and environment for statistical computing. Vienna, Austria.
- Thies, M., & Spiecker, H. (2004). Evaluation and future prospects of terrestrial laser scanning for standardized forest inventories. *Forest*, *2*, 1.
- Tinley, K. (1982). *The influence of soil moisture balance on ecosystem patterns in southern Africa*. Springer.
- Torres, R., Snoeij, P., Geudtner, D., Bibby, D., Davidson, M., Attema, E., Potin, P., Rommen, B., Floury, N., Brown, M. et al. (2012). GMES Sentinel-1 mission. *Remote Sensing of Environment*, *120*, 9–24.
- Urbazaev, M., Thiel, C., Mathieu, R., Naidoo, L., Levick, S. R., Smit, I. P., Asner, G. P., & Schmullius, C. (2015). Assessment of the mapping of fractional woody cover in southern african savannas using multi-temporal and polarimetric ALOS PALSAR L-band images. *Remote Sensing of Environment*, *166*, 138–153.
- Van Der Werf, G. R., Randerson, J. T., Giglio, L., Van Leeuwen, T. T., Chen, Y., Rogers, B. M., Mu, M., Van Marle, M. J., Morton, D. C., Collatz, G. J. et al. (2017). Global

- fire emissions estimates during 1997-2016. *Earth System Science Data*, *9*, 697–720.
- Van Wyk, P. (1971). Veld burning in the kruger national park, an interim report of some aspects of research. In *Proceedings of the Tall Timbers Fire Ecology Conference* (pp. 9–31). volume 11.
- Vaughn, N. R., Asner, G. P., Smit, I. P., & Riddel, E. S. (2015). Multiple scales of control on the structure and spatial distribution of woody vegetation in African savanna watersheds. *PloS one*, *10*, e0145192.
- Venter, F. (1986). Soil patterns associated with the major geological units of the Kruger National Park. *Koedoe*, *29*, 125–138.
- Venter, F. J., Scholes, R. J., & Eckhardt, H. C. (2003). The abiotic template and its associated vegetation pattern. *The Kruger experience: Ecology and management of savanna heterogeneity*, *83*, 129.
- Wagenmakers, E.-J., & Farrell, S. (2004). Aic model selection using akaike weights. *Psychonomic Bulletin & Review*, *11*, 192–196.
- Wagner, W. (2010). Radiometric calibration of small-footprint full-waveform airborne laser scanner measurements: Basic physical concepts. *ISPRS Journal of Photogrammetry and Remote Sensing*, *65*, 505–513.
- Walter, H., & Burnett, J. H. (1971). *Ecology of tropical and subtropical vegetation*. 581.5264 W3. Oliver and Boyd Edinburgh.
- Ward, D., Wiegand, K., & Getzin, S. (2013). Walter’s two-layer hypothesis revisited: back to the roots! *Oecologia*, *172*, 617–630.
- Wessels, K. J., Mathieu, R., Erasmus, B., Asner, G., Smit, I., Van Aardt, J., Main, R., Fisher, J., Marais, W., Kennedy-Bowdoin, T. et al. (2011). Impact of communal land use and conservation on woody vegetation structure in the lowveld savannas of south africa. *Forest Ecology and Management*, *261*, 19–29.
- Wigley, B. J., Bond, W. J., & Hoffman, M. T. (2010). Thicket expansion in a South African savanna under divergent land use: local vs. global drivers? *Global Change Biology*, *16*, 964–976.
- van Wilgen, B. W. (2009). The evolution of fire management practices in savanna protected areas in South Africa. *South African Journal of Science*, *105*, 343–349.
- van Wilgen, B. W., Govender, N., & Biggs, H. C. (2007). The contribution of fire research to fire management: a critical review of a long-term experiment in the Kruger National Park, South Africa. *International Journal of Wildland Fire*, *16*, 519.
- van Wilgen, B. W., Govender, N., Smit, I. P., & MacFadyen, S. (2014). The ongoing development of a pragmatic and adaptive fire management policy in a large African savanna protected area. *Journal of Environmental Management*, *132*, 358–368.
- Wilkes, P., Lau, A., Disney, M., Calders, K., Burt, A., de Tanago, J. G., Bartholomeus, H., Brede, B., & Herold, M. (2017). Data acquisition considerations for terrestrial laser

-
- scanning of forest plots. *Remote Sensing of Environment*, 196, 140–153.
- Williams, R., Mueller, W., Wahren, C.-H., Setterfield, S., & JS, C. (2003). Fire in tropical savannas: The Kapalga experiment. *Vegetation. In: Andersen AN, Cook GD, Williams RJ, editors.*, (pp. 79–106).
- Williams, R. J., Hutley, L. B., Cook, G. D., Russell-Smith, J., Edwards, A., & Chen, X. (2004). Assessing the carbon sequestration potential of mesic savannas in the northern territory, australia: approaches, uncertainties and potential impacts of fire. *Functional Plant Biology*, 31, 415–422.
- Woodhouse, I. H. (2006). Predicting backscatter-biomass and height-biomass trends using a macroecology model. *IEEE Transactions on Geoscience and Remote Sensing*, 44, 871–877.
- Woodhouse, I. H., Mitchard, E. T., Broolly, M., Maniatis, D., & Ryan, C. M. (2012). Radar backscatter is not a ‘direct measure’ of forest biomass. *Nature Climate Change*, 2, 556–557.
- Woodward, F. I., Lomas, M. R., & Kelly, C. K. (2004). Global climate and the distribution of plant biomes. *Philosophical Transactions of the Royal Society of London. Series B: Biological Sciences*, 359, 1465–1476.
- Xu, X., Medvigy, D., & Rodriguez-Iturbe, I. (2015). Relation between rainfall intensity and savanna tree abundance explained by water use strategies. *Proceedings of the National Academy of Sciences*, 112, 12992–12996.
- Xu, X., Medvigy, D., Trugman, A. T., Guan, K., Good, S. P., & Rodriguez-Iturbe, I. (2018). Tree cover shows strong sensitivity to precipitation variability across the global tropics. *Global Ecology and Biogeography*, 27, 450–460.
- Yao, T., Yang, X., Zhao, F., Wang, Z., Zhang, Q., Jupp, D., Lovell, J., Culvenor, D., Newnham, G., Ni-Meister, W. et al. (2011). Measuring forest structure and biomass in new england forest stands using echidna ground-based lidar. *Remote Sensing of Environment*, 115, 2965–2974.

Selbstständigkeitserklärung

Ich erkläre, dass ich die vorliegende Arbeit selbstständig und nur unter Verwendung der angegebenen Hilfsmittel, persönlichen Mitteilungen und Quellen angefertigt habe.

Jenia Singh

Jena, December 18, 2019

